Accuracy and Sensitivity Analysis of Bioelectromagnetic Field Modeling in the Human Brain

Cumulative Habilitation Thesis

to obtain the Venia Docendi in

Biomedizinische Technik / Biomedical Engineering

submitted by

Dr. Johannes Vorwerk

– January 2025 –

universität innsbruck

Department of Mechatronics

Abstract

The simulation of bioelectromagnetic fields is an important tool for several applications in the field of neuroscience. The simulated fields are not limited to naturally occurring ones resulting from brain activity as in the analysis of electroencephalography (EEG) and magnetoencephalography (MEG), but can also be externally impressed as in the simulation of invasive and non-invasive brain stimulation. To draw reliable conclusions based on these simulation results, it is important to understand the accuracy of the numerical methods used for the electromagnetic field simulations and in how far the simulation results are sensitive towards model simplifications or uncertainties of the input parameters, such as the inter-individually varying tissue conductivities. In this thesis, several studies investigating accuracy, sensitivity, and applications of bioelectromagnetic field modeling in the human brain are discussed. A focus is put on studies in the field of EEG/MEG source analysis but also some results and conclusions for the field of brain stimulation, which shares the same underlying mathematical equations, are presented.

EEG and MEG are important tools for non-invasive functional neuroimaging due to their unique time resolution. To perform EEG/MEG source analysis, i.e., determine the active brain areas underlying the measured signal, an ill-posed inverse problem has to be solved. For reliable EEG/MEG source analysis, it is necessary to accurately simulate the electric and magnetic fields generated by active brain tissue. This so-called forward problem of EEG/MEG has to be solved numerically when aiming to consider the individual shape and conductivity distribution of the subject's head. Therefore, it is necessary to create an (individual) head volume conductor model.

The accuracy of the EEG/MEG forward solution and in consequence of the source analysis is amongst others influenced by the chosen numerical method, the geometric accuracy of the head volume conductor model, and a correct choice of the tissue conductivities. In this thesis, several studies are presented that aim to improve the accuracy and understanding of EEG/MEG source analysis by addressing these aspects. Novel numerical methods that improve the accuracy of EEG/MEG forward solutions are presented, the influence of head model detail and geometric accuracy on EEG/MEG source analysis is evaluated, and the sensitivity of EEG/MEG source analysis towards tissue conductivity uncertainties is quantified. Furthermore, applications of highly accurate head volume conductor models for EEG/MEG source analysis and improved electric brain stimulation in practice as well as toolboxes that easily allow for the use of such head models are presented.

Zusammenfassung

Die Simulation bioelektromagnetischer Felder ist ein wichtiges Instrument in verschiedenen Anwendungen im Bereich der Neurowissenschaften. Die zu simulierenden Felder sind dabei nicht auf solche beschränkt, die natürlicherweise durch Hirnaktivität erzeugt werden, wie etwa bei der Analyse von Elektroenzephalographie (EEG) und Magnetenzephalographie (MEG), sondern können auch von außen eingeleitet werden, wie bei der Simulation invasiver und nichtinvasiver Hirnstimulation. Um basierend auf den Simulationsergebnissen verlässliche Schlüsse ziehen zu können, ist es wichtig, die Genauigkeit der für die elektromagnetischen Feldsimulationen verwendeten numerischen Methoden zu verstehen und zu analysieren, inwieweit die Simulationsergebnisse durch Modellvereinfachungen oder Unsicherheiten der Eingangsparameter, wie die interindividuell variierenden Gewebeleitfähigkeiten, beeinflusst werden. In dieser Habilitationsschrift werden mehrere Studien vorgestellt, die die Genauigkeit, Sensitivität gegenüber Modellvereinfachungen und Parameterunischerheiten und praktische Anwendungen der Modellierung bioelektromagnetischer Felder im menschlichen Gehirn untersuchen. Der Schwerpunkt liegt dabei auf Studien im Bereich der EEG/MEG-Quellenanalyse, aber auch einige Ergebnisse und Schlussfolgerungen für den Bereich der Hirnstimulation, welchem dieselben mathematischen Gleichungen zu Grunde liegen, werden vorgestellt.

EEG und MEG sind auf Grund ihrer einzigartigen zeitlichen Auflösung wichtige Methoden für die nicht-invasive funktionelle Neurobildgebung. Um EEG/MEG-Quellenanalyse durchzuführen, d. h. die aktiven Hirnareale zu bestimmen, die dem gemessenen Signal zu Grunde liegen, muss ein schlecht gestelltes inverses Problem gelöst werden. Für eine zuverlässige EEG/MEG-Quellenanalyse ist es notwendig, die von aktiven Hirnarealen erzeugten elektrischen und magnetischen Felder akkurat zu simulieren. Wenn man die individuelle Form und Leitfähigkeitsverteilung des Kopfes der Versuchsperson berücksichtigen will, muss dieses so genannte Vorwärtsproblem des EEG/MEG numerisch gelöst werden. Dafür ist es notwendig ein (individuelles) Volumenleitermodell des Kopfes zu erstellen.

Die Genauigkeit der EEG/MEG-Vorwärtslösung und damit auch der darauf basierenden Quellenanalyse wird unter anderem durch die gewählte numerische Methode, die Genauigkeit des Volumenleitermodells und einer korrekten Wahl der Gewebeleitfähigkeiten beeinflusst. In dieser Arbeit werden mehrere Studien vorgestellt, die zum Ziel haben den Einfluss dieser Aspekte auf die EEG/MEG-Quellenanalyse besser zu verstehen und die Genauigkeit der Quellanalyse zu verbessern. Es werden neue numerische Methoden vorgestellt, welche die Genauigkeit von EEG/MEG-Vorwärtslösungen verbessern, der Einfluss des Detailgrades und der geometrischen Genauigkeit des Kopfmodells auf die

EEG/MEG-Quellenanalyse wird analysiert, und die Empfindlichkeit der EEG/MEG-Quellenanalyse gegenüber Unsicherheiten bezüglich der Gewebeleitfähigkeiten wird quantifiziert. Darüber hinaus werden Anwendungen akkurater Volumenleitermodelle des Kopfes für die EEG/MEG-Quellanalyse und verbesserte elektrische Hirnstimulation in der Praxis sowie Toolboxen, welche die Verwendung solcher Kopfmodelle auf einfache Weise ermöglichen, vorgestellt.

Contents

List of Figures

List of Tables

List of Abbreviations

AEP	auditory evoked potential.
BCI	brain-computer interface.
BEM	boundary element method.
BEM-FMM	boundary element fast multipole method.
CDR	current density reconstruction.
CG	continuous Galerkin.
CSF	cerebrospinal fluid.
CT	computed tomography.
DBS	deep brain stimulation.
DG	discontinuous Galerkin.
DSI	diffusion spectrum imaging.
ECD	equivalent current dipole.
ECoG	electrocorticography.
EEG	electroencephalography.
EIT	electrical impedance tomography.
FCM	functional cortical mapping.
FEM	finite element method.
fMRI	functional magnetic resonance imaging.
FVM	finite volume method.
GFS	goal function scan.
gPC	generalized polynomial chaos.
IC	internal capsule.
IED	interictal epileptic discharge.
iEEG	intracranial EEG.
LCMV	linearly-constrained minimum variance.
MEG	magnetoencephalography.
MRI	magnetic resonance imaging.
NIRS	near-infrared spectroscopy.
PDE	partial differential equation.
PED	presurgical epilepsy diagnosis.
PET	positron emission tomography.
sEEG	stereo EEG.
SEP	somatosensory evoked potential.
SNR	signal-to-noise ratio.
SPECT	single-photon emission computed tomography.

tDCS	transcranial direct current stimulation.
TMS	transcranial magnetic stimulation.
Vc	ventralis caudalis.
VIM	ventrointermediate nucleus.

List of Relevant Publications

J. Vorwerk, M. Clerc, M. Burger, and C. Wolters (2012). "Comparison of boundary element and finite element approaches to the EEG forward problem". In: *Biomedical Engineering/Biomedizinische Technik* 57.SI-1-Track-O, pp. 795–798

J. Vorwerk, J.-H. Cho, S. Rampp, H. Hamer, T. R. Knösche, and C. H. Wolters (2014). "A guideline for head volume conductor modeling in EEG and MEG". in: *NeuroImage* 100, pp. 590–607

Ü. Aydin, **J. Vorwerk**, P. Küpper, M. Heers, H. Kugel, A. Galka, L. Hamid, J. Wellmer, C. Kellinghaus, S. Rampp, H. Stefan, and C. H. Wolters (2014). "Combining EEG and MEG for the reconstruction of epileptic activity using a calibrated realistic volume conductor model". In: *PloS one* 9.3, e93154

J.-H. Cho, **J. Vorwerk**, C. H. Wolters, and T. R. Knösche (2015). "Influence of the head model on EEG and MEG source connectivity analyses". In: *NeuroImage* 110, pp. 60–77

Ü. Aydin, **J. Vorwerk**, M. Dümpelmann, P. Küpper, H. Kugel, M. Heers, J. Wellmer, C. Kellinghaus, J. Haueisen, S. Rampp, H. Stefan, and C. H. Wolters (2015). "Combined EEG/MEG can outperform single modality EEG or MEG source reconstruction in presurgical epilepsy diagnosis". In: *PloS one* 10.3, e0118753

J. Vorwerk, C. Engwer, S. Pursiainen, and C. H. Wolters (2016). "A mixed finite element method to solve the EEG forward problem". In: *IEEE Transactions on Medical Imaging* 36.4, pp. 930–941

S. Pursiainen, **J. Vorwerk**, and C. H. Wolters (2016). "Electroencephalography (EEG) forward modeling via H (div) finite element sources with focal interpolation". In: *Physics in Medicine & Biology* 61.24, p. 8502

L. D. J. Fiederer, **J. Vorwerk**, F. Lucka, M. Dannhauer, S. Yang, M. Dümpelmann, A. Schulze-Bonhage, A. Aertsen, O. Speck, C. H. Wolters, and T. Ball (2016). "The role of blood vessels in high-resolution volume conductor head modeling of EEG". in: *NeuroImage* 128, pp. 193–208

C. Engwer*, **J. Vorwerk***, J. Ludewig, and C. H. Wolters (2017). "A discontinuous Galerkin method to solve the EEG forward problem using the subtraction approach". In: *SIAM Journal on Scientific Computing* 39.1, B138–B164. **The first two authors contributed equally to this work.*

J. Vorwerk, R. Oostenveld, M. C. Piastra, L. Magyari, and C. H. Wolters (2018). "The FieldTrip-SimBio pipeline for EEG forward solutions". In: *Biomedical Engineering Online* 17, pp. 1–17

J. Vorwerk, Ü. Aydin, C. H. Wolters, and C. R. Butson (2019a). "Influence of head tissue conductivity uncertainties on EEG dipole reconstruction". In: *Frontiers in Neuroscience* 13, p. 531

J. Vorwerk, A. A. Brock, D. N. Anderson, J. D. Rolston, and C. R. Butson (2019b). "A retrospective evaluation of automated optimization of deep brain stimulation parameters". In: *Journal of Neural Engineering* 16.6, p. 064002

J. Vorwerk, A. Hanrath, C. H. Wolters, and L. Grasedyck (2019c). "The multipole approach for EEG forward modeling using the finite element method". In: *NeuroImage* 201, p. 116039

J. Vorwerk, D. McCann, J. Krüger, and C. R. Butson (2020). "Interactive computation and visualization of deep brain stimulation effects using Duality". In: *Computer Methods in Biomechanics and Biomedical Engineering: Imaging & Visualization* 8.1, pp. 3–14

J. Vorwerk, C. H. Wolters, and D. Baumgarten (2024). "Global Sensitivity of EEG Source Analysis to Tissue Conductivity Uncertainties". In: *Frontiers in Human Neuroscience* 18, p. 1335212

1 Introduction

Over the last decades, neuroscience has made significant progress which not only resulted in a better understanding of the functioning of the human brain, but also led to novel approaches in the diagnosis and treatment of neurological disorders. An important driver of this progress is the still ongoing (further) development of neuroimaging methods, enabling a more and more detailed insight into the spatial and temporal organization of brain activity. These methods can be subdivided into structural and functional imaging methods. Whereas structural imaging methods such as magnetic resonance imaging (MRI) and computed tomography (CT) allow to examine the tissue structure of the brain enabling the detection of (possibly pathological) anomalies such as lesions, functional imaging methods provide information about timing and location of brain activity.

One of the first methods developed to measure brain activity was the electroencephalography (EEG), which was for the first time recorded in a human in the 1920s by Hans Berger (Berger, 1929). The EEG measures the potential differences at the head surface that result from neural activity. In the 1960s also the magnetic counterpart of the EEG, the magnetoencephalography (MEG), was first measured (Cohen, 1968, 1972). Whereas both EEG and MEG offer a very high temporal resolution in the millisecond range, the spatial resolution of early EEG and MEG was very limited and was largely based on the user's interpretation.

In the following decades, further methods for functional brain imaging were developed, such as positron emission tomography (PET), single-photon emission computed tomography (SPECT), functional magnetic resonance imaging (fMRI), and near-infrared spectroscopy (NIRS), which often achieved a higher spatial resolution than EEG and MEG. Though, their temporal resolution is clearly lower as they do not image brain activity directly, but indirectly by tracking metabolic processes or blood flow. In the case of fMRI and NIRS, this is achieved by imaging the change of blood oxygenation and for PET and SPECT through radioactive tracers. The exposure to ionizing radiation caused by these tracers has to be taken into account when considering the use of PET or SPECT, especially as they are often combined with CT for structural imaging; fMRI - just like common MRI - exposes the subject to strong magnetic fields, which is usually unproblematic as long as the subject does not have metallic implants. As probably the most invasive option for

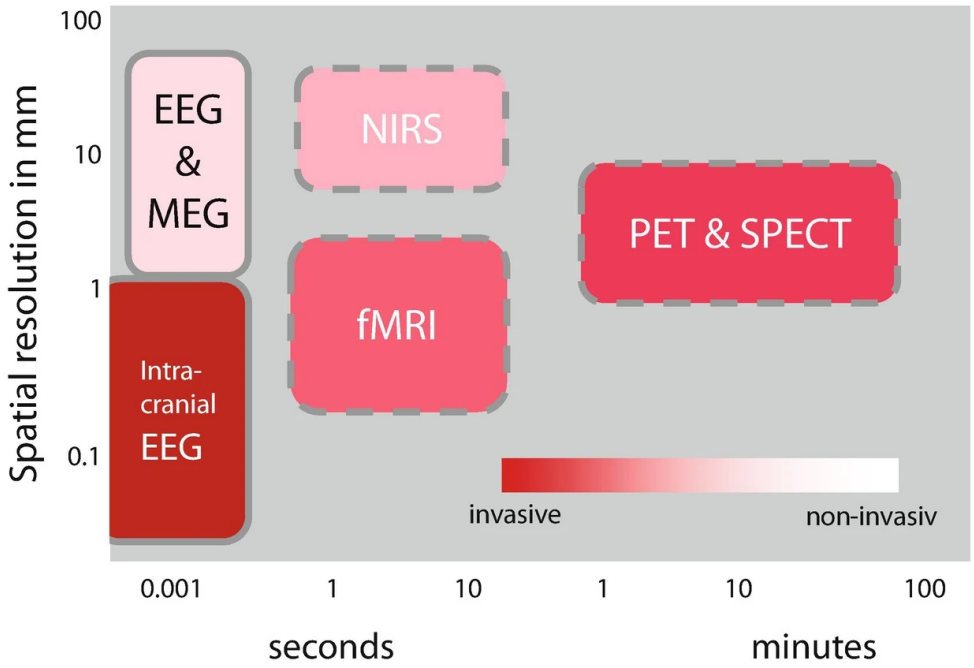

Figure 1.1: Overview of spatial and temporal resolutions as well as the degree of invasiveness for some of the most important functional brain imaging modalities in humans: EEG, MEG, intracranial EEG (surface or depth electrodes), fMRI, NIRS, PET, and SPECT. Dashed frames indicate indirect (metabolic) methods and solid ones direct (electrophysiological) methods. Figure from Knösche and Haueisen (2022). Reproduced with permission from Springer Nature.

functional brain imaging, intracranial EEG (iEEG) recordings use either electrodes placed directly on the cortex (electrocorticography/ECoG) or depth electrodes implanted in the brain tissue (stereo EEG/sEEG) so that the spatial resolution can be increased while the same temporal resolution as for EEG is achieved.

Meanwhile, several improvements both in EEG/MEG technology and analysis have been made, so that nowadays also a quantitative analysis with a resolution up to a few millimeters is possible in some scenarios (Knösche and Haueisen, 2022). On the one hand, the number of sensors both in EEG and MEG has been significantly increased and is nowadays in the range of up to a few hundred resulting in an improved spatial sampling of the signal. On the other hand, aided by the rapid increase in available computational power, numerical methods that allow to solve the EEG/MEG inverse problem, i.e., to locate the active brain areas underlying a measured signal using computational methods, have been developed and continuously improved. The process of solving the EEG/MEG inverse problem is often also referred to as EEG/MEG source analysis.

An overview of the temporal and spatial resolution as well as an assessment of the invasiveness of the different methods for functional brain imaging is shown in Fig. 1.1. As a consequence of their invasiveness/radiation exposure, PET, SPECT, and iEEG can only be considered for functional brain imaging if medical reasons exist, whereas fMRI, NIRS as well as EEG and MEG can be used for healthy subjects. Another aspect to be considered

is the portability of devices. Most of the mentioned imaging techniques rely on complex, stationary machinery. Only EEG and NIRS are portable and even offer the possibility for mobile measurements outside the lab environment, whereas the other techniques mostly restrict the subject to a lying position. MEG allows a somewhat higher flexibility with regard to subject position as subjects can often be either seated or in a lying position.
This thesis is primarily devoted to studying novel methodology to improve the accuracy of EEG/MEG source analysis and investigating the sensitivity of EEG/MEG source analysis to model simplifications and parameter variations, e.g., the influence of the used head volume conductor models or of head tissue conductivity uncertainties. Furthermore, some results obtained in the simulation of invasive and non-invasive brain stimulation are presented and discussed. The simulation of brain stimulation is related to EEG/MEG source analysis through the underlying physical equations so that some of the methodology and simulation results obtained for EEG/MEG source analysis can be translated to the simulation of brain stimulation and vice versa.

1.1 EEG and MEG

Electroencephalography and magnetoencephalography measure the electric and magnetic fields, respectively, evoked by electrical currents in the brain, such as postsynaptic potentials. Whereas action potentials do not evoke an exploitable EEG/MEG signal, as they are too short (0.5-2 ms), insufficiently synchronized, and their far-field induced by the resulting ion currents is dominated by the quadrupole term (Plonsey, 1977), the simultaneous generation of post-synaptic potentials with a duration of tens of milliseconds by some ten-thousand neighboring and similarly oriented neurons, which correspond to a patch of a few square millimeters of cortex surface, results in a measurable dipolar electromagnetic field (Murakami and Okada, 2006; Okada, 1993). Murakami and Okada (2006) estimate that about 50.000 pyramidal neurons might be sufficient to generate a source strength of about 10 nAm, which was suggested to be a lower bound for measurable cortical generators in humans by Hämäläinen et al. (1993).
To generate a measurable electric and magnetic field, respectively, it is important that the activated neurons are not only synchronized but also spatially aligned, i.e., oriented in a similar direction. The highest concentration of similarly oriented neurons is given for the approximately 10^9 pyramidal cells that are mainly found in the cortex but also in the hippocampus and the amygdala. Thus, the major contribution to the EEG/MEG signals originates from these areas. As the orientation of the pyramidal cells is perpendicular to the cortex surface, the orientation of the resulting primary current representing a patch of active cortex is roughly perpendicular to the cortex surface as well and can be approximated by an accordingly oriented current dipole (Fig. 1.2).
The primary current gives rise to volume currents within the conductive head tissues

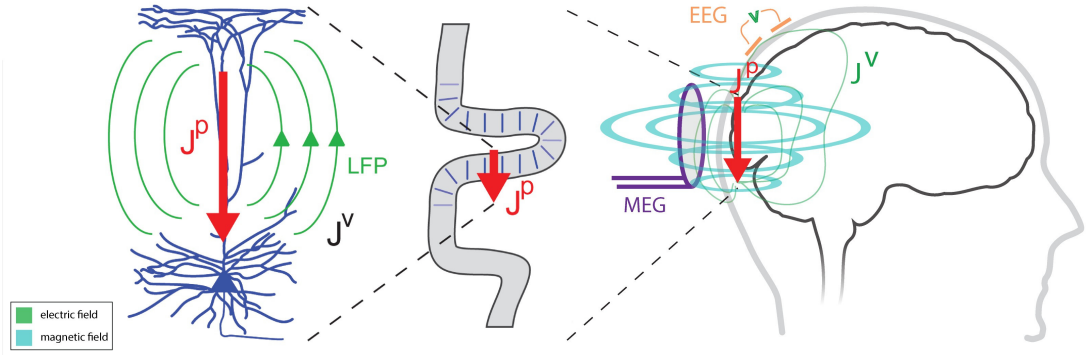

Figure 1.2: Origin of EEG and MEG signals. Synchronized post-synaptic potentials evoke a primary current $\mathbf{j}^p$ oriented perpendicular to the cortex surface and volume currents $\mathbf{j}^v$. If the number of activated neurons is sufficient, the resulting electric and magnetic fields can be detected by EEG and MEG, respectively. Figure from Neymotin et al. (2020) licensed under CC BY 4.0 DEED.

causing an electric potential distribution. The resulting electric potential differences between different positions on the head surface are measured as EEG. The topography of the potential distribution is influenced by the properties of the head as a volume conductor, i.e., the geometry and electric conductivities of the different head tissues such as white matter, gray matter, cerebrospinal fluid (CSF), skull, or skin. The air surrounding the head is considered as an isolator. As the primary current approximately represents a current dipole, it also evokes a measurable magnetic field, the so-called primary magnetic field. Furthermore, the volume currents in the conductive head tissues also lead to a magnetic field, the so-called secondary magnetic field. The signal measured by MEG accordingly consists of the sum of primary and secondary magnetic field. Measurable EEG/MEG signals are commonly in the range of microvolts (μV) and femtotesla (fT), respectively. For quasi-radial orientations of the primary current, i.e., pointing perpendicular towards the head surface, as it occurs, e.g., for brain activity localized on top of gyri, the total magnetic field (almost) vanishes so that such sources have a very weak MEG signal.

1.2 EEG/MEG Source Analysis

EEG/MEG source analysis aims at reconstructing the active brain areas underlying a measured signal. Analysis in the *source space* - instead of in the *sensor space* - is advantageous in many applications of EEG/MEG. In a clinical context, source analysis is especially of interest in presurgical evaluations to either determine the brain areas to be resected or brain areas required for critical functions that need to remain intact. To determine the location of eloquent cortical areas possibly overlapping with a resection zone, presurgical functional cortical mapping (FCM) is common clinical practice for which both invasive and non-invasive methods, including EEG and MEG, are applied (Kreidenhuber

et al., 2019).
Another clinical example of the use of EEG/MEG source analysis is pharmacoresistant epilepsy, which is also topic of multiple studies included in this thesis. A requirement for (successful) epilepsy surgery is the accurate and unambiguous localization of the epileptogenic zone, i.e., the brain area responsible for the seizure onset, whose resection and/or disconnection should render the patient seizure-free. An important step to accurately define the epileptogenic zone in presurgical epilepsy diagnosis (PED) is the localization of the irritative zone, whose location is suggested to correlate with the epileptogenic zone (Rosenow and Lüders, 2001). The irritative zone is defined as the brain area producing synchronous discharges of nerve cell clusters in the time between seizures that can be observed in EEG and/or MEG (interictal epileptic discharges/IEDs). This makes EEG/MEG source analysis an important tool to accurately localize the irritative zone, and - in consequence - also the epileptogenic zone. Due to the severe consequences of resective epilepsy surgery, greatest care has to be taken in the determination of the epileptogenic zone. However, incomplete resection of the epileptogenic zone is a predictor of poor surgery outcome (Ryvlin et al., 2014).
In basic neuroscience, EEG/MEG source analysis is for example of interest to study evoked responses, e.g., of the primary sensory and motor systems (Knösche and Haueisen, 2022). In some cases, the analysis of evoked responses even has diagnostic value in clinical applications (Walsh et al., 2005; Wolters et al., 2021). Auditory (Pantev et al., 1989), somatosensory (Buchner et al., 1995), or visual stimuli (Makeig et al., 2002) can be repeated hundreds of times within a short amount of time; the measured signals can then be averaged in relation to the stimulus onset so that noise can be decreased and the signals of interest related to the processing of the stimulus can be extracted. This allows to identify the involved brain areas and the chronological order of their activation. This is not only of interest for simple stimuli but also in the processing of complex stimuli, e.g., faces or emotion (Olivares et al., 2015; Schupp et al., 2006). To better understand the interplay of these different activated brain areas, EEG/MEG source analysis is often also used as a basis for source space functional connectivity analysis (Schoffelen and Gross, 2009).
Besides these classical applications, EEG/MEG source analysis has recently also gained interest in the development of non-invasive brain-computer interfaces (BCI). When trying to identify the intention of the patient/subject, expressed through the intentional activation of specific brain areas, source analysis can help to separate signals from different origins (Grosse-Wentrup et al., 2009).
To perform EEG/MEG source analysis, two mathematical problems need to be solved, first the *EEG/MEG forward problem* and subsequently the *EEG/MEG inverse problem*. Consequentially, the accuracy of the inverse solution crucially depends on the accuracy of the forward solution (Akalin Acar and Makeig, 2013; Cho, **Vorwerk**, et al., 2015).

1.2.1 EEG/MEG Forward Problem

The EEG/MEG forward problem consists of simulating the electric/magnetic field at the sensor positions evoked by brain activity in a predefined brain area. Commonly, this brain activity is modeled by a point-like dipole source with a fixed position and dipole moment. A set of such dipoles can be used to model almost arbitrary distributions of brain activity in the following processing steps.
The first step to solving the EEG/MEG forward problem is simulating the electric potential distribution in the head. This directly leads to the EEG forward solution by reading out the electric potential at the electrode positions. Following, the law of Biot-Savart allows to calculate the magnetic field at the MEG sensor positions based on the potential distribution.
The common starting point to solve the EEG/MEG forward problem is the quasi-static approximation of Maxwell's equations (Hämäläinen et al., 1993). Assuming that the permeability of the head's tissue is that of free space, i.e., $\mu = \mu_0$, these read

$$\nabla \cdot \mathbf{E} = \frac{\rho}{\epsilon_r \epsilon_0}, \tag{1.1}$$

$$\nabla \cdot \mathbf{B} = 0, \tag{1.2}$$

$$\nabla \times \mathbf{E} = -\frac{\partial \mathbf{B}}{\partial t}, \tag{1.3}$$

$$\nabla \times \mathbf{B} = \mu_0 \mathbf{j} + \mu_0 \epsilon_r \epsilon_0 \frac{\partial \mathbf{E}}{\partial t}, \tag{1.4}$$

where $\mathbf{E}$ denotes the electric field, $\mathbf{B}$ the magnetic flux density, ρ the charge density, $\mathbf{j}$ the current density, ϵ_0 and ϵ_r the permittivity of free space and the relative permittivity, respectively, and μ_0 the permeability of free space.
Through the analysis of electric fields with a harmonic time-dependency, i.e., $\mathbf{E}(t) = \mathbf{E}_0 e^{-i\omega t}$, it can be shown that for $|\epsilon_r \epsilon_0 \omega / \sigma| \ll 1$ the time derivative in (1.4) can be neglected. With $\sigma \approx 0.3$ S/m, $\epsilon_r \approx 10^5$ and a frequency $f = \omega / 2\pi \approx 100$ Hz, which is assumed to be an upper bound for frequencies in neuroelectromagnetism (Hämäläinen et al., 1993), we have $\epsilon_r \epsilon_0 \omega / \sigma \approx 2 \cdot 10^{-3} \ll 1$. Similarly, it can be shown that the time-derivative in (1.3) can be neglected as the characteristic wavelength is much larger than the diameter of the human head so that the quasi-static assumption is valid for solving the EEG/MEG forward problem.
As we now have $\nabla \times \mathbf{E} = 0$ in (1.3), $\mathbf{E}$ is a gradient field and can be related to a scalar potential u:

$$\mathbf{E} = -\nabla u. \tag{1.5}$$

We further separate the current density $\mathbf{j}(x)$ into two parts: the *primary current* $\mathbf{j}^p(x)$, which is a direct result of the brain activity and is commonly spatially limited to a small

volume, and the *volume current* or *return current*, $\mathbf{j}^v(\mathbf{x}) = \sigma(\mathbf{x})\mathbf{E}(\mathbf{x})$:

$$\mathbf{j}(\mathbf{x}) = \mathbf{j}^p(\mathbf{x}) + \mathbf{j}^v(\mathbf{x}) = \mathbf{j}^p(\mathbf{x}) + \sigma(\mathbf{x})\mathbf{E}(\mathbf{x}) = \mathbf{j}^p(\mathbf{x}) - \sigma(\mathbf{x})\nabla u(\mathbf{x}). \tag{1.6}$$

The conductivity $\sigma(\mathbf{x})$ is either a non-negative scalar or a positive definite tensor, i.e., for a head domain Ω, which is assumed to be open and connected with a sufficiently regular boundary, we have $\sigma : \Omega \to \mathbb{R}^+$ or $\sigma : \Omega \to \mathbb{R}^{3\times3}$. A tensor-valued conductivity is, e.g., used to incorporate the effects of the anisotropic structure of white matter on the electric/magnetic fields (Güllmar et al., 2010; Wolters et al., 2006).
Taking the divergence of (1.4) in the quasi-static approximation and exploiting $\nabla\cdot\nabla\times B = 0$, together with (1.6) we can either formulate a system of two coupled first-order partial differential equations (PDE)

$$\begin{aligned} \mathbf{j} + \sigma\nabla u &= \mathbf{j}^p \\ \nabla\cdot\mathbf{j} &= 0 \end{aligned} \quad \text{in } \Omega, \tag{1.7a}$$

$$\langle \mathbf{j}, \mathbf{n}\rangle = 0 \quad \text{on } \partial\Omega = \Gamma. \tag{1.7b}$$

or by eliminating $\mathbf{j}$ one second-order PDE

$$\nabla\cdot(\sigma\nabla u) = f = \nabla\cdot\mathbf{j}^p \quad \text{in } \Omega, \tag{1.8a}$$

$$\sigma\partial_{\mathbf{n}} u = 0 \quad \text{on } \partial\Omega = \Gamma \tag{1.8b}$$

The homogeneous Neumann boundary condition is chosen as there is no current flowing through the head surface. f is introduced as an abstract source term, and the actual definition of f depends on the representation of the primary current $\mathbf{j}^p$. Commonly, $\mathbf{j}^p$ is chosen to be a current dipole defined by its position $\mathbf{x}_0$ and its moment $\mathbf{p}$,

$$\mathbf{j}^p(\mathbf{x}) = \mathbf{p}\delta_{\mathbf{x}_0}(\mathbf{x}), \tag{1.9}$$

where $\delta_{\mathbf{x}_0}$ is the Dirac delta distribution and $\mathbf{p}$ the dipole moment.
For EEG/MEG, the current dipole is a good approximation of the smallest unit of the neural generators, whose far-field is mainly dipolar (De Munck et al., 1988; Hämäläinen et al., 1993; Sarvas, 1987). Due to the linearity of the problem (1.8), forward solutions for different dipole positions and orientations can be linearly combined to obtain a forward solution for a general current density in the brain. Some studies have also examined other choices of $\mathbf{j}^p$ as an alternative or supplement to dipoles in special situations, e.g., quadrupoles (Jerbi et al., 2004; Nolte and Curio, 1997; Riera et al., 2012; **Vorwerk** et al., 2019c). However, the fields of these higher-order contributions decay much faster than the dipole fields so that their influence is usually negligible. Thus, we focus on the choice of a current dipole as the primary current.

The EEG forward problem now consists in finding a solution u or $(\mathbf{j}, u)$ to the equivalent equation systems (1.8) or (1.7), respectively. With (1.6), the solution to the forward problem of MEG follows directly from the solution of the respective EEG forward problem via the *law of Biot-Savart*:

$$\begin{aligned}\mathbf{B}(\mathbf{x}) &= \frac{\mu_0}{4\pi}\int_\Omega \mathbf{j}(\mathbf{x}') \times \frac{\mathbf{x}-\mathbf{x}'}{\|\mathbf{x}-\mathbf{x}'\|_2^3}\,\mathrm{d}x' \\ &= \frac{\mu_0}{4\pi}\int_\Omega [\mathbf{j}^p(\mathbf{x}') - \sigma(\mathbf{x}')\nabla u(\mathbf{x}')] \times \frac{\mathbf{x}-\mathbf{x}'}{\|\mathbf{x}-\mathbf{x}'\|_2^3}\,\mathrm{d}x'.\end{aligned} \tag{1.10}$$

Splitting up the integral in the second line of (1.10), one recognizes the first term involving $\mathbf{j}^p$ as the primary magnetic flux density, which is directly evoked by the primary current, whereas the second term corresponds to the secondary magnetic flux density evoked by the volume currents.

To obtain accurate EEG/MEG forward solutions, it is necessary to consider the individual geometry of the subject's head represented by the domain Ω and the conductivity distribution $\sigma(x)$. However, the limitations in available computational power only allowed the use of (quasi-)analytical solutions to (1.8) in the early days of EEG/MEG source analysis. Such (quasi-)analytical solutions only exist for some simple geometries, such as nested spheres. In consequence, the head volume conductor was approximated by a set of nested spheres resulting in forward solutions with significant inaccuracies, especially for the EEG. As the influence of an accurate representation of the head volume conductor is assumed to be less significant for the MEG, sphere models are sometimes still used for MEG source analysis nowadays. This is due to the fact that the primary magnetic field only depends on the position, strength, and orientation of the primary current and the primary magnetic flux density in (1.10) can even be easily calculated analytically. Only the secondary magnetic field is influenced by the head volume conductor model. However, for quasi-radial sources in a spherical model the MEG signal completely vanishes. Calculating the secondary magnetic flux using a realistic head volume conductor model a weak but usually non-zero MEG signal remains.

With the increase of the available computational power over the last decades, novel methods to solve the EEG/MEG forward problem that allow for a better representation of the geometry of the head volume conductor have been developed. Boundary element methods (BEM) transform the PDE (1.8) into an integral equation on the surfaces separating regions of different conductivities. The advantage of this method is that only the resulting region surfaces have to be discretized, which leads to a relatively small number of unknowns. Drawbacks are the dense matrices in the resulting linear equation system, the limitation to isotropic conductivities, and restrictions with regard to the discretized geometry, which result from the need to keep the number of unknowns and the related computational effort within limits. Therefore, BEMs are often used in combination with rather coarse

three-compartment head volume conductor models distinguishing skin, skull, and brain compartments, where the homogenized "brain" compartment represents both gray and white matter as well as the highly conducting CSF through a single conductivity value. In contrast to BEM, finite volume methods (FVM) or finite element methods (FEM) rely on a volumetric discretization of the head volume conductor into small volumetric elements such as tetra- or hexahedrons. Both FVM and FEM can model complex geometries without a significant increase in computation time. To solve the EEG/MEG forward problem, FVM is based on a discretization of the electric current over element interfaces, whereas FEMs are usually based on a representation of the electric potential through basis functions defined on the volumetric elements.

Evaluation of Numerical Approaches to Solve the EEG Forward Problem

To compare the accuracy of different methods to solve the EEG/MEG forward problem, it is necessary to introduce suitable error measures. Commonly used error measures are the relative difference measure (RDM) and the magnitude error (MAG) (Meijs et al., 1989). The RDM quantifies the change in signal topography in comparison to a reference solution, which was shown to be linked to source localization accuracy, whereas the MAG measures the change in signal magnitude. RDM and MAG are defined as follows:

$$\begin{aligned} RDM(u^{test}, u^{ref}) &= \left\| \frac{u^{test}}{\|u^{test}\|_2} - \frac{u^{ref}}{\|u^{ref}\|_2} \right\|_2, \\ MAG(u^{test}, u^{ref}) &= \frac{\|u^{test}\|_2}{\|u^{ref}\|_2}, \end{aligned} \tag{1.11}$$

where u^{ref} corresponds to the vector of electrode potentials for a reference solution and u^{test} corresponds to the vector of electrode potentials for a method to be tested. The RDM is 0 for an exact solution and 2 for the maximal error, and the MAG is 1 for an exact solution and deviates towards 0 and $+\infty$ for a too small or too large signal magnitude, respectively. Besides the MAG sometimes also the lnMAG is applied, which is obtained by taking the logarithm of the MAG and thus is 0 for an exact solution. In some studies the RDM is indicated in %, which is achieved by normalizing the RDM to the interval from 0 to 1, i.e., dividing the RDM from (1.11) by 2 and multiplying it with 100.
As a first step to evaluate novel numerical methods, comparisons in sphere models are frequently chosen, where u^{ref} can be calculated analytically. Commonly, four-layer sphere models representing brain, CSF, skull, and skin are used and either triangular surface meshes of the tissue interfaces (BEM) or tetra- or hexahedral volume meshes (FEM) are generated. Dipole sources are placed at different radii - often also described by the eccentricities, which is the ratio between the radius at which the source is positioned and the radius of the innermost tissue interface - and usually both radial and tangential dipole orientations are studied. For practical applications, especially the numerical accuracy for

dipoles with a high eccentricity, i.e., very close to the brain/CSF interface, is of interest, since this scenario is also common in realistic head models.
To study the accuracy of numerical methods in realistically shaped head models, u^{ref} is usually computed using a head model with a very fine mesh resolution, whereas u^{test} is computed using a head model with a resolution that is commonly applied in practice. RDM and MAG are also used to study the influence of head model detail on the EEG/MEG forward solution. In this case, u^{ref} is calculated using a more detailed head model and u^{test} using a simplified head model, e.g., neglecting the distinction between two or more conductive compartments such as gray and white matter. To study the sensitivity of the EEG/MEG forward solution towards tissue conductivity variations, u^{ref} is calculated using standard values for the tissue conductivities, and u^{test} is computed using varying tissue conductivities.

Finite Element Methods to Solve the EEG/MEG Forward Problem

One focus of this thesis is novel FEMs to solve the EEG/MEG forward problem. FEMs are also used for essentially all bioelectromagnetic field simulations in this thesis, i.e., not only to solve the EEG/MEG forward problem but also to simulate electric brain stimulation. Therefore, we briefly present the basics of the most common FEM approach used to solve the EEG/MEG forward problem and simulate electric brain stimulation, the continuous Galerkin (CG) or Lagrange-FEM. For more details of the derivation and the definitions of the used function spaces, we refer the interested reader to a FEM textbook such as Braess (2007) or the PhD thesis **Vorwerk** (2016). The basics of the FEMs newly developed to solve the EEG/MEG forward problem within the scope of this thesis, such as discontinuous Galerkin (DG) and Mixed-FEM, are presented together with the summaries of the respective publications in Sec. 3.2.
The starting point to introduce the CG-FEM to solve the EEG/MEG forward problem is the weak formulation of (1.8). Using a linear test function space V the weak formulation reads:

$$\text{Find } u \in V \text{ such that } \int_\Omega \langle \sigma \nabla u, \nabla v \rangle \, \mathrm{d}x = \int_\Omega f v \, \mathrm{d}x \text{ for all } v \in V. \tag{1.12}$$

The weak formulation can be obtained by multiplying (1.8) with a test function v, integrating over the domain Ω, applying Gauss's theorem (multi-dimensional integration by parts), and exploiting the homogeneous Neumann boundary condition (1.8b). To show the existence and uniqueness of a solution using the *Lemma of Lax-Milgram*, V needs to be chosen to be a Hilbert space. For the CG-FEM, V is usually chosen to be $H^1(\Omega)$.

Introducing the notation

$$a(u,v) = (\sigma u, v)_{L^2(\Omega)^3} = \int_\Omega \langle \sigma \nabla u, \nabla v \rangle \, \mathrm{d}x \text{ for } u, v \in V, \tag{1.13a}$$

$$l(v) = (f, v)_{L^2(\Omega)} = \int_\Omega f v \, \mathrm{d}x \text{ for } v \in V \tag{1.13b}$$

(1.12) can be reformulated to

$$\text{Find } u \in V \text{ such that } a(u,v) = l(v) \text{ for all } v \in V. \tag{1.14}$$

To solve (1.14) using the Ritz-Galerkin method, we choose a finite-dimensional subspace $V_n \subset V$ (Braess, 2007). This subspace is defined based on a subdivision of the head domain Ω into small volume elements, usually tetrahedrons or hexahedrons. This subdivision should allow to represent the shape of the head volume conductor and the boundaries of the conductivity distribution σ as good as possible so that the number of elements is often in the range of a few million. Based on this subdivision, often called *mesh* or *grid*, a basis for the space V_n can be defined.
For the (first-order) CG-FEM, we choose $V_n = P_1(\mathcal{M})$, where $P_1(\mathcal{M})$ is the space of piecewise (tri-)linear functions implicitly defined on the mesh $\mathcal{M}(\Omega)$. A basis S_n of $P_1(\mathcal{M})$ can be defined by *hat functions*. A hat function $s_i \in S_n \subset P_1$ admits the value 1 on vertex $\mathbf{x}_i$, 0 on all other vertices, and the decay is (piecewise) linear and defined by $s_i(\mathbf{x}_k) = \delta_{i,k}$ for all $\mathbf{x}_k \in V(\mathcal{M})$ with $V(\mathcal{M})$ the set of vertices of $\mathcal{M}$.
If we replace $H^1(\Omega)$ by its approximation $V_n = \operatorname{span} S_n$, it is sufficient to use the elements of S_n as test functions as this is a linear space. We further replace u by its approximation $u_n \in V_n$ and find the discretized problem

$$\text{Find } u_n \in V_n, \text{ such that } \quad \int_\Omega \langle \sigma \nabla u_n, \nabla s_i \rangle \, \mathrm{d}x = \int_\Omega f s_i \, \mathrm{d}x \quad \text{for all } s_i \in S_n. \tag{1.15}$$

Based on the operators (1.13), we can now define

$$A_{ij} = a_n(s_i, s_j) \coloneqq \int_\Omega \langle \sigma \nabla s_i, \nabla s_j \rangle \, \mathrm{d}x \tag{1.16}$$

$$b_i \coloneqq l_h(s_i) = \int_\Omega f s_i \, \mathrm{d}x, \tag{1.17}$$

and obtain a discretized formulation of (1.14) that can be expressed as a linear equation system

$$Au = b. \tag{1.18}$$

For pure Neumann boundary conditions, A is only positive semidefinite so that (1.18) does not have a unique solution. This can, e.g., be fixed by specifying the potential u at a

single point. As the dimension of A equals the number of mesh vertices, i.e., potentially a few million, it is not efficient to solve (1.18) through matrix inversion. Instead, it is solved using iterative solvers such as preconditioned conjugate gradient solvers, e.g., using incomplete Cholesky preconditioning with zero fill-in (IC(0)) or algebraic multigrid (AMG) preconditioning (Lew et al., 2009; Wolters et al., 2002).
If $\mathbf{j}^p$ is chosen to be a current dipole, b_i in (1.17) cannot be integrated directly. Different approaches to circumvent this problem have been developed; a short overview of such methods and a summary of some novel developments is given in Sec. 3.1.

1.2.2 EEG/MEG Inverse Problem

The EEG/MEG inverse problem consists in determining the active brain areas underlying a measured signal. Whereas the existence and uniqueness of a solution for the EEG/MEG forward problem have been proven, the EEG/MEG inverse problem is non-unique (Sarvas, 1987). In consequence, prior assumptions regarding the brain activity underlying the measured signal have to be made to select one out of the infinitely many possible solutions. These (sometimes implicit) prior assumptions are reflected in the different classes of inverse approaches, such as equivalent current dipole (ECD) reconstruction (Fuchs et al., 1998; Mosher et al., 1992; Scherg and Von Cramon, 1985), current density reconstruction (CDR) (Hämäläinen and Ilmoniemi, 1994; Pascual-Marqui, 1999), and spatio-temporal filters, such as beamforming methods (Sekihara and Nagarajan, 2008). In all of these approaches, the brain activity is modeled through current dipoles as the smallest source unit for which the EEG/MEG signal is simulated by solving the EEG/MEG forward problem.
Under the prior assumption that the brain activity is confined to few, small brain regions, it can be explained by fitting a set of ECDs (Mosher et al., 1992; Scherg and Von Cramon, 1985). The number of dipoles has to be fixed in advance and following the locations, orientations, and/or magnitudes of these dipoles are optimized to explain the measured signal. Dipole fits perform well for a small number of sources and in simple geometries, such as sphere models, but they tend to become unstable for a larger number of dipoles and more complex geometries of the source region.
An alternative, more robust approach for the reconstruction of (single) dipole sources is the goal function scan (GFS) (Fuchs et al., 1998). Instead of performing a continuous optimization in the source volume, a discrete set of source locations (and possibly also orientations) that covers the source volume is selected. Now, the optimal source position within this discrete set can be easily determined without any risk of getting stuck in local optima. GFS works very well for scenarios that can be explained by a single source (Aydin, **Vorwerk**, et al., 2015, 2014; Rullmann et al., 2009; **Vorwerk** et al., 2019a), whereas it is seldomly applied in scenarios where multiple sources are active simultaneously due to the increasing complexity of the scanning procedure.

Both dipole fits and GFS share the same objective function, which is given by

$$f(\mathbf{x}_1, \mathbf{x}_2, \dots, \mathbf{p}_1, \mathbf{p}_2, \dots) = \|m - \sum_i L(\mathbf{x}_i)\mathbf{p_i}\|_2 \tag{1.19}$$

Here, m is the measurement result, $\|\cdot\|_2$ is the Euclidian norm, $L(\mathbf{x}_i) = L_i$ is the $\#sensors \times 3$ leadfield matrix for position $\mathbf{x}_i$, i.e., a matrix containing the forward simulation results for dipoles with unit moments oriented in each of the three cartesian directions at the source position, and $\mathbf{p}_i$ the dipole moment for position $\mathbf{x}_i$. Especially for EEG source analysis, the dipole moment is often directly estimated using the Moore-Penrose pseudoinverse L_i^+. For the one dipole case, (1.19) thus transforms to

$$\tilde{f}(\mathbf{x}) = \|m - L_i L_i^+ m\|_2. \tag{1.20}$$

For CDR methods, the prior assumption is that one or multiple significantly large brain areas are simultaneously activated so that the brain activity can no longer reasonably be approximated by a current dipole. Instead, CDR methods approximate this brain activity by a current distribution, which is modeled through a large number of current dipoles at fixed positions inside the source region. To achieve the uniqueness of the solution and to dampen the influence of measurement noise, regularization of the source activity in the CDR reconstruction is necessary. The choice of the regularization method has a strong influence on the reconstructed current density and defines the different CDR methods (Hämäläinen and Ilmoniemi, 1994; Pascual-Marqui, 1999).
As a variation of CDR methods, hierarchical Bayesian methods (HBM) have been introduced, which promise huge flexibility such that they allow for the reconstruction of both focal and distributed sources without a priori knowledge about the number of sources. Simulation studies comparing HBMs to classical CDR methods have obtained promising results (Calvetti et al., 2009; Lucka et al., 2012). Recently, also first results applying HBMs in practical scenarios were obtained (Costa et al., 2017; Rezaei et al., 2020). However, the flexibility of HBMs comes at the cost of a complex parametrization and an increased computational effort.
The third common group of methods for EEG/MEG source analysis are spatial or spatio-temporal filters, such as beamforming methods (Sekihara and Nagarajan, 2008). Spatial filter methods aim to construct a filter for each source position that can be applied to the sensor data and let activity from this source position pass while suppressing activity from all other source positions. This way, the time course of source activity for each position can be reconstructed. The construction of the filter weights requires a leadfield matrix, as it is also needed for CDR and GFS, and often additional inputs such as the sensor covariance matrix (Van Veen et al., 1997). Especially beamformer approaches are beneficial to resolve deeper sources and to suppress external noise. However, the accuracy of some beamformer

methods can be severely affected when correlated sources are present, as is for example the case for auditory evoked potentials (AEP).
As EEG/MEG source analysis is either applied to simulated dipole activity or to measurements of focal, single source brain activity (epileptic activity, somatosensory evoked potentials/SEPs) within the scope of this thesis, GFS was used as inverse approach in most of the included studies.

2 Scope of this Thesis

Despite the improvements achieved in the simulation of bioelectromagnetic fields and particularly in EEG/MEG source analysis through the introduction of numerical methods to solve the EEG/MEG forward problem using realistic head volume conductor models, a variety of challenges remain. Even state-of-the-art numerical methods can still have non-negligible numerical errors and the used head volume conductor models rely on certain simplifications. Understanding these numerical errors, the effects of head volume conductor model simplifications, and the sensitivity towards parameter uncertainties, such as inter-individual variations of tissue conductivities, is highly important for reliable EEG/MEG source analysis.
Accurate bioelectromagnetic field simulations are not only a necessity in EEG/MEG source analysis but also in the related field of electric brain stimulation. Thus, many results and methods can be translated between these two research areas, and this thesis includes some examples for applications in deep brain stimulation (DBS) research.
Finally, demonstrating the benefits of modern numerical methods and highly-detailed head volume conductor models for, e.g., EEG/MEG source analysis is of limited value if it is impossible for the majority of researchers to generate and apply such models. In this thesis, we present some efforts to make these methods easily accessible in practice.

Considering these challenges, this thesis covers the following topics:

Chapter 3 is dedicated to the derivation and evaluation of novel and existing FEMs to solve the EEG/MEG forward problem. Advanced approaches for dipole modeling in CG-FEM that allow for more reliable EEG/MEG forward simulations are presented and compared to established approaches, and novel, current-preserving FEMs that overcome some weaknesses of CG-FEM in certain scenarios are introduced.

Chapter 4 gives an overview of the influence of head volume conductor accuracy on EEG/MEG source analysis. In Sec. 4.1, the influence of differently detailed head volume conductor models on EEG/MEG source analysis is analyzed to understand which are the most important conductive tissues to be distinguished. In Sec. 4.2, the sensitivity of EEG

source analysis toward tissue conductivity uncertainties is investigated to understand which tissue conductivity uncertainties have the greatest impact on source analysis accuracy.

Chapter 5 is devoted to examples for and pathways to an application of FEMs and highly-realistic head volume conductor models for EEG/MEG source analysis in practice. Two studies in which state-of-the-art head volume conductor modeling is applied for combined EEG/MEG source analysis in PED are presented. In these studies, both the effects of combining EEG and MEG for source analysis and of highly detailed volume conductor modeling were evaluated. Furthermore, the implementation of a user-friendly pipeline to easily obtain FEM-calculated EEG forward solutions based on realistic head volume conductor models is presented.

Chapter 6 presents examples for applications of detailed head volume conductor modeling using FEM in the simulation and optimization of electric brain stimulation, particularly DBS. These efforts are not limited to the development and evaluation of novel algorithms to improve DBS outcomes, but also include approaches to make these methods easily accessible in (clinical) practice.

Each of these chapters is preceded by an introduction to the specific research topic, followed by summaries of those publications relevant for this thesis that are related to the respective research topic. The thesis is completed by a Discussion (Chapter 7) and Conclusion (Chapter 8).

3

Advanced Finite Element Methods to Solve the EEG/MEG Forward Problem

This chapter is devoted to studying FEMs for solving the EEG/MEG forward problem and the accuracy of different developed numerical approaches. Different sources of numerical errors influencing the numerical accuracy exist. These errors are mainly a result of the used numerical methods for solving the EEG/MEG forward problem and have to be distinguished from errors introduced due to simplifications or inaccuracies in defining the head volume conductor model, such as inaccurate conductivities or not distinguishing certain head tissues. The latter ones are in detail evaluated in Chapter 4.

One source of numerical error is the necessary discretization of the head volume conductor model into small volumes such as tetra- and hexahedrons and following solving (1.12) in a corresponding discrete subspace (1.15). This results in an approximation error, which depends amongst others on the mesh resolution and the order of the FE basis functions. This error can, e.g., be studied in convergence studies. In this thesis, we mostly refrain from studying this error in detail for the commonly used CG-FEM and use mesh resolutions that are as fine as possible but still allow reasonable computation times on standard hardware. Another source of numerical error specific to the EEG/MEG foward problem is the integration of the right-hand side (1.17) for the choice of $\mathbf{j}^p$ as a current dipole. Due to the resulting irregularity of the integrand $f = \nabla \cdot \mathbf{j}^p$, no direct integration is possible. Different ways to circumvent this problem have been proposed. Within this thesis, we focus on *direct approaches*, for which the dipole source is approximated by a distribution of electrical monopoles/current sinks and sources. The numerical accuracy of advanced direct approaches for the CG-FEM is studied in Sec. 3.1.

When studying CG-FEM to solve the EEG/MEG forward problem, it became apparent

that in some scenarios, especially in hexahedral meshes, the numerical accuracy collapsed and large numerical errors were observed (Sonntag, **Vorwerk**, et al., 2013). Further investigations found this to be caused by an effect later termed *skull leakage*, where an unphysical, large current flow between mesh elements of CSF and skin that only touch in a single point or edge occurs. This motivated the development of current-preserving FEMs to solve the EEG/MEG forward problem, which enforce physically plausible current flows and prevent leakage effects. In Sec. 3.2 two such current-preserving FEMs are presented, DG-FEM and Mixed-FEM.

3.1 Continuous Galerkin FEM

The first FEM approaches proposed for EEG/MEG forward simulations where *partial integration* and *St. Venant* approach (Buchner et al., 1997; Yan et al., 1991), which are both considered direct approaches. For the partial integration approach, Gauss's theorem, i.e., multi-dimensional partial integration, is applied to the right-hand side (1.17). Following, the integral can be evaluated easily due to the δ-function in $\mathbf{j}^p$. In result, the right-hand side b is non-zero only for basis functions s_i that are non-zero on the element that contains the dipole position. Heuristically, this approach blurs the dipole source into a distribution of current sinks and sources on the vertices belonging to the mesh element containing the source $\mathbf{j}^p$. For the St. Venant approach, the mesh vertex next to the source position is identified and all neighboring mesh vertices, i.e., sharing an edge, are identified. Following, a distribution of current sinks and sources placed at these vertex positions is determined that optimally matches the moments of the original dipole (Buchner et al., 1997; **Vorwerk**, 2016; **Vorwerk** et al., 2019c).

Partial integration and St. Venant approach were evaluated in several studies and achieved good accuracies both in tetrahedral and hexahedral sphere models (Köstler et al., 2007; Lew et al., 2009; **Vorwerk**, 2011). However, a dependency of the numerical accuracy on the local mesh structure was observed as well as a sudden increase of the numerical errors for the highest eccentricities (Lew et al., 2009; **Vorwerk**, 2011). In earlier studies also the high computational load was problematic, as the linear equation system (1.18) had to be solved once for each dipole. This problem was solved by the introduction of fast AMG-CG solvers (Wolters et al., 2002) and especially of transfer matrices (Weinstein et al., 2000; Wolters et al., 2004), which made it possible that the linear equation system had to be evaluated only once per measurement channel.

The FEM subtraction approach was introduced to improve the robustness and accuracy of EEG/MEG forward simulations. For the subtraction approach, the dipole potential is calculated using the analytical formula for a homogeneous volume conductor, and only a correction potential to account for the conductivity distribution is calculated using the CG-FEM (Drechsler et al., 2009; Wolters et al., 2008). This allows for a detailed

theoretical analysis, e.g., proving convergence estimates for the numerical solution. While the subtraction approach overcame the mesh dependency of the numerical accuracy, the accuracy was in the same range as that of the direct approaches and the computation times were clearly higher, making an application in practice infeasible. The high computation times could also only barely be reduced through the introduction of the analytical subtraction approach (Beltrachini, 2019).
The Whitney approach defines the source through vector-valued basis functions, which are then mapped to the FE space (Pursiainen, 2012; Pursiainen et al., 2011). This approach achieved good accuracies for a specific choice of dipole directions in sphere models, and the computational effort is comparable to St. Venant and partial integration approach. However, for random dipole directions, the St. Venant still showed a higher accuracy (Bauer et al., 2015).
These results motivated the further development of (direct) FEM approaches to solve the EEG/MEG forward problem to improve accuracy and particularly robustness for arbitrary dipole positions and orientations. Furthermore, most of the cited studies only performed evaluations in sphere models so that comparison studies in realistic head volume conductor models were necessary to understand which approaches offer the best accuracy in realistic scenarios.

Relevant Publications

J. Vorwerk, M. Clerc, M. Burger, and C. Wolters (2012). "Comparison of boundary element and finite element approaches to the EEG forward problem". In: *Biomedical Engineering/Biomedizinische Technik* 57.SI-1-Track-O, pp. 795–798

S. Pursiainen, **J. Vorwerk**, and C. H. Wolters (2016). "Electroencephalography (EEG) forward modeling via H (div) finite element sources with focal interpolation". In: *Physics in Medicine & Biology* 61.24, p. 8502

J. Vorwerk, A. Hanrath, C. H. Wolters, and L. Grasedyck (2019c). "The multipole approach for EEG forward modeling using the finite element method". In: *NeuroImage* 201, p. 116039

3.1.1 H(div) Approach

In the study Pursiainen, **Vorwerk**, et al. (2016), an expansion of the Whitney approach for EEG forward simulations (Pursiainen, 2012; Pursiainen et al., 2011) is presented and evaluated in combination with the optimization techniques introduced in Bauer et al. (2015), which are necessary to model arbitrary source directions. Whereas the Whitney approach relied on vector-valued first-order $H(\mathrm{div};\Omega)$ basis functions (Raviart-Thomas

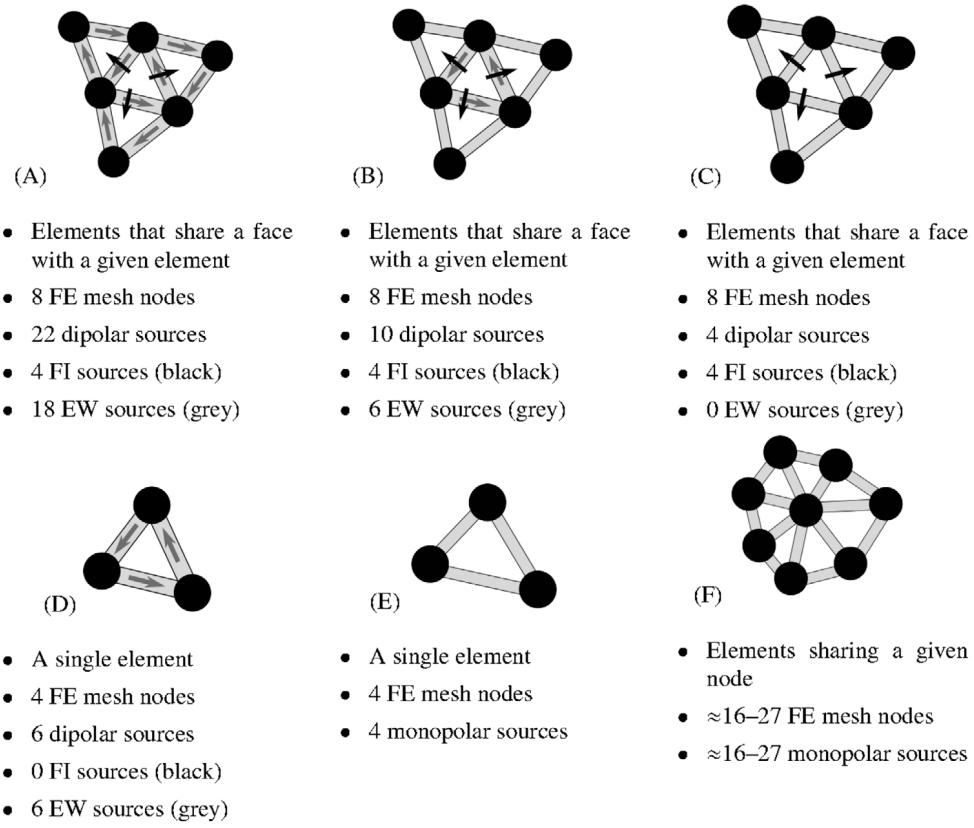

Figure 3.1: 2D illustrations of $H(\mathrm{div};\Omega)$ conforming sources involving first- and second-order basis functions (A, B), first-order basis functions (C), and second-order basis functions (D). As reference partial integration (E) and St. Venant approach (F) are depicted. Figure from Pursiainen, **Vorwerk**, et al. (2016).

elements) to model $\mathbf{j}^p$, Pursiainen, **Vorwerk**, et al. (2016) additionally considered second-order $H(\mathrm{div};\Omega)$ basis functions. Whereas the first-order - or linear - basis functions can be identified with element faces, as they are supported on two elements sharing a face, the second-order - or quadratic - basis functions can be identified with element edges. To model dipolar sources with arbitrary orientations, it is necessary to (linearly) combine several of these basis functions. Bauer et al. (2015) proposed two approaches to calculate the weights for such a combination, the position-based optimization (PBO) and the mean position/orientation (MPO) methods. These two methods were expanded to different combinations of first- and second-order $H(\mathrm{div};\Omega)$ basis functions in Pursiainen, **Vorwerk**, et al. (2016).

Fig. 3.1 illustrates different explored combinations of first- and second-order $H(\mathrm{div};\Omega)$ basis functions for a tetrahedral mesh. These differ with regard to the number of degrees of

Table 3.1: Shell radii and tissue conductivities for four-layer sphere model

Compartment	Skin	Skull	CSF	Brain
Outer shell radius (mm)	92	86	80	78
Tissue conductivity (S/m)	0.33	0.0042/0.01	1.79	0.33

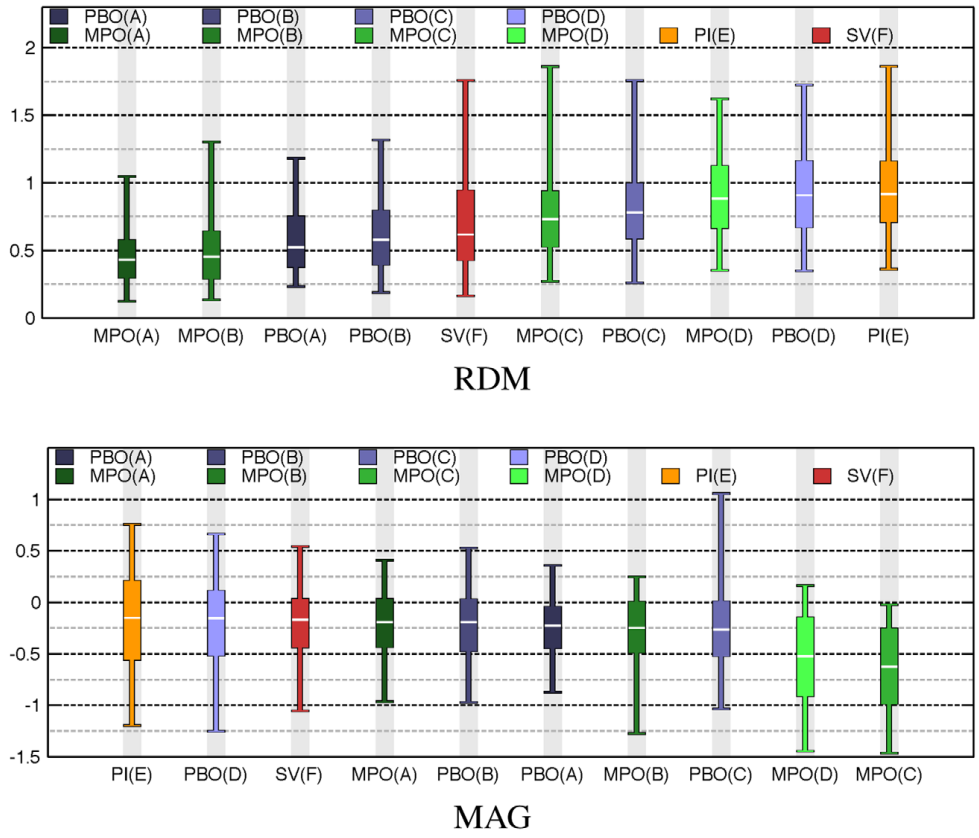

Figure 3.2: RDM (in %, i.e., 0% is best and 100% is worst) and MAG for optimized approximation of 200 dipole sources randomly placed at an eccentricity of 99%. The optimization schemes are ranked in ascending order from best (left) to worst (right) based on the absolute value of the median. Figure from Pursiainen, **Vorwerk**, et al. (2016).

freedom for the approximation of the source orientation and their focality, i.e., the number of mesh nodes/FE basis functions in the approximation of the source. The number of FE basis functions corresponds to the number of non-zero entries for the right-hand side (1.17) and is either 8 (A-C) or 4 (D). For comparison, also partial integration and St. Venant approaches are listed, for which the number is either 4 (E, partial integration) or about 16 to 27 (F, St. Venant). For the St. Venant approach, this number is mesh dependent and can vary for every node in a tetrahedral mesh.

The numerical accuracy of the four different combinations of $H(\mathrm{div};\Omega)$ basis functions combined with the two different optimization schemes was compared to that of partial integration and St. Venant approach in a four-layer sphere model with a skull conductivity of 0.0042 S/m. All shell radii and tissue conductivities of the sphere model are given in Table 3.1.

The numerical evaluations in Pursiainen, **Vorwerk**, et al. (2016) showed very good accuracies of the $H(\mathrm{div};\Omega)$ approach when a dipole source could be represented by exactly one first- or second-order basis function. To easily allow for arbitrary source orientations, it is necessary to combine multiple basis functions using the optimization schemes MPO

or PBO. The resulting numerical accuracies for sources at an eccentricity of 99% are evaluated in Fig. 3.2. For the RDM, which is considered the most important error measure for EEG/MEG source analysis accuracy, for all approaches the maximal errors were below 2% RDM. For both optimization schemes source configuration A leads to the best RDM results with regard to the median and maximal error. Furthermore, the RDM median for the MPO optimization scheme was found to be significantly smaller than that of the PBO interpolation scheme. Overall, source configurations A and B were found to result in significantly more accurate results than the other source configurations and mostly also than partial integration and St. Venant approaches. For the MAG, most differences were found to be insignificant; only MPO in combination with source configurations C and D led to significantly worse accuracies.
Based on the numerical results, it would be desirable to obtain forward solutions based on non-interpolated first- or second-order $H(\mathrm{div};\Omega)$ basis functions. These approaches not only lead to highly accurate forward simulations but are also based on a very focal support, which is advantageous for the placement of sources within the gray matter. Unfortunately, an application of these approaches in practice would require specifically constructed FE meshes to allow for the desired source orientations and the generation of such meshes would add a significant additional effort.
For arbitrary source orientations, source configuration A in combination with the optimization scheme MPO led to the best numerical accuracies. However, the numerical accuracy was not found to be significantly better than that of the established St. Venant approach, and source configuration A was amongst the least focal of the tested source configurations, potentially only slightly more focal than the St. Venant approach.
EEG forward modeling based on first- and second-order $H(\mathrm{div};\Omega)$ basis functions was further evaluated, especially also in realistic head models, by Miinalainen et al. (2019), and implementations in the open-source toolboxes DUNEuro (Schrader et al., 2021) and Zeffiro (He et al., 2020) were presented, allowing for an easy application in practice.

3.1.2 Multipole Approach

The multipole approach was introduced in **Vorwerk** et al. (2019c) to further improve the numerical accuracy and stability of the St. Venant approach while retaining a similar numerical efficiency. This is achieved by correcting an inconsistency in the original definition of the St. Venant approach.
The fundamental idea of the St. Venant approach is to approximate a dipole source through a distribution of current sinks and sources that matches the "moments" of the dipole source. The sinks and sources are distributed on the mesh nodes connected to the mesh node closest to the source position via mesh edges. In the original formulation of the St. Venant approach, the moments are defined as the net sum of the currents (zeroth order), the

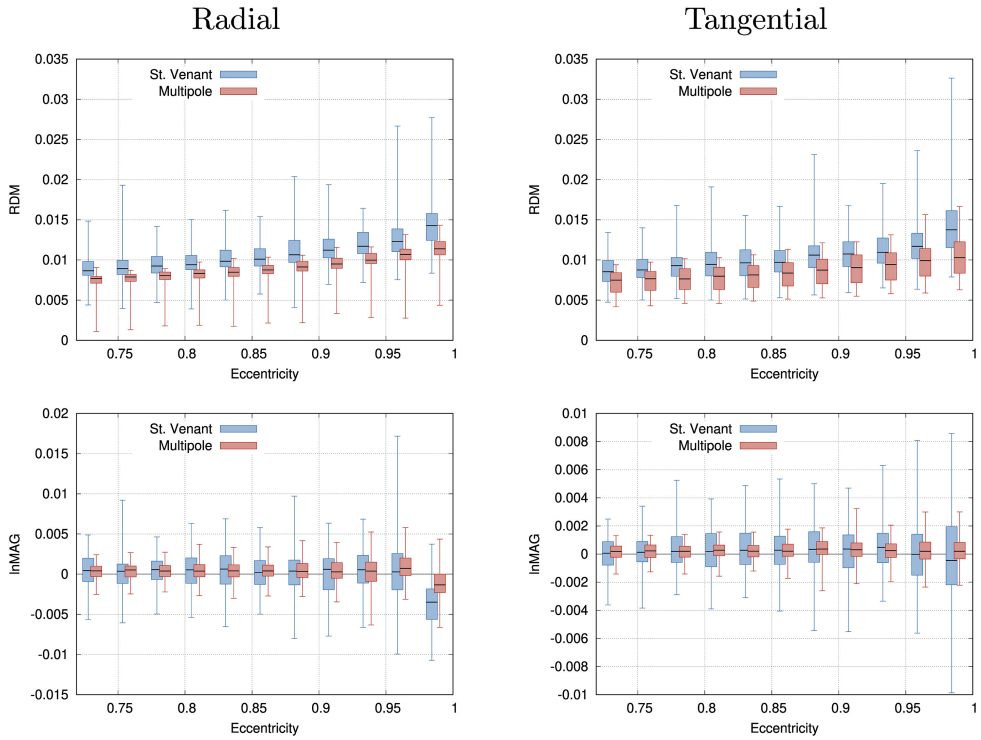

Figure 3.3: RDM (top row) and lnMAG (bottom row) for radial (left column) and tangential (right column) source orientations for four-layer tetrahedral sphere model. For better readability, the boxes for St. Venant and multipole approach at the same eccentricity are slightly shifted toward a lower and higher eccentricity, respectively. Figure from **Vorwerk** et al. (2019c).

dipole moment (first order), and higher order moments, which were defined similar to the dipole moment but with an increased exponent (Buchner et al., 1997). The strength of sinks and sources was then determined to match the dipole moment, while all other moments should be zero. To account for a possible over- or underdetermination of the resulting equation system, an additional regularization was introduced. This approach was shown to lead to good numerical accuracies both in tetrahedral and hexahedral meshes while demonstrating a high computational efficiency in various studies (Köstler et al., 2007; Lew et al., 2009; Pursiainen, **Vorwerk**, et al., 2016; **Vorwerk**, 2011) and was applied in several experimental studies (Antonakakis et al., 2020; Aydin, **Vorwerk**, et al., 2015, 2014; Gao et al., 2019).

However, evaluation studies showed that the accuracy of the St. Venant approach did not smoothly vary with the source eccentricity (Köstler et al., 2007; Lew et al., 2009). **Vorwerk** (2011) showed that the accuracy was to a certain degree depending on the local position of the dipole source within the mesh and the best accuracy was found if the source was positioned directly on a mesh node.

Vorwerk et al. (2019c) suggest that this behavior is due to a not optimal definition of the higher-order moments in the St. Venant approach and propose to instead use the moments that are derived from the multipole expansion (Jackson, 2021). Taking into account

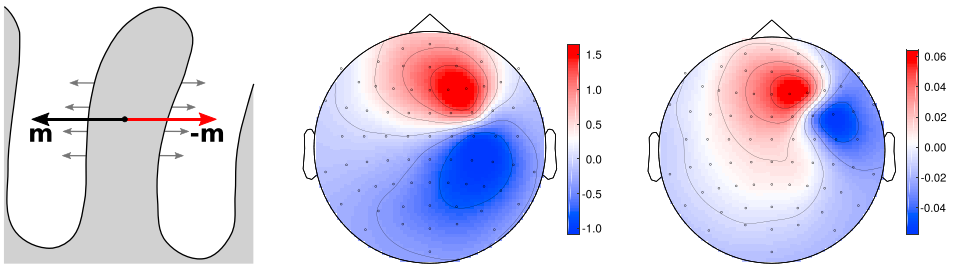

a) Quadrupolar Source b) Dipole topography c) Quadrupole topography

Figure 3.4: Schematic illustration of a scenario that creates a quadrupolar source consisting of two dipoles with opposite dipole moments (a) distributed neural activity on both sides of the gyrus (gray arrows) leads to overall dipole moments $\mathbf{m}$ and $-\mathbf{m}$ (black and red arrows), so that the net dipole moment is zero, but a quadrupole moment $\mathbf{Q}$ remains. Topoplot of dipolar (b) and quadrupolar (c) source in the somatosensory cortex, simulated in a realistic head model for 10-10 EEG cap. Please observe the difference in color bar range in Subfigures b and c. Figure from **Vorwerk** et al. (2019c).

the quadrupole moment in the calculation of the strength of sinks and sources requires additionally optimizing for three "mixed terms" that are neglected in the St. Venant approach.

The accuracy of multipole and St. Venant approaches were compared in tetrahedral and hexahedral four-layer sphere models with a skull conductivity of 0.01 S/m (Table 3.1) and in a realistic head model. Fig. 3.3 shows the results for the tetrahedral sphere model. At all eccentricities, the numerical errors both measured with RDM and lnMAG are clearly lower for the multipole approach than for the St. Venant approach. Also, the mesh dependency is clearly reduced for the multipole approach. These results were also confirmed in a realistic tetrahedral head model in **Vorwerk** et al. (2019c), whereas the improvement in a hexahedral model was less pronounced.

As a side effect, the multipole approach does not only allow for the modeling of dipolar sources but also of higher-order source configurations such as quadrupoles (Fig. 3.4). The additional consideration of quadrupolar sources was shown to be beneficial in some scenarios, e.g., for MEG and iEEG (Jerbi et al., 2004; Riera et al., 2012). The multipole approach can be easily implemented based on the St. Venant approach, as it was done for FieldTrip-SimBio and DUNEuro (Schrader et al., 2021; **Vorwerk** et al., 2018), allowing for a direct application in practice.

3.1.3 Comparison of FEM and BEM in Realistic Head Models

Adequately representing the folded structure of the cortical surfaces requires a high surface mesh resolution. Including such a surface in the head volume conductor model severely increases the computational load for most BEMs, making the use of head volume conductor models that distinguish CSF, gray, and white matter not feasible in practice. Thus, BEM

is mostly used in combination with three-layered head volume conductor models (skin, skull, homogenized brain). In contrast, the computational load for FEM is only barely affected by complex geometries so that head volume conductor models resolving at least five-compartments including white matter, gray matter, and CSF can easily be applied. Therefore, the goal of **Vorwerk** et al. (2012) was to not only perform a comparison of the numerical accuracy of BEM and FEM approaches to solve the EEG forward problem, but to also set the observed numerical errors in relation to the errors introduced by model simplifications - in this case neglecting the CSF compartment.
As numerical methods **Vorwerk** et al. (2012) considered St. Venant, partial integration, and subtraction FEM as well as the double-layer and symmetric BEM, respectively (Hamalainen and Sarvas, 1989; Kybic et al., 2005). Unbiased comparisons between FEM and BEM are in general hard to achieve due to the very different distribution of the computational effort. Whereas for the FEM the set-up of the matrices and right-hand side vectors is generally rather cheap (especially for St. Venant and partial integration approach) and the main computational effort lies in repeatedly solving the linear equation system (1.18), the set-up of the matrices and right-hand side vectors is the most costly part for BEM. Of course, the computational effort is also directly influenced by the resolution of the used volumetric or surface meshes, respectively. To achieve a somewhat unbiased comparison, **Vorwerk** et al. (2012) chose to adjust the resolution of the used volumetric and surface meshes so that the computation times for an EEG leadfield were about the same for all tested approaches.
As a result, **Vorwerk** et al. (2012) found that the symmetric BEM led to the smallest numerical errors in a three-layer sphere and a three-layer realistic head model. Similarly small numerical errors were found for St. Venant and subtraction FEM and the highest numerical errors were found for partial integration FEM and double-layer BEM. However, the errors introduced by not considering a CSF compartment were by far larger than all numerical errors both in the spherical and realistic head models.
These results demonstrate the importance of enabling the use of more detailed head volume conductor models in practice to improve the accuracy of EEG/MEG source analysis. Furthermore, it is important to understand the effects that model simplifications might have on the results of EEG/MEG source analysis. In this regard, several studies investigating the influence of head model inaccuracies and simplifications on EEG/MEG source analysis are summarized in Chapter 4, and some applications of highly realistic head volume conductor models in practice are demonstrated in Chapter 5.

3.2 Current-Preserving FEM

While significant effort was put into improving and evaluating the accuracy of FEM approaches such as St. Venant, partial integration, or subtraction in sphere and realistic,

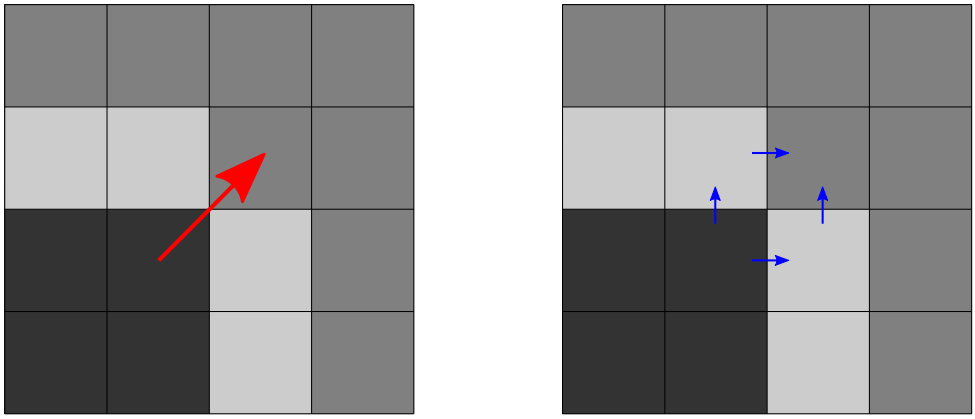

Figure 3.5: CG-FEM simulations lead to an overestimated electric current at degenerated vertices of the skull (light gray voxels). This effect is due to the vertex-based discretization, which considers only the potential, but not the electric current. DG-FEM and Mixed-FEM enforce a physically plausible current through cell faces. Therefore, these methods do not overestimate the electric current, even in the presence of segmentation artifacts. Figure adapted from Engwer*, **Vorwerk***, et al. (2017).

tetrahedral and hexahedral head models, little to no efforts were made to change the underlying FEM approach based on piecewise linear basis functions (CG-FEM/Lagrange-FEM) as introduced in Sec. 1.2.1. This changed when Sonntag, **Vorwerk**, et al. (2013) discovered a sudden increase of numerical errors in hexahedral models that did not follow the expected continuous increase of numerical errors usually observed in convergence studies.

As the reason for this effect, an unphysically large current flow through the skull was identified. This effect occurs when the thickness of the skull compartment is in the range of the mesh resolution. As a result, the higher conducting skin and CSF compartments "touch" in single mesh nodes, enabling an unphysical "leakage" of current through this single node, bypassing the lower conducting skull compartment (Fig. 3.5, left). This is possible since the CG-FEM neither enforces a physically plausible flow of the electric currents nor guarantees the conservation of charge.

In the following, two approaches are presented that resolve the problem of skull leakage, the Mixed-FEM and the DG-FEM. Both methods enforce physically plausible electric currents and guarantee the conservation of charge (Fig. 3.5, right). However, the approaches to achieving this goal are clearly different.

Relevant Publications

J. Vorwerk, C. Engwer, S. Pursiainen, and C. H. Wolters (2016). "A mixed finite element method to solve the EEG forward problem". In: *IEEE Transactions on Medical Imaging* 36.4, pp. 930–941

C. Engwer*, **J. Vorwerk***, J. Ludewig, and C. H. Wolters (2017). "A discontinuous Galerkin method to solve the EEG forward problem using the subtraction approach". In: *SIAM Journal on Scientific Computing* 39.1, B138–B164. **The first two authors contributed equally to this work.*

3.2.1 Mixed Finite Element Method

The starting point for the Mixed-FEM is the system of two coupled first-order PDEs (1.7). Instead of eliminating the current $\mathbf{j}$ to obtain the second-order PDE (1.8), as it is done to derive the CG-FEM, the current is kept as an additional, explicitly modeled variable in the Mixed-FEM and the equation system (1.7) is discretized. This requires two sets of basis functions: scalar ones to approximate the scalar potential u and test the second, scalar equation and vector ones to approximate the vector-valued current $\mathbf{j}$ and test the first, vector-valued equation. The correct choice of scalar- and vector-valued basis functions is crucial not only to achieve the desired properties, such as conservation of charge, but also to ensure the existence and uniqueness of a solution. In **Vorwerk** et al. (2016), the scalar space $L^2(\Omega)$ was approximated by piecewise constant functions P_0, and the vector-valued space $H(\mathrm{div};\Omega)$ was approximated by lowest-order Raviart-Thomas elements RT_0.
The Mixed-FEM results in an equation system with saddle point structure so that it cannot efficiently be solved using iterative solvers commonly used for CG-FEM, such as AMG-CG. An efficient solver based on the conjugated Uzawa iteration was derived and evaluated in **Vorwerk** et al. (2016). As no derivative is applied to the source $\mathbf{j}^p$ in (1.7), unlike for the CG-FEM no special treatment of $\mathbf{j}^p$ is necessary here, since $\mathbf{j}^p$ can be integrated directly. However, two options to introduce the source exist, as it can either be modeled as a current source, referred to as direct approach, or as a voltage source, referred to as projected approach. Furthermore, interpolation is necessary to model arbitrary dipole orientations with the Mixed-FEM, similar to the CG-FEM approaches based on $H(\mathrm{div};\Omega)$ basis functions (Sec. 3.1.1).
The Mixed-FEM was implemented for regular hexahedral meshes in **Vorwerk** et al. (2016). For the evaluation on the one hand regular hexahedral meshes of common sphere models (Table 3.1) with different mesh resolutions (1 mm, 2 mm, 4 mm) and different resolutions of the underlying segmentation (1 mm, 2 mm, 4 mm) and sphere models with a reduced thickness of the skull compartment (between 2 mm and 4 mm) were used. The models with the reduced skull thickness were especially generated to demonstrate leakage effects

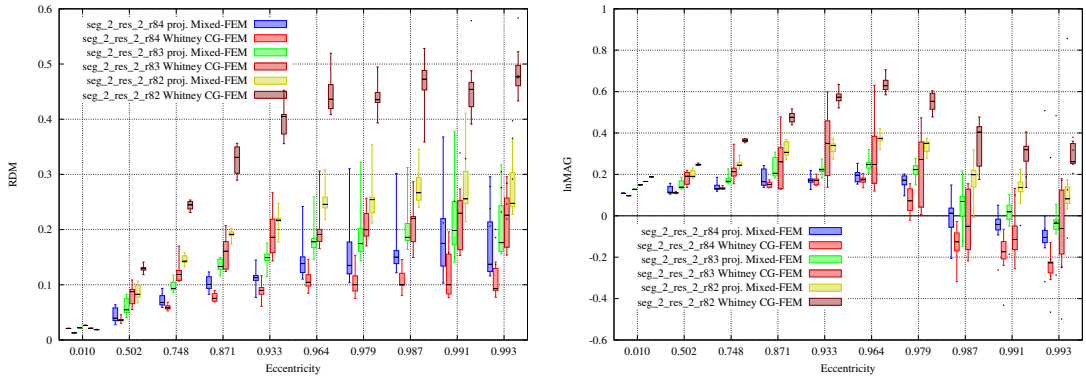

Figure 3.6: Comparison of projected Mixed-FEM and Whitney CG-FEM in meshes with a thin skull compartment. Results for random dipole positions. Visualized are boxplots of RDM (left) and lnMAG (right). Dipole positions falling outside the brain compartment in the discretized models are marked as dots. Note the logarithmic scaling of the x-axes. Figure from **Vorwerk** et al. (2016).

and to evaluate whether the Mixed-FEM could prevent these. Furthermore, an evaluation in a realistic head model was performed. As a comparison, the Whitney CG-FEM was used.

Due to the use of regular hexahedral meshes and the resulting worse approximation of the underlying geometry, the observed numerical errors were in general increased compared to other studies evaluating approaches for EEG/MEG forward modeling. In the common sphere models, projected Mixed-FEM and Whitney CG-FEM obtained comparable accuracies, whereas the direct Mixed-FEM led to less accurate results especially for coarser meshes. For the meshes with a reduced skull thickness (Fig. 3.6), the projected Mixed-FEM achieved better numerical accuracies than the Whitney CG-FEM, demonstrating the effective prevention of skull leakages through the Mixed-FEM. The unphysical current flow for the CG-FEM and the improved current flow for the Mixed-FEM are also visualized in Fig. 3.7. Also, the comparison in a 2 mm hexahedral realistic head model showed the highest numerical accuracies for the Mixed-FEM.

The numerical results presented for the Mixed-FEM in **Vorwerk** et al. (2016) are promising, and the computational efficiency is in principle sufficient for an application in practice. However, the original implementation in DUNEuro only allowed the use of regular hexahedral meshes, which led to a reduced numerical accuracy compared to tetrahedral or geometry-adapted hexahedral meshes due to the worse approximation of the underlying geometry. Therefore, the implementation and evaluation of the Mixed-FEM for geometry-adapted hexahedral and/or tetrahedral meshes is necessary before an application in practice can be considered. First steps in this direction were taken in Stubbemann (2021). Furthermore, Stubbemann (2021) derived and implemented the transfer matrix approach for the Mixed-FEM, which is essential to achieve computation times that are feasible in practice.

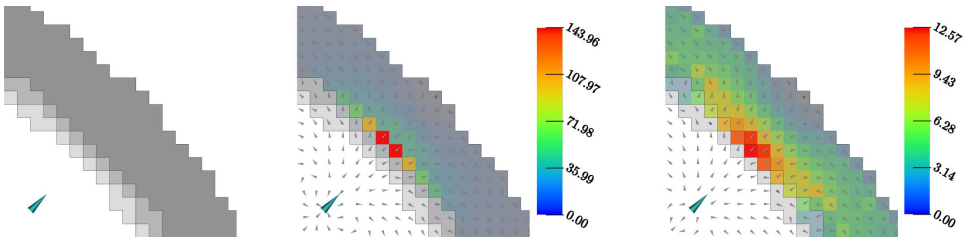

Figure 3.7: Geometry of leaky four-layer sphere model (left, compartments from in- to outside/bottom left to top right are brain, CSF, skull, skin, and air) and visualization of strength (only skull and skin, in $\mu A/mm^2$) and direction of volume currents for CG-FEM (middle) and Mixed-FEM simulation (right). Figure from **Vorwerk** et al. (2016).

3.2.2 Discontinuous Galerkin Finite Element Method

Like the CG-FEM, the DG-FEM solves the EEG/MEG forward problem based on the second-order PDE (1.8). In consequence, also for the DG-FEM it is necessary to deal with the problem of the singularity in the source term $\mathbf{j}^p$, and approaches similar to the CG-FEM, such as partial integration or subtraction, can be applied. However, as the name suggests, the DG-FEM does not enforce a continuous solution of the electric potential u, as is the case for the CG-FEM, but allows for discontinuities across (mesh) element boundaries. The basis functions used for the DG-FEM are only supported on a single mesh element, e.g., in Engwer*, **Vorwerk***, et al. (2017) orthonormal linear functions that are non-zero on a single mesh element and zero everywhere else were used. Locally, i.e., viewed on a single mesh element, this basis is equivalent to the basis for a linear CG-FEM. The potential discontinuity across element boundaries requires the addition of "internal skeleton" terms when deriving the weak formulation of (1.8) for the DG-FEM. These skeleton terms establish the coupling between basis functions on different elements and are linked to the current flow across element boundaries. Thereby, the across-element coupling in DG-FEM has certain similarities to FVM. To further control the discontinuity of the electric potential, a penalty term integrating the jumps of the electric potential across element boundaries is introduced. An increased weighting of this penalty term reduces the extent of jumps of the potential at element boundaries, leading to a "more continuous" solution of the electric potential at the cost of a worse conservation of charge. In the limit case, i.e., an increasingly strong weighting of the penalty term, the DG-FEM solution converges to the CG-FEM solution.
A DG-FEM formulation of the subtraction approach was derived in Engwer*, **Vorwerk***, et al. (2017) and the existence and uniqueness of a solution as well as conservation of charge were shown. As for the evaluation of the Mixed-FEM, the numerical accuracy of CG-FEM and DG-FEM was compared in common hexahedral sphere models with different mesh resolutions, in sphere models with a reduced skull thickness, and a realistic hexahedral head volume conductor model.

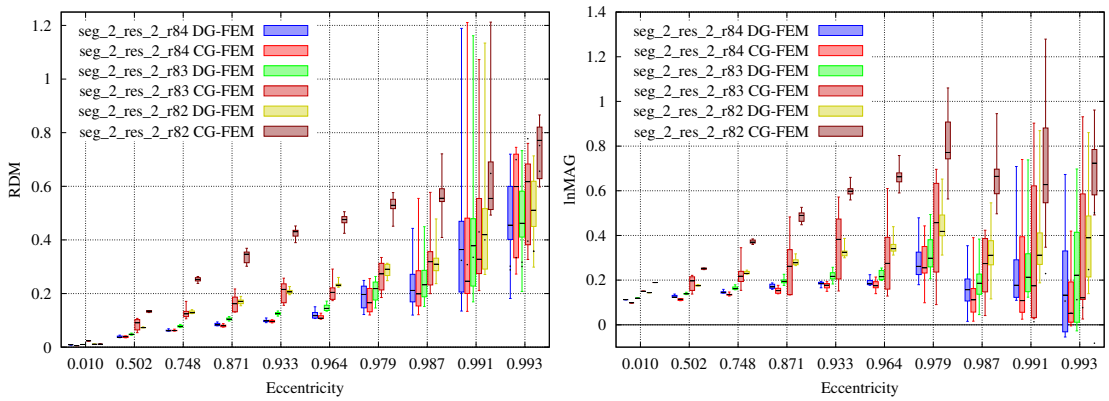

Figure 3.8: Comparison of increase of errors for decreasing skull thickness between the CG-FEM and DG-FEM for radial dipoles. Visualized are boxplots of the RDM (left) and lnMAG (right). Dipole positions that are outside the brain compartment in the discretized models are marked as dots. Note the different scaling of the x-axes. Figure adapted from Engwer*, **Vorwerk***, et al. (2017).

For common sphere models, no significant differences in numerical accuracy between CG- and DG-FEM subtraction approaches were observed. However, in the sphere models with a reduced skull thickness, the DG-FEM achieves a better numerical accuracy especially for radial dipole orientations demonstrating that also the DG-FEM subtraction approach effectively suppresses skull leakage effects. Also in the realistic head model, the DG-FEM results in a better numerical accuracy than the CG-FEM.
The subtraction DG-FEM is implemented and freely available in the open-source toolbox DUNEuro (Schrader et al., 2021). DUNEuro also provides further source models for DG-FEM, such as the partial integration and St. Venant approach, which are computationally more efficient than the subtraction approach (Nüßing, 2018).

4

Realistic Head Modeling in EEG/MEG Source Analysis

As demonstrated exemplarily by **Vorwerk** et al. (2012) (Sec. 3.1.3), not only the accuracy of the numerical methods but also the level of detail and the correct parametrization of the head volume conductor model have an important influence on EEG/MEG forward solutions. In this chapter, several studies are presented that evaluate the effects of head volume conductor simplifications and tissue conductivity uncertainties on EEG/MEG forward and inverse solutions.

4.1 Influence of Head Modeling Detail on EEG/MEG Source Analysis

Starting from three-layer realistically shaped head models (skin, skull, homogenized brain) as commonly used with BEM (Fuchs et al., 2001; Geselowitz, 1967) the progress of numerical methods, computing power, and especially also of structural brain imaging and automated segmentation methods made it possible to add more and more detail to head volume conductor models. This increased level of model detail allowed to overcome the homogenized compartment inside the inner skull surface and distinguish the highly-conducting CSF as well as gray and white matter (Lanfer et al., 2012; Ramon et al., 2004; Wendel et al., 2008). Diffusion spectrum imaging (DSI) even allows to investigate the effects of the anisotropic structure of the white matter on EEG/MEG source analysis and can be modeled with FEM (Güllmar et al., 2010). Modeling the skull as a closed shell of isotropic conductivity enveloping the brain and the CSF disregards the influence of the layered structure of the skull (Akhtari et al., 2002; Dannhauer et al., 2011) and the importance of modeling skull holes and inhomogeneity accurately (Lanfer et al., 2012; Montes-Restrepo et al., 2014; Ollikainen et al., 1999; Pohlmeier et al., 1997). As many of these modeling steps make the head model generation more complex and potentially increase the computational complexity, it is of interest to study how large the influence

of each of these modeling steps is in comparison to the others. Thereby it is possible to optimize the head model detail for each study depending, e.g., on the necessary source analysis accuracy and the available resources for head model generation.

Relevant Publications

J. Vorwerk, J.-H. Cho, S. Rampp, H. Hamer, T. R. Knösche, and C. H. Wolters (2014). "A guideline for head volume conductor modeling in EEG and MEG". in: *NeuroImage* 100, pp. 590–607

J.-H. Cho, **J. Vorwerk**, C. H. Wolters, and T. R. Knösche (2015). "Influence of the head model on EEG and MEG source connectivity analyses". In: *NeuroImage* 110, pp. 60–77

L. D. J. Fiederer, **J. Vorwerk**, F. Lucka, M. Dannhauer, S. Yang, M. Dümpelmann, A. Schulze-Bonhage, A. Aertsen, O. Speck, C. H. Wolters, and T. Ball (2016). "The role of blood vessels in high-resolution volume conductor head modeling of EEG". in: *NeuroImage* 128, pp. 193–208

4.1.1 A Guideline for EEG/MEG Head Volume Conductor Modeling

In the two studies **Vorwerk** et al. (2014) and Cho, **Vorwerk**, et al. (2015), the effects of a reduction of model detail were investigated for EEG and MEG forward and inverse analysis, respectively, based on a highly realistic six-compartment (white matter, gray matter, CSF, skull compacta, skull spongiosa, skin) head model including white matter conductivity anisotropy.

EEG/MEG Forward Modeling

To evaluate the effects on forward modeling, **Vorwerk** et al. (2014) took a three-compartment head model (homogenized brain, skull, skin) as starting point and step-by-step added another level of detail in the order CSF, gray/white matter distinction, skull compacta/spongiosa distinction, and anisotropic white matter conductivity. Additionally, a head model considering all model details but with an especially high mesh resolution was created to evaluate the numerical errors. Source positions were distributed uniformly on the cortex surface and EEG/MEG forward simulations were performed for all differently detailed head models. Following, the difference in signal topography (RDM) and signal magnitude (lnMAG) of the EEG/MEG forward solutions between two modeling steps was calculated for each source position and visualized on an inflated cortex surface. This surface visualization allows to determine which source positions are especially (or less affected) by a certain modeling step so that researchers can determine what level of detail might be necessary to accurately localize the sources expected in their study.

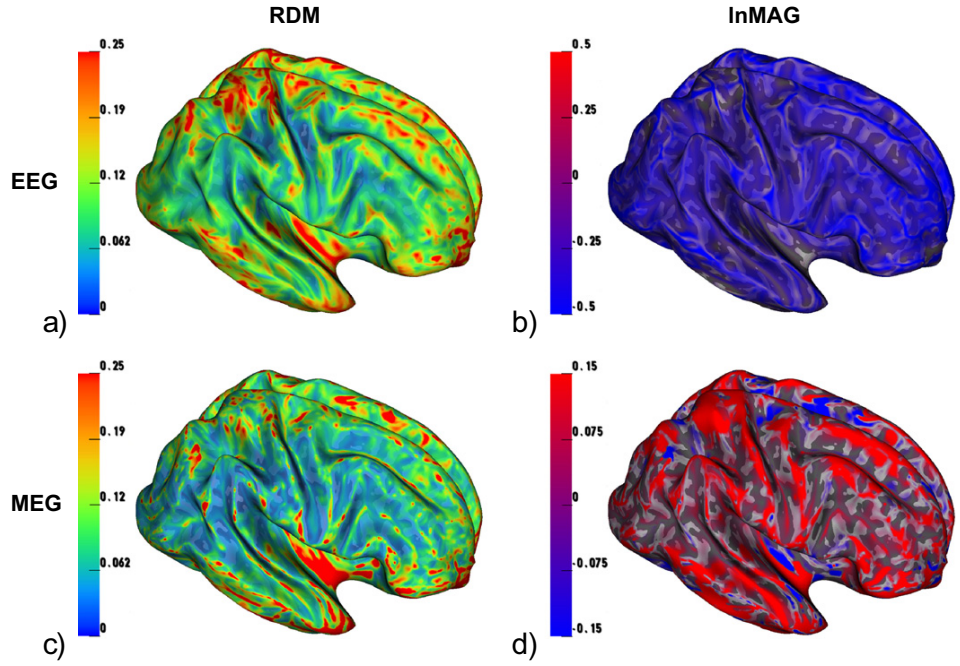

Figure 4.1: Effect of CSF distinction on EEG/MEG forward solution. Difference between three-compartment and four-compartment head models plotted on the brain surface. Figure from **Vorwerk** et al. (2014).

Vorwerk et al. (2014) found the strongest effect on both EEG and MEG forward solutions for the distinction of the CSF compartment and the distinction between gray and white matter. For both modalities, the highest influence on both signal topography and magnitude of not distinguishing the CSF compartment was found for sources on top of gyral crowns and especially for sources at the top of the brain (Fig. 4.1). Most of these sources are assumed to have a quasi-radial orientation. Furthermore, a strong influence was found for sources in the insula. Also for the distinction between gray and white matter, the strongest influence on the signal topography was found for sources on top of gyral crowns, whereas the strongest influence on the signal magnitude was found for sources inside of sulci in this case. For the distinction of tissue conductivity anisotropy, the influence on signal topography and magnitude showed a less clear pattern, but a tendency towards a higher influence for deeper sources could be observed.
Neglecting the distinction between skull spongiosa and compacta only showed a negligible effect for large parts of the brain (Fig. 4.2) and in general for the MEG. Only for sources in regions for which the covering skull mostly consists of compact bone, such as the temporal lobe, a notable effect was found. However, this observed influence on signal topography and magnitude is still weaker than for the other considered modeling steps. Overall, this justifies the use of a homogenized skull compartment for most scenarios when the conductivity for the homogenized skull is chosen adequately (Dannhauer et al., 2011).

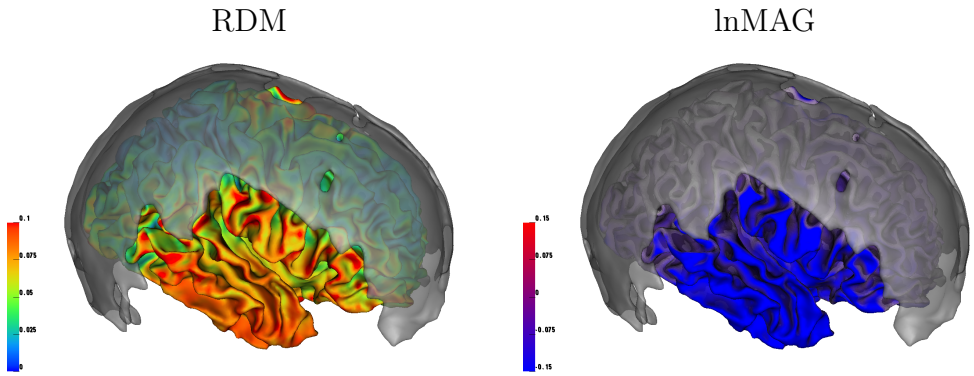

Figure 4.2: Effect of skull compacta/spongiosa distinction on EEG/MEG forward solution. Difference between five-compartment and six-compartment isotropic head models plotted on the brain surface.

EEG/MEG Source Reconstruction and Connectivity Analysis

The study by Cho, **Vorwerk**, et al. (2015) largely built upon **Vorwerk** et al. (2014) and expanded the evaluations to EEG/MEG source reconstruction and connectivity analysis. It is important to set the results of forward simulation studies such as **Vorwerk** et al. (2014) in relation to the effects observed in source and connectivity analysis, as it is not immediately clear if and how much the changes or errors in the forward simulations correlate to changes in source reconstruction and connectivity analysis. Such comparisons thus allow to demonstrate the benefit of forward simulation studies, which are often easier to perform than extensive source or connectivity analysis studies.

The head volume conductor model used in Cho, **Vorwerk**, et al. (2015) was identical to the one used in **Vorwerk** et al. (2014), but instead of increasing the model detail step-by-step the starting point was always the six-compartment head model, which was then simplified by neglecting a single refinement step such as gray/white matter distinction or CSF distinction. Furthermore, a three-compartment head model was investigated. As inverse approach, a linearly-constrained minimum variance (LCMV) beamformer was used (Van Veen et al., 1997). The change in output SNR in a two-source scenario was analyzed to investigate the influence of the model simplifications on beamformer source reconstruction. Furthermore, the influence on connectivity analysis using imaginary coherence (ICoh) and generalized partial directed coherence (GPDC) was evaluated (Baccala et al., 2007; Nolte et al., 2004).

As for the EEG/MEG forward simulations, also for the source reconstruction and connectivity analysis neglecting the distinction between CSF, gray, and white matter caused the largest errors. Neglecting the distinction between skull spongiosa and compacta only resulted in relatively small errors when using an optimized conductivity for the homogenized skull compartment. Consequently, the errors observed for the three-compartment

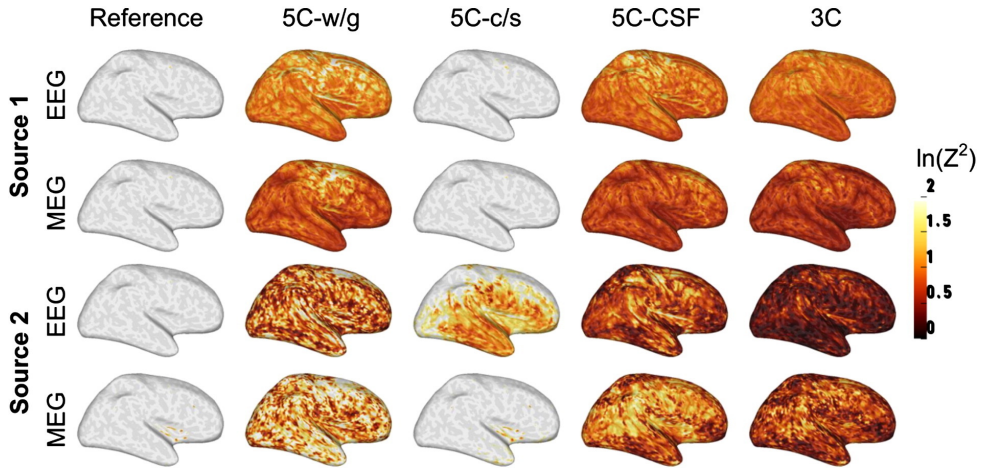

Figure 4.3: Influence of head volume conductor model detail on EEG and MEG beamformer output. Output SNR $\ln(Z^2)$ for sources 1 and 2 in EEG and MEG with input SNR of 300, plotted on the inflated white/gray matter interface. Note that in the maps for source 1, the $\ln(Z^2)$ value for source 1 is mapped onto the corresponding location of source 2 for visualization purposes because the location of source 1 is fixed in one location and only the location of source 2 varies. Figure from Cho, **Vorwerk**, et al. (2015).

head model are the largest out of all considered head models. The regions for which large errors in the source reconstruction and the connectivity analysis are found correspond to those for which large errors in the forward simulation study were observed. The rather conservative ICoh was found to be relatively safe from crosstalk effects due to simplified head volume conductor models, whereas the GDPC is clearly more affected.

4.1.2 The Role of Blood Vessels in Head Volume Conductor Modeling for EEG

Whereas the five- or six-compartment head volume conductor models as evaluated in Cho, **Vorwerk**, et al. (2015) and **Vorwerk** et al. (2014) constitute a clear improvement over the three-compartment model and can be generated with an effort that enables an application in practice (Aydin, **Vorwerk**, et al., 2015, 2014; **Vorwerk** et al., 2018), they of course still rely on several simplifications of the head's conductivity distribution. Thus, it is worthwhile to explore if and which further conductive compartments exist that could and should be additionally considered once the further development of imaging techniques and segmentation methods facilitates their distinction.

The use of MRIs with an isotropic resolution of 0.6 mm^3 measured with a 7T MRI system enabled Fiederer, **Vorwerk**, et al. (2016) to create a high-resolution nine-compartment head volume conductor model that additionally distinguishes blood vessels, dura mater, and soft tissue (Fig. 4.4). This head volume conductor model represents blood vessels and dura mater with an unprecedented level of detail, making a detailed analysis of their influence on EEG source analysis possible. Dipole sources were distributed uniformly in

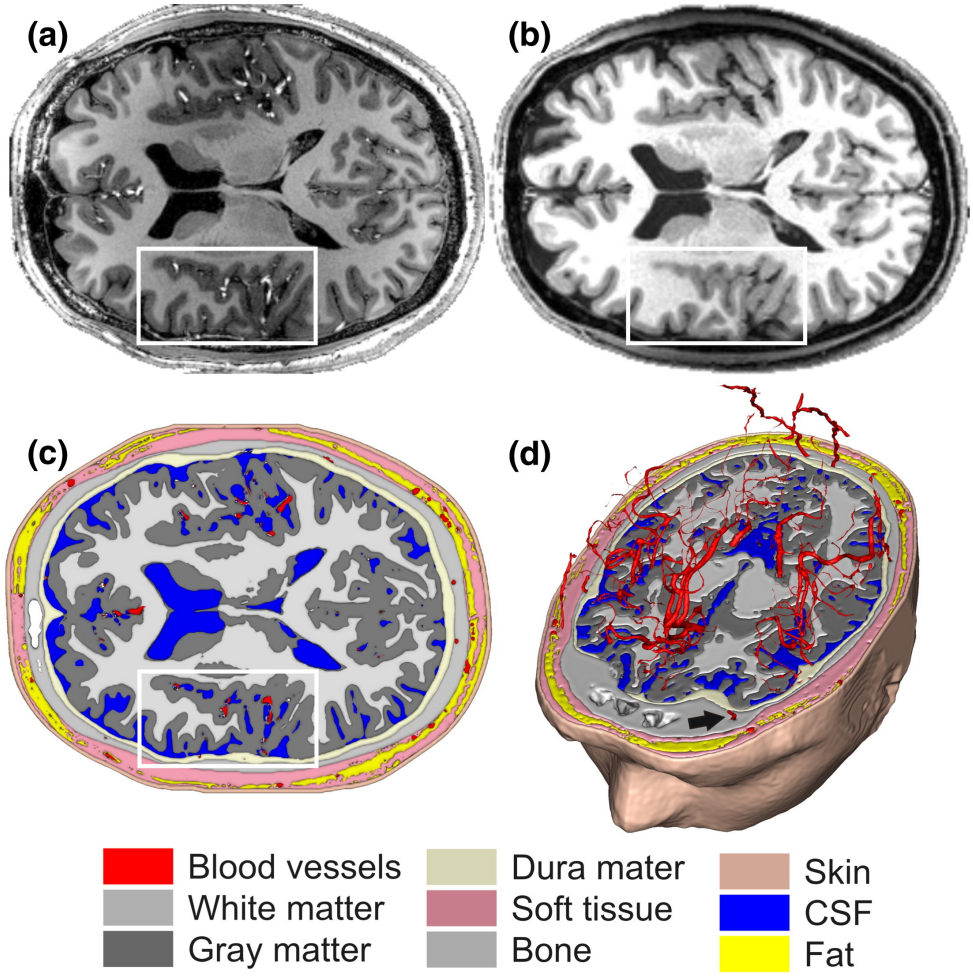

Figure 4.4: 7T structural MRI data and nine-compartment head volume conductor model. (a) 7T T1 MPRAGE MRI data at 0.6-mm isotropic resolution used to derive the volume conductor head model. Arteries are, for example, visible as bright tubular structures in the insular region (white box). Note that the dataset was acquired without any contrast agent. (b) 3T T1 MPRAGE dataset obtained in the same subject. Arteries in the same region (white box) are not clearly visible. (c) Axial slice through the head volume conductor model derived from the 7T data by tissue segmentation. The white box again highlights the insular region as in (a) and (b). Segmented blood vessels are shown in red. Note that neither the hematopoietic nor the fatty bone marrow was included in the segmentation. (d) 3D visualization of intracranial and intraosseous blood vessels; the black arrow indicates an example of an intraosseous vein. Figure from Fiederer, **Vorwerk**, et al. (2016).

the gray matter compartment with an orientation normal to the cortex surface. For each source, the EEG topography and source analysis error resulting from not distinguishing blood vessels was calculated. The source analysis error was determined by simulating an EEG signal using the fully detailed head volume conductor model and performing EEG source analysis using the head model not distinguishing blood vessels. As it is not possible to distinguish between vessel walls and the blood-filled lumen in the head volume conductor model, these were modeled as one compartment, and three different

compound conductivities were tested. To set the errors resulting from not distinguishing blood vessels in relation, the same calculations were performed for simplified head models not distinguishing the CSF and the dura mater, respectively.
A strong effect of not distinguishing blood vessels was for all considered conductivities observed around cerebral arteries, especially the three major brain arteries (anterior, middle, and posterior cerebral arteries). For the high and intermediate blood vessel conductivities tested, also significant errors in the vicinity of skull foramina and intraosseous vessels were found. These were most pronounced in the region of the carotid canal. The observed localization errors were as high as up to 20 mm for all considered blood vessel conductivities. Not distinguishing the CSF and modeling it with gray matter conductivity instead led to similarly strong errors as not distinguishing blood vessels, but a higher proportion of affected sources was observed and consequently also a higher mean error. Not considering the dura mater and modeling it with skull or CSF conductivities led to similar strong errors as not distinguishing the CSF.
In conclusion, the modeling of blood vessels is mainly of interest when reconstructing sources close to the carotid arteries and in regions with dense arterial vasculature such as the insula or the medial temporal lobe. Furthermore, the study demonstrated the significant influence of not distinguishing the dura mater as a separate compartment but assigning it with the much lower skull or much higher CSF conductivity instead.

4.2 Influence of Tissue Conductivity Uncertainties on EEG/MEG Source Analysis

Most of the studies investigating the effects of differently detailed head volume conductor models on EEG/MEG forward and inverse analysis assume exactly known tissue conductivities, neglecting interindividual variations that occur, e.g., due to age or disease state (Antonakakis et al., 2020; McCann et al., 2019). Variations of skin and skull conductivities were found to have a strong influence on EEG source analysis in three- and four-compartment head models, and it was underlined that MEG source analysis is clearly less affected by tissue conductivity uncertainties (Gençer and Acar, 2004; Vallaghé and Clerc, 2008). The strongest influence on MEG source analysis was found for conductivity variations around the source (Gençer and Acar, 2004). However, most of these studies only investigated a few selected source positions, but especially in highly-detailed head volume conductor models the choice of the source positions might have a strong influence on the results.
Most sensitivity studies give a general idea about the quality of the influence of tissue conductivity uncertainties on EEG/MEG source analysis and which sources of uncertainty are relevant but do not actually quantify and visualize the risk that the estimated (maximal)

errors occur in a specific analysis. However, for many applications, it is desirable to actually quantify the likelihood with which certain deviations occur for a specific subject/patient and a specific analysis of measured brain activity.

A first approach to quantify the uncertainty in EEG/MEG source analysis was the introduction of confidence ellipsoids to estimate the effects of measurement noise/low SNRs (Fischer et al., 2005; Fuchs et al., 2017, 2004). Confidence ellipsoids can be computed through deviation scans around the source positions or by analyzing the scatter of several source reconstructions, e.g., by analyzing subaverages or several IEDs, which is especially tempting to determine the extent of the irritative zone in PED. However, given the low signal-to-noise ratio (SNR) one has to take care to distinguish the effects of measurement noise from actual variations of the source location (Fischer et al., 2005; Fuchs et al., 2017).

Another potential source of uncertainty in EEG/MEG source analysis is inaccuracies in the parametrization of the head volume conductor model used to obtain the forward solutions, particularly inaccurately defined tissue conductivities. The influence of these uncertainties on simulations of invasive and non-invasive electric or magnetic brain stimulation was demonstrated in multiple studies. Schmidt et al. (2012) applied Monte-Carlo methods to investigate the influence of tissue conductivity uncertainties on simulations of DBS effects. To perform the necessary large number of simulations, generalized polynomial chaos (gPC) expansions that allow for the rapid and accurate approximation of bioelectric field simulations for varying tissue conductivities were used, and based on prior probability distributions of the tissue conductivities derived from the literature, probabilistic representations of the volume of tissue activated by DBS were determined. This approach was later adopted for other brain stimulation methods, such as transcranial direct current stimulation (tDCS) and transcranial magnetic stimulation (TMS) (Saturnino et al., 2019; Schmidt et al., 2015; Weise et al., 2015).

The results obtained in simulations of brain stimulation give an idea about the potential error sources for EEG/MEG source analysis. However, a specific analysis especially focusing on the influence of head tissue conductivity uncertainties on EEG/MEG source analysis is desirable. In this section, we summarize the results of two studies adopting this approach to investigate the effects of tissue conductivity uncertainties for EEG source analysis.

Relevant Publications

J. Vorwerk, Ü. Aydin, C. H. Wolters, and C. R. Butson (2019a). "Influence of head tissue conductivity uncertainties on EEG dipole reconstruction". In: *Frontiers in Neuroscience* 13, p. 531

J. Vorwerk, C. H. Wolters, and D. Baumgarten (2024). "Global Sensitivity of EEG Source Analysis to Tissue Conductivity Uncertainties". In: *Frontiers in Human Neuroscience* 18, p. 1335212

4.2.1 Influence of Head Tissue Conductivity Uncertainties on EEG Dipole Reconstruction

As a first step, **Vorwerk** et al. (2019a) investigated the influence of head tissue conductivity uncertainties for the source reconstruction of a dipolar source in the primary somatosensory cortex. Realistic measurement data obtained through electrical stimulation of the medianus nerve were used as the basis for the source reconstruction and a detailed five-compartment head model (white matter, gray matter, CSF, skull, skin) of the subject was created. Following the ideas of Saturnino et al. (2019) and Schmidt et al. (2015), a gPC approach was implemented to easily obtain EEG leadfields for varying conductivities.
Based on the gPC expansion, a Monte Carlo approach was applied to estimate the influence of the conductivity variations on EEG source analysis. For 10,000 sets of randomly drawn tissue conductivities, EEG source analysis of the SEP was performed and the distribution of the resulting source localizations was evaluated. Furthermore, the same approach was repeated for variations of a single tissue conductivity only. This allows to understand which tissue conductivity uncertainties have the strongest influence on EEG source analysis.
The range within which each conductivity could vary was obtained from the literature and a uniform distribution of each conductivity within the respective range was assumed (Table 4.1). This represents a "worst case" scenario, as the ranges in general were chosen rather wide and the conductivity distribution is certainly not uniform. However, these assumptions reflect our lack of knowledge about the actual conductivity distributions and the obtained results reflect the maximal errors that could occur.
Fig. 4.5 visualizes the distribution of EEG source localizations for the multivariate conductivity distribution, i.e., the conductivities of white matter, gray matter, skull,

Table 4.1: Tissue conductivity intervals [mS/m].

Tissue	Min.	Max.	Standard	Reference
Skin	280.0	870.0	430.0	Haueisen et al. (1997) and Ramon et al. (2004)
Skull	1.6	33.0	10.0	Akhtari et al. (2002) and Hoekema et al. (2003); Dannhauer et al. (2011)
CSF	1769.6	1810.4	1790.0	Baumann et al. (1997)
GM	220.0	670.0	330.0	Haueisen et al. (1997) and Ramon et al. (2004)
WM	90.0	290.0	140.0	Haueisen et al. (1997) and Ramon et al. (2004)

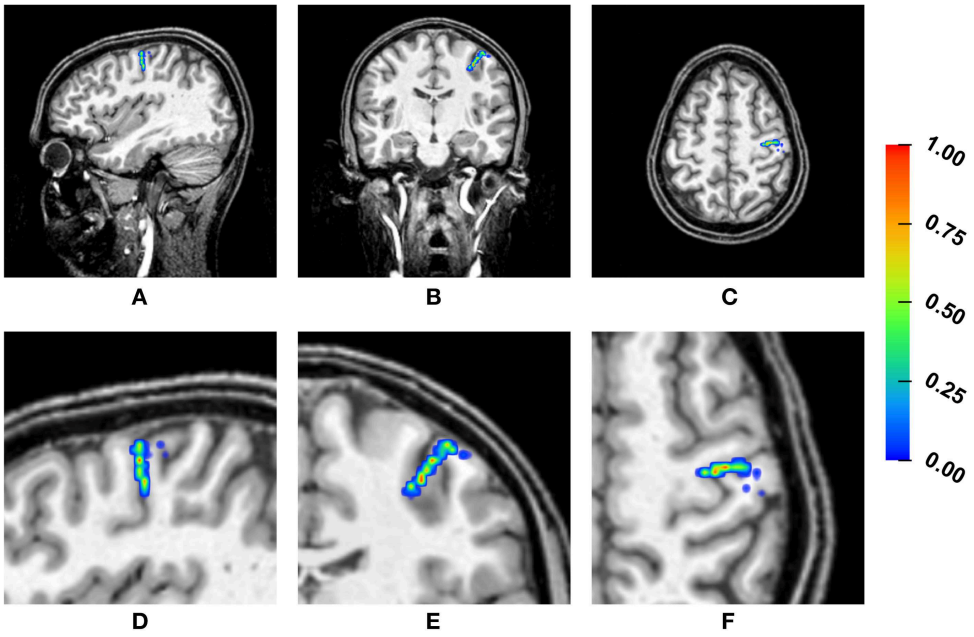

Figure 4.5: Visualization of the source localizations for the multivariate distribution overlaid on the T1-MRI showing the full head (A-C) and a detail around the source locations (D-F). From left to right showing sagittal (A,D), coronal (B,E), and axial slices (C,F). The color bar ranges from low frequency of source localizations (blue) to high frequency of source localizations (red). Values are normalized to the maximum for each slice. Figure from **Vorwerk** et al. (2019a).

and skin were considered uncertain simultaneously. Due to its negligible inter-individual variability, the CSF conductivity was not considered uncertain. It is clearly visible that the distribution of the obtained source localizations mainly occurs in a quasi-radial direction, i.e., the depth of the reconstructed source changes. The extent of the point cloud of source reconstructions along its principal axis is about 2 cm. Analyzing the effects of uncertainties of each tissue's conductivity separately shows that only skin and skull conductivity uncertainties have a significant influence on the source localization and the influence of the skull conductivity is found to be stronger. Furthermore, the effects of skin and skull conductivity uncertainties are opposing - a higher skull conductivity results in an increasing depth of the reconstructed source, whereas a higher skin conductivity results in a decreasing depth of the reconstructed source. In practice, the effects of skin and skull conductivity uncertainties could thus annihilate or reinforce each other, depending on whether the conductivities are over- or underestimated.

Whereas gray matter and white matter conductivities were found to have negligible influence on source localization, their influence on the orientation of the reconstructed source was significant. In most cases, the orientation of the reconstructed source is of less interest. However, such deviations might be misleading when trying to align the orientation of the reconstructed source with the orientation of the cortex surface to account for suspected source localization errors.

4.2.2 Global Sensitivity of EEG Source Analysis to Tissue Conductivity Uncertainties

A shortcoming of prior studies investigating the influence of head tissue conductivity uncertainties on EEG source analysis - including the one presented in the previous section - is that these focused on the analysis of only a few source positions, e.g., in the primary somatosensory cortex (Vallaghé and Clerc, 2008; **Vorwerk** et al., 2019a). Thus, it remained unclear if and to what extent the results of these studies could be translated to general source positions. To resolve this deficit, the aim of **Vorwerk** et al. (2024) was to determine the influence of head tissue conductivity uncertainties on EEG source analysis for arbitrary cortical sources, similar to the approach taken by Cho, **Vorwerk**, et al. (2015) and **Vorwerk** et al. (2014) for the effects of head volume conductor model simplifications. To avoid any influence of individual variations of head anatomy on the results, a head volume conductor model based on a template was used, the New York Head (Huang et al., 2016). Source positions were distributed uniformly in the gray matter. For each source position, EEG measurements were simulated using literature conductivity values. Following, the influence of tissue conductivity uncertainties on EEG forward and inverse solutions was evaluated using a Monte Carlo approach, again employing gPC expansions as in **Vorwerk** et al. (2019a).

The strongest influence on the signal topography of EEG forward solutions for almost all sources up to a depth of 4 cm is found for variations of the skull conductivity. A notable effect is also found for variations in skin conductivity. The influence of gray and white matter conductivity variations is only notable for a few source positions on gyral crowns. However, for even deeper sources, e.g., located deep in the longitudinal fissure, an increasing influence of the white matter conductivity is found.

Particularly for quasi-tangential sources on sulcal walls, the tissue conductivity variations translate to significant changes in source localization, whereas source localizations of quasi-radial sources on the top of gyri are less affected. Fig. 4.6 (top) shows that source positions inside the sulci are clearly more sensitive to localization errors due to conductivity uncertainties than superficial source positions on top of the gyri. Maximal average localization errors of up to 10 mm are found for sources deep inside of sulci, whereas the average localization errors remain below 5 mm for very superficial sources. Fig. 4.6 (bottom) shows that the changes in source localization due to conductivity variations are mainly driven by changes in source depth as also observed in **Vorwerk** et al. (2019a). For rather superficial sources in the longitudinal fissure large localization errors are found as well, whereas the localization errors for deep brain regions that can be attributed to subcortical structures are small. The variations of source localizations and especially the depth of the reconstructed sources show a strong correlation with the skull conductivity, especially for quasi-tangential sources on sulcal walls. A clear but weaker correlation is

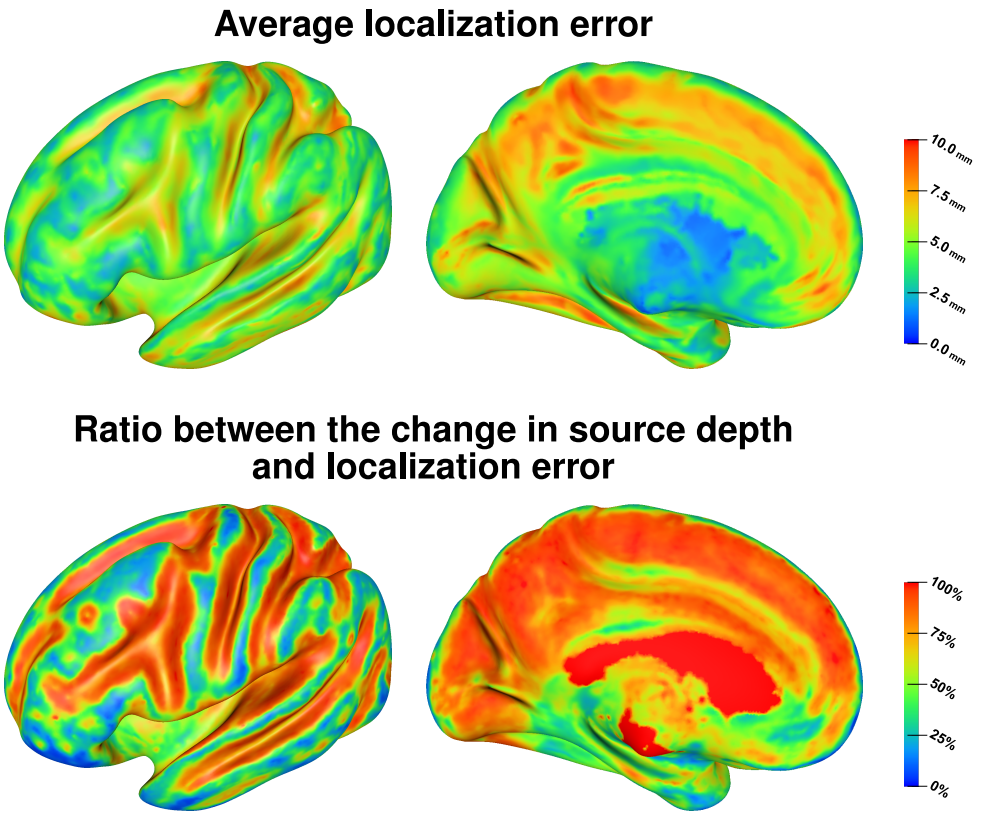

Figure 4.6: Average localization error (top) and the average ratio between the change in source depth and localization error (bottom) resulting from head tissue conductivity uncertainties visualized on inflated cortex surface; (fronto-)lateral (left column) and medial (right column) view. Figure from **Vorwerk** et al. (2024).

also found between the depth of the reconstructed source and the skin conductivity. These results demonstrate that the results of sensitivity studies only investigating a few selected sources such as Vallaghé and Clerc (2008) and **Vorwerk** et al. (2019a) can be generalized quite well for sources that are similar to the investigated sources with regard to source location (gyral crown/sulcal wall/sulci bottom), source orientation (quasi-tangential/quasi-radial), and source depth. For rather deep sources, the obtained results differ significantly from region to region so that the effects for these regions have to be considered individually.

5

Application of Realistic Head Modeling in EEG/MEG Source Analysis

The studies presented in Chapters 3 and 4 demonstrate the importance of accurate EEG/MEG forward solutions for reliable EEG/MEG source analysis. However, the increased accuracy comes at the price of additional efforts, be it due to the necessity to use and get accustomed to new tools for the computation of EEG/MEG forward solutions or to generate more complex head volume conductor models. Therefore, it is important to not only point out the benefit of such novel computational methods and sophisticated head volume conductor models in abstract studies but their actual application in practice should be demonstrated. Two such exemplary studies applying realistic six-layer head volume conductor models in PED are summarized in Sec. 5.1.
Furthermore, it is important that switching to novel numerical methods is as easy as possible for the user. A good approach to achieve this is the integration into popular, well-documented and -maintained open-source toolboxes, which optimally even support various operating systems. This saves the user from having to deal with several different data formats or even compile their own binaries, which would deter many potential users. In Sec. 5.2 the implementation of a pipeline that easily allows the application of the St. Venant approach (Sec. 3.1) together with individual five-compartment head volume conductor models in the popular open-source toolbox FieldTrip is described.

5.1 EEG/MEG Source Analysis in Presurgical Epilepsy Diagnosis

Determining the irritative zone in PED is an important clinical application of EEG/MEG (Sec. 1.2). The analysis of epilepsy data recorded with EEG/MEG typically consists of two main steps: First, the epileptic activity is identified by reviewing the sensor data. This

is commonly done by a trained expert, but automated approaches have been significantly improved recently (Dimakopoulos et al., 2019). Second, EEG/MEG source analysis is performed to localize the irritative zone. If the irritative zone is assumed to be focal, ECD reconstructions can be applied for source analysis and have been validated for temporal and frontal lobe epilepsy (Tanaka and Stufflebeam, 2014). If the IEDs originate from more widespread brain activity or in cases of multifocal epilepsy, CDR methods or beamforming approaches can be applied (Rullmann et al., 2009). In non-trivial cases, the results of different inverse approaches can be compared to obtain a better picture.

A combined analysis of EEG and MEG measurements to improve the accuracy of source analysis is desirable due to the complimentary information measured by EEG and MEG (Dassios et al., 2007), and the advantages of a combined EEG/MEG source analysis were shown in many studies (Baillet et al., 1999; Cohen and Cuffin, 1987; Fuchs et al., 1998; Huang et al., 2007). In PED, not only the superior spatial resolution and increased stability is relevant, but also the finding that some interictal epileptic spikes can only be detected in MEG and not in EEG and vice versa (Barkley and Baumgartner, 2003; Iwasaki et al., 2005).

To ensure an accurate EEG, MEG, or combined EEG/MEG source analysis in PED, some pitfalls have to be avoided. A major source of inaccuracy in the localization of the irritative zone is the commonly low SNR of single IEDs. Averaging of different IEDs can help to alleviate this problem but requires an accurate clustering. Also inaccuracies in the EEG/MEG source analysis methods, such as inaccurate volume conductor models, can impair the localization of the irritative zone. In this regard, the accurate choice of the head tissue conductivities is especially critical for combined EEG/MEG source analysis. Due to the different influence of tissue conductivity inaccuracies on EEG and MEG forward solutions, an incorrect parametrization of the head volume conductor model may cause sub-optimal results of the combined EEG/MEG source analysis.

In the following, two studies investigating these challenges are presented. Aydin, **Vorwerk**, et al. (2014) demonstrated that the use of highly realistic head volume conductor models including white matter anisotropy and individual skull conductivity estimation for combined EEG/MEG source analysis can significantly increase the accuracy of source analysis in PED. Aydin, **Vorwerk**, et al. (2015) evaluated the effect of (sub-)averaging of epileptic spikes on the estimated location and extent of the irritative zone.

Relevant Publications

Ü. Aydin, **J. Vorwerk**, P. Küpper, M. Heers, H. Kugel, A. Galka, L. Hamid, J. Wellmer, C. Kellinghaus, S. Rampp, H. Stefan, and C. H. Wolters (2014). "Combining EEG and MEG for the reconstruction of epileptic activity using a calibrated realistic volume conductor model". In: *PloS one* 9.3, e93154

Ü. Aydin, **J. Vorwerk**, M. Dümpelmann, P. Küpper, H. Kugel, M. Heers, J. Wellmer, C. Kellinghaus, J. Haueisen, S. Rampp, H. Stefan, and C. H. Wolters (2015). "Combined EEG/MEG can outperform single modality EEG or MEG source reconstruction in presurgical epilepsy diagnosis". In: *PloS one* 10.3, e0118753

5.1.1 Combining EEG and MEG for the Reconstruction of Epileptic Activity Using a Calibrated Realistic Head Volume Conductor Model

Aydin, **Vorwerk**, et al. (2014) investigated the benefit of combined EEG/MEG source analysis in comparison to single-modality EEG and MEG source analysis. To achieve optimal accuracy, EEG/MEG-based skull conductivity fitting was performed before the combined EEG/MEG analysis of the epileptic activity. The skull conductivity calibration was performed following the approach proposed by Wolters et al. (2010). For SEP/SEF measurements of medianus nerve stimulation the source localization of the MEG is chosen as ground truth, and following the skull conductivity is adjusted until the EEG measurement can optimally be explained.

The subject was a 17-year-old female diagnosed with pharamaco-resistant focal epilepsy. Prior (video-)EEG measurements had shown early temporal left and bifrontal/frontal left seizure activity. During a combined EEG/MEG measurement 40 minutes of spontaneous brain activity were measured for spike detection and 7 minutes of left median nerve SEP for the conductivity calibration. Epileptic spikes were marked by three clinical reviewers and clustered according to the electrode at which the maximum negativity occurred. Overall 568 spikes were marked. After preprocessing, all spikes with an SNR smaller than 3 were discarded. FT9 and F9 spike clusters consisting of 350 and 218 spikes, respectively, were selected for further evaluation. T1-, T2-, and diffusion spectrum MRIs were measured for the construction of the individual head volume conductor model. A six-compartment (white matter, gray matter, CSF, skull compacta, skull spongiosa, skin) geometry-adapted hexahedral head volume conductor model with a mesh resolution of 1 mm and anisotropic white matter conductivity was generated. A source space with a resolution of 2 mm restricted to the gray matter compartment was defined and the St. Venant approach was used for the calculation of EEG/MEG leadfields. As the EEG/MEG inverse approach,

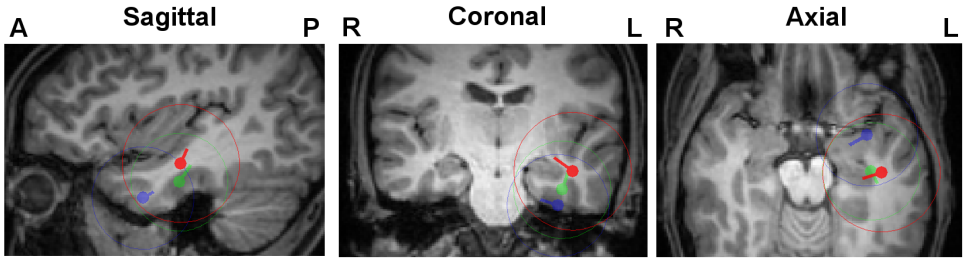

Figure 5.1: Centroids of FT9 spike cluster source reconstructions and standard deviation for EEG, MEG, and combined EEG/MEG. FT9 centroids and spread spheres plotted on T1-weighted MRI for combined EEG/MEG (red), MEG (green), and EEG (blue) using the six-compartment head model conductor model with calibrated skull conductivity. The centroid location of the combined reconstruction was used for the selection of MRI slices and all results were projected on these slices. Figure from Aydin, **Vorwerk**, et al. (2014).

GFS was selected both for the conductivity calibration and the analysis of the epileptic activity. A (compact) skull conductivity of 0.024 S/m was obtained from the conductivity calibration; the conductivity of the skull spongiosa was scaled accordingly. For the calibrated skull conductivity and four selected skull conductivities, source reconstructions were performed for each spike, and the resulting centroid and standard deviation of the source reconstructions were calculated.

A strong influence of the skull conductivity on the centroid location was observed particularly for the EEG source reconstruction. For both FT9 and F9 clusters, a variation of more than 2 cm was observed, where the main change of source localization occurred with regard to the depth of the reconstructed sources. For the MEG, a clearly smaller variation of less than 1 cm was observed. No significant change in the standard deviations of the source localizations between different skull conductivity values was observed for both EEG and MEG.

Comparing the results of EEG, MEG, and combined EEG/MEG source analysis using the head volume conductor model with calibrated skull conductivity, a deviation from the centroid obtained for combined EEG/MEG of up to 3 cm for the EEG and of up to 1 cm for the MEG were observed. Fig. 5.1 shows the centroids and standard deviations for the FT9 cluster. With regard to reconstructed source orientation, a deviation of around 20 degrees between EEG and combined EEG/MEG average was observed, whereas a difference of 70 degrees between MEG and combined EEG/MEG average was observed. This shows that the reconstructed source localization is clearly - but not purely - dominated by the MEG, whereas the EEG has a strong influence on the reconstructed source orientation. With deviations of slightly more than 1 cm, variations of the skull conductivity had a higher influence on the combined EEG/MEG than on the MEG source reconstructions. However, the deviations were clearly smaller than for the EEG.

5.1.2 Influence of (Sub-)Averaging on EEG/MEG Source Reconstruction of Epileptic Activity

The large number of epileptic spikes obtained for the patient evaluated in Aydin, **Vorwerk**, et al. (2014) raised the question of what an optimal strategy for the evaluation of such a large number of resulting source localizations is. On the one hand, an averaging of spikes is beneficial to reduce the noise bias and potentially obtain a more accurate reconstruction of the irritative zone. On the other hand, the variation of source localizations might provide information regarding the extent of the irritative zone that can be lost by spike averaging. From the detected spikes, 10 left temporal spikes, which was the most frequent spike type, were selected. Following, a template search was used to identify further spikes of this type, and 200 spikes without any clear artifacts were selected for further analysis. For each spike, the peak of the EEG was determined. For 10 different sample sizes between 5 and 50, spikes were randomly drawn from the full set of 200 spikes, (sub-) averaged, and EEG, MEG, and combined EEG/MEG source reconstructions were performed. This was performed 200 times for each sample size, resulting in 200 source reconstructions per sample size. Furthermore, source reconstructions of the 200 single spikes and the grand average of all 200 spikes were performed. For each sample size, the distribution of the source reconstructions, the centroid of the source reconstructions, and the distribution of the SNRs for each subaverage were calculated. As propagation of the epileptic activity was hypothesized, this analysis was performed at 33, 23, 13, and 3 ms before the peak.
The centroids of the source reconstructions for subaverages with 10 or more spikes are located within a very small distance, whereas the centroids of source reconstructions for the single spikes and subaverages with 5 spikes clearly deviate (Fig. 5.2). Akin to the results of Aydin, **Vorwerk**, et al. (2014), also in this case there is a significant distance between the EEG and MEG centroids for all sample sizes. Again, the centroids for the combined EEG/MEG source reconstructions are closer to the MEG centroids. However, the combined EEG/MEG centroids are not located in between the EEG and MEG results as one might expect but are localized more inferior than both EEG and MEG centroids. This suggests that combining EEG and MEG can reveal more information than a joint analysis of the single-modality results.
A comparison of the point clouds representing the 200 source reconstructions for each subaverage sample size shows a clear reduction of the extent of the point clouds with an increasing sample size for both EEG, MEG, and combined EEG/MEG. However, whereas the point cloud of EEG source reconstructions converges in the vicinity of the temporal pole, the MEG point cloud converges in a more posterior area of the temporal lobe and the combined EEG/MEG source reconstructions converge along the inferior temporal gyrus. A comparison with the irritative zone determined from invasive sEEG measurements shows that for 10 samples per average especially for combined EEG/MEG the point cloud of

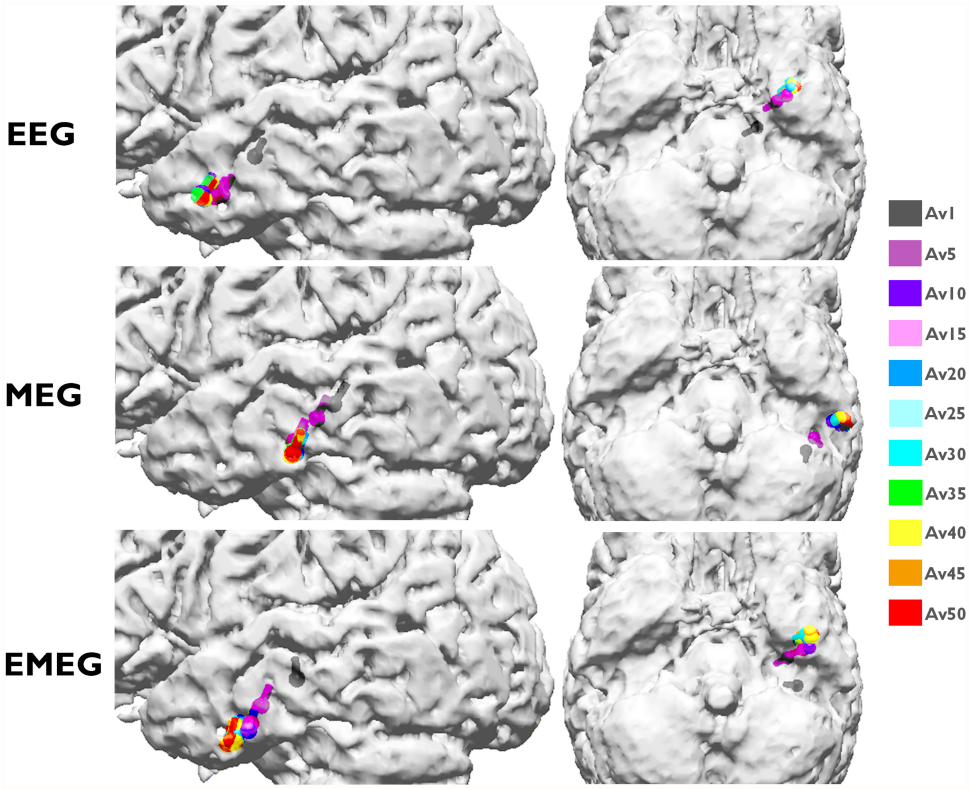

Figure 5.2: Centroids of EEG (top), MEG (middle) and combined EEG/MEG (bottom) for different subaverages at 23 ms before peak. Each color shows centroids for different subaverages and Av1 is the centroid for single spike reconstructions. Only those of the 200 random realizations for each group with an SNR larger than 3 were included. Figure from Aydin, **Vorwerk**, et al. (2015).

source reconstructions covers the irritative zone very well. For the subaverages with a higher number of samples, the extent of the point cloud of source reconstructions tends to be too small, whereas for smaller sample sizes the results are still overly affected by noise. A comparison of the source reconstructions at different time points prior to the determined peak with the propagation pathway determined using sEEG again shows that only combined EEG/MEG correctly estimates the onset zone, whereas EEG and MEG do not lead to a stable localization at very early time points. Furthermore, single-modality EEG and MEG do not accurately estimate the correct extent of the epileptic activity also at later time points. Validated through the sEEG results, these findings demonstrate the benefit of combined EEG/MEG to accurately estimate the propagation pathway of the epileptic activity even at early time points.

5.2 Toolboxes

Open-source toolboxes for EEG/MEG analysis have become highly popular especially in research environments (Delorme and Makeig, 2004; Esch et al., 2019; Gramfort et al., 2013;

Oostenveld et al., 2011; Tadel et al., 2011). A major advantage over commercially available toolboxes is the traceability of calculations, the faster development cycles, the higher flexibility, and often also the compatibility with several operating systems. Especially toolboxes implemented in Matlab or Python easily allow for individual adaptations and expansions. A drawback of most open-source toolboxes is the lack of certifications that allow for an (official) use in clinical applications.

The benefit of using FEM to calculate EEG/MEG forward solutions based on highly-realistic head volume conductor models for EEG/MEG source analysis was demonstrated in Chapter 4. Therefore, it is desirable to enable the use of such head models for a large number of researchers. Most of the novel methods for EEG/MEG forward simulations presented in Sec. 3 have been implemented in freely available open-source toolboxes (He et al., 2020; Schrader et al., 2021) and are thus accessible to everyone at no charge. However, the functionality of these toolboxes is mostly limited to EEG/MEG forward simulations, requiring the user to perform data processing and head volume conductor generation using separate tools. This often leads to tedious conversion processes between different data formats and possibly even incompatibilities. Some of these platforms, such as SimBio and DUNEuro, also require the user to compile the binaries themselves. Overall, this (perceived) complexity represents a (too) high barrier to entry for many users.

A promising approach to promote the use of highly realistic head volume conductor models in the calculation of EEG/MEG forward solutions and to close the gap between methodological studies and the practical challenges encountered by researchers in scientific praxis is to directly include this calculation within the workflow of toolboxes with comprehensive functionalities for EEG/MEG (source) analysis and large user bases. This requires the integration of a complete pipeline for leadfield generation including at least basic MRI segmentation and head volume conductor generation. For more experienced users, the open-source nature of the toolboxes then still offers the possibility to improve the results of the pipeline, e.g., by loading more detailed head models generated with an external tool such as ROAST (https://www.parralab.org/roast/) or SimNIBS (https://simnibs.github.io) (Huang et al., 2019; Puonti et al., 2020).

In the following, we summarize the implementation of the FieldTrip-SimBio pipeline, which allows the straight-forward use of realistic five-compartment head volume conductor models for leadfield generation within FieldTrip based on the SimBio algorithms. Similarly, DUNEuro has been made directly available as an option for leadfield computation within Brainstorm recently (https://neuroimage.usc.edu/brainstorm/Introduction) (Medani et al., 2023). The core of the FieldTrip-SimBio pipeline has later also been used to enable FEM simulations of DBS in the popular LeadDBS toolbox (Horn et al., 2019).

Relevant Publications

J. Vorwerk, R. Oostenveld, M. C. Piastra, L. Magyari, and C. H. Wolters (2018). "The FieldTrip-SimBio pipeline for EEG forward solutions". In: *Biomedical Engineering Online* 17, pp. 1–17

5.2.1 FieldTrip-SimBio Pipeline

The FieldTrip-SimBio pipeline aims to provide easy access to EEG source analysis using FEM-generated leadfields based on five-compartment (white matter, gray matter, CSF, skull, skin) head volume conductor models for a large user base. While the main focus during the implementation was to achieve a clear improvement in accuracy over EEG source analysis using the previously common three-compartment (homogenized brain, skull, skin) head volume conductor models, other important aspects were an easy application and a computational load that can be handled by standard desktop computers. This led to the decision to rely on geometry-adapted hexahedral head volume conductor models as these can be directly generated from segmented MRIs within a few minutes, while still achieving a high accuracy. In comparison, the generation of accurate tetrahedral head volume conductor models is much more complex and at the time of the implementation of the FieldTrip-SimBio pipeline no open-source tools reliably performing this task without user intervention were available. This led to the decision to not go for the highest accuracy

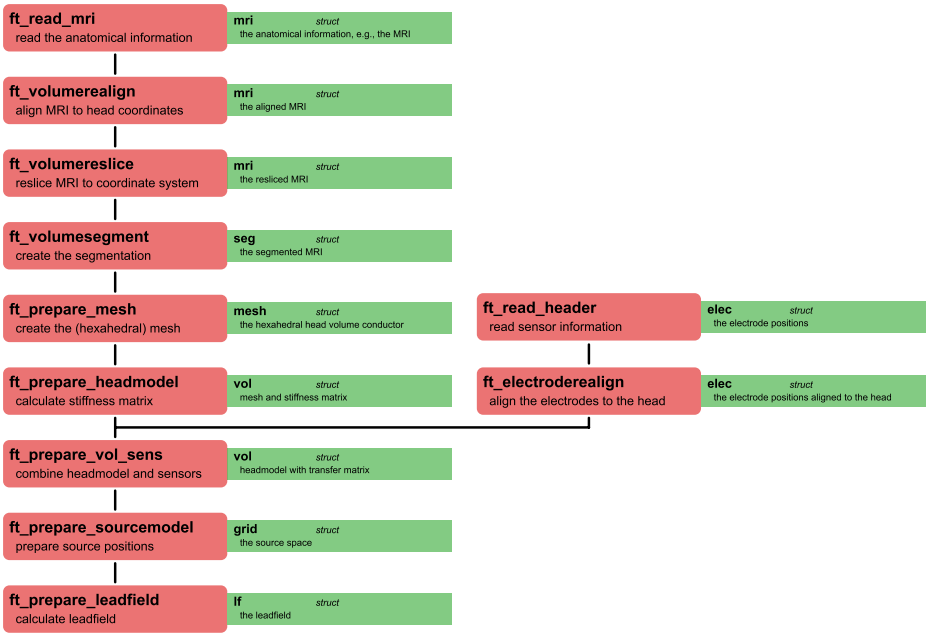

Figure 5.3: Sketch of the FieldTrip-SimBio pipeline (workflow goes from top to bottom). Red background indicates Matlab/FieldTrip functions, green background (main) output of the respective function. Figure from **Vorwerk** et al. (2018).

of the skull segmentation but to rely on a rather robust segmentation that prevents any possibility for skull leakages (see Sec. 3.2). Of course, the possibility to include self-generated hexahedral or tetrahedral head volume conductor models for more experienced users was also considered. For the subsequent FEM computations, core routines of SimBio were made accessible in Matlab through the generation of mex-files for multiple platforms (Windows, Linux, MacOS). Fig. 5.3 gives an overview of the full FieldTrip-SimBio pipeline. To demonstrate the benefit of the FieldTrip-SimBio pipeline for the accuracy of EEG source analysis, we evaluated the EEG forward solutions calculated with the obtained five-compartment head model in comparison to EEG forward solutions obtained with the highly accurate six-compartment tetrahedral head volume conductor model used in Cho, **Vorwerk**, et al. (2015) and **Vorwerk** et al. (2014), which was created with extensive manual interventions. Furthermore, we included simplified versions of the tetrahedral head volume conductor model in the comparison that were generated by step-by-step neglecting an additional model detail (distinction skull compacta/spongiosa, gray matter/white matter, CSF/brain) until a three-compartment model remained akin to the approach in Sec. 4.1.1. The evaluation showed that the automatically generated five-compartment head volume conductor was about as accurate as the four-compartment version of the highly accurate head volume conductor model and clearly more accurate than the three-compartment version of the highly accurate head volume conductor model. This demonstrates a significant improvement over the three-compartment head models previously available within FieldTrip, while not requiring a significantly increased effort from the user.

Nowadays, tools are available that reliably generate highly realistic tetrahedral head volume conductor models upon button press (Huang et al., 2019; Puonti et al., 2020). These can be included in the FieldTrip-SimBio pipeline with minimal effort by more experienced users. However, the generation of a single head volume conductor model using these tools has a computation time of multiple hours.

6

Simulation and Optimization of Electric Brain Stimulation

The equations derived in Chapter 1 not only cover the EEG/MEG forward problem but are also the basis for the simulation of invasive and non-invasive brain stimulation. Therefore, the focus of the thesis is widened in the following and some results from the field of brain stimulation are presented. The simulation of tDCS, TMS, and DBS has recently gained popularity to improve the understanding of treatment effects and to provide individually optimized stimulation patterns. Similar to EEG/MEG source analysis (see Chapter 4), the influence of differently detailed head volume conductor models or tissue conductivity uncertainties on simulation results or the optimization algorithms based on these have been investigated for brain stimulation (Saturnino et al., 2019; Schmidt et al., 2015; Wagner et al., 2013; Weise et al., 2015). The similarity of the underlying equations not only allows to use the same numerical methods for EEG/MEG forward simulations and simulations of brain stimulation, but often even the conclusions drawn from modeling studies translate to the other application. Due to this close relationship, methodological research in both areas is closely intertwined and an exchange of both methods and ideas is highly beneficial. In this chapter, two applications of bioeletromagnetic field simulations with realistic head volume conductor models from DBS research are presented.

6.1 Deep Brain Stimulation

DBS is an established treatment for several neurological diseases such as Parkinson's disease, essential tremor, and epilepsy (Deuschl et al., 2006; Salanova et al., 2015; Weaver et al., 2009) and is currently evaluated as a treatment for a variety of other neurological disorders (Lee et al., 2019). DBS is applied through leads implanted in specific anatomical targets in the brain, which are chosen depending on a patient's diagnosis and symptoms. The DBS leads are connected to a pulse generator that is usually implanted subcutaneously in the patient's chest. A few weeks after the implantation of the DBS lead, an initial programming session is performed. During this session, the stimulation is activated for

the first time and optimal stimulation parameters for the specific patient are determined. Therefore, a comprehensive monopolar review is performed, i.e., the stimulation strength for different activated contacts is incrementally increased and the resulting therapeutic and side effects are observed. Further parameters that can be varied to modify the stimulation are the pulse width and pulse frequency. This review is necessary due to the variability in lead placement, e.g., due to the limited accuracy in stereotactic surgery and clinician preferences, but also (or especially) due to the different patient responses to stimulation. Nowadays, a variety of different DBS leads exist, which differ with regard to the number, size, shape, and arrangement of contacts. Whereas early DBS leads usually consisted of four cylindrical contacts, novel DBS leads with up to eight cylindrical contacts or even segmented contacts, for which some of the cylindrical contacts are subdivided into three or four contacts that can be separately controlled, have been introduced (Krauss et al., 2021). Together with a novel generation of pulse generators that allow for higher flexibility in the choice of stimulation parameters, this innovation has caused an exponential growth of the parameter space so that a complete sampling during a manual review is no longer feasible. Simulations of DBS effects can support clinicians during programming to reduce the time effort and improve treatment outcomes. This can be achieved by simply providing the clinician with a visualization of the stimulated brain tissue (Butson et al., 2012) or through an automated optimization of stimulation parameters (Anderson et al., 2018; Peña et al., 2017; Xiao et al., 2015). The automated optimization of stimulation parameters is especially interesting to fully capitalize on the possibilities of novel lead models, for which the interplay between several simultaneously activated contacts is becoming less intuitive. As a basis, these applications require simulations of the bioelectromagnetic fields evoked by DBS in the brain and computational methods to determine the activation of individual neurons through DBS (Duffley et al., 2019). At the same time, these computational methods can also help to better understand the mechanisms underlying DBS (Anderson et al., 2019) or to identify and evaluate novel DBS targets and targeting strategies (Horn et al., 2017). Several open-source toolboxes to perform DBS simulations exist (Horn et al., 2019).

As the computational methods to simulate DBS rely on several simplifications and uncertain parameters, it is important to validate the results obtained in simulation studies in practice. Such a validation is a non-trivial task not only for practical but also for ethical reasons. In the following, we summarize a study performing a retrospective evaluation of the optimization algorithm presented by Anderson et al. (2018). Furthermore, it is important to make the results of such simulations easily accessible in clinical practice. Therefore, we present an approach to interactively visualize optimized DBS parameters in near real-time on a tablet computer.

Relevant Publications

J. Vorwerk, A. A. Brock, D. N. Anderson, J. D. Rolston, and C. R. Butson (2019b). "A retrospective evaluation of automated optimization of deep brain stimulation parameters". In: *Journal of Neural Engineering* 16.6, p. 064002

J. Vorwerk, D. McCann, J. Krüger, and C. R. Butson (2020). "Interactive computation and visualization of deep brain stimulation effects using Duality". In: *Computer Methods in Biomechanics and Biomedical Engineering: Imaging & Visualization* 8.1, pp. 3–14

6.1.1 A Retrospective Evaluation of Automated Optimization of Deep Brain Stimulation Parameters

Whereas the benefits of an individual optimization of DBS parameters have been suggested in several computational studies, most studies lack an evaluation in practice. Retrospective studies are one option for a first validation and towards an application in practice. In **Vorwerk** et al. (2019b), detailed notes about the occurrence of therapeutic and unwanted side effects of DBS at different stimulation settings were used to evaluate the automatic determination of optimal DBS parameters based on the optimization algorithm proposed by Anderson et al. (2018). The data were obtained during the initial programming session for three patients (five electrodes) diagnosed with essential tremor and implanted with a Medtronic 3387 lead, which has four cylindrical contacts. Furthermore, comprehensive pre- and post-operative imaging (CT, MRI) was obtained for each patient, and individual models to simulate DBS effects and compute optimized DBS parameters were generated.

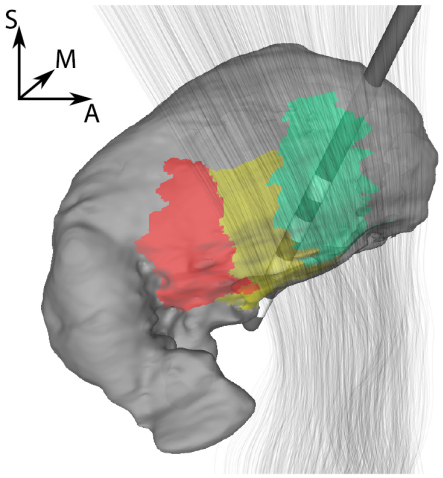

Figure 6.1: Surface visualization of lead placement relative to the thalamus (gray) and IC (gray lines) for right-hemisphere stimulation. Selected subregions of the thalamus are highlighted (Vc - red, VIM - yellow, Vop - green). Figure from **Vorwerk** et al. (2019b).

The optimization algorithm is based on a definition of target and avoidance regions for which the stimulation should be maximized or for which the stimulation has to be kept below a certain threshold, respectively. Subsequently, a multipolar stimulation pattern, i.e., multiple contacts can be activated simultaneously, is computed that takes into account target and avoidance regions, while minimizing the consumed energy. For essential tremor, the ventrointermediate nucleus (VIM) was chosen as the target region, and the ventralis caudalis (Vc) and internal capsule (IC) as avoidance regions (Fig. 6.1). The threshold below which the stimulation of the avoidance region needs to be kept could in theory be estimated based on computational models (Duffley et al., 2019). However, it is not clear how well these estimates work in practice. Therefore, **Vorwerk** et al. (2019b) propose to instead determine the threshold empirically by incrementally raising the threshold while closely monitoring the patient for therapeutic and side effects of the stimulation. In the retrospective study, this approach was implemented by increasing the threshold until for one of the active contacts a voltage was reached at which side effects were observed during the monopolar review.

The comparison of the automatically optimized DBS parameters with the results of the monopolar review showed a good agreement. In all cases, the optimization algorithm assigned the highest voltage to the contact that was clinically selected. Furthermore, the predicted target activation for the optimized DBS parameters was at least equal to the clinically determined settings, and in four out of five cases the predicted target activation was improved. Equally, the estimated power consumption was reduced or equal to the clinically determined settings in four out of five cases. For the single case in which the power consumption was increased for the optimized DBS parameters, the increase in target activation was still clearly higher than the increase in power consumption. Thus, this retrospective analysis provides a first demonstration that the optimization algorithm in combination with the chosen target and avoidance regions leads to meaningful DBS parameters that may improve stimulation effectiveness and efficiency.

6.1.2 Interactive Computation and Visualization of Deep Brain Stimulation Effects

To make computational models of DBS usable in clinical practice, an interactive, intuitive visualization of the results is necessary while providing high flexibility regarding the choice of parameters and methods. Furthermore, the presentation device should be highly mobile to seamlessly integrate into the clinical workflow. Both a visualization on desktop computers and the presentation of precomputed results on tablet computers are not well suited for this purpose as each of them lacks one of these requirements. Even if the computing power of today's tablet computers would allow for the (near) real-time computation of DBS simulations and optimizations, the integration of the necessary

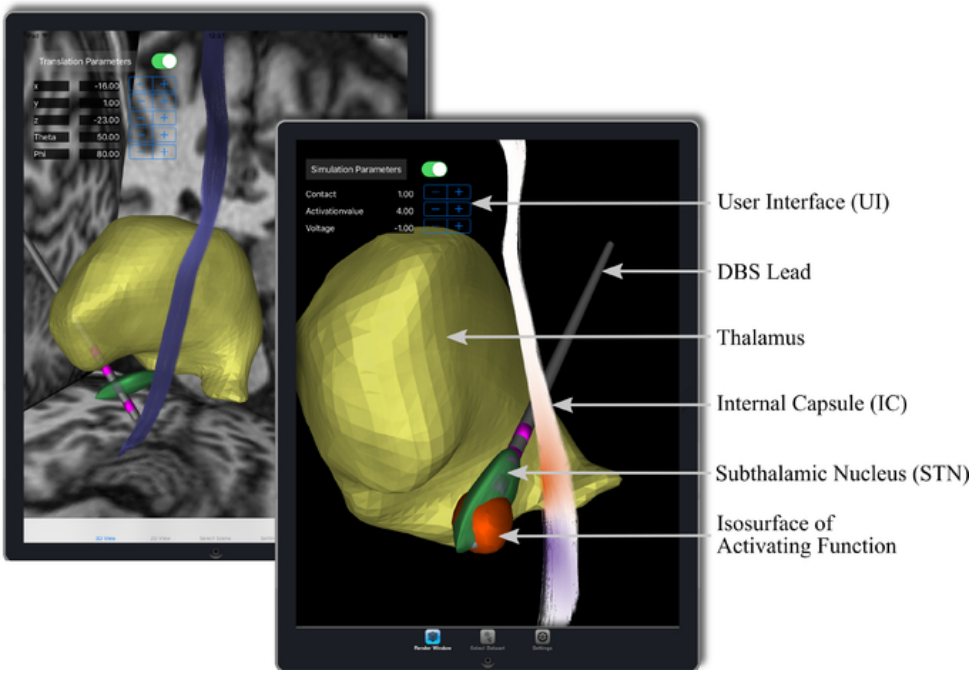

Figure 6.2: Illustration of the iPad-app. Visualization of the activating function through an isosurface, i.e., the VTA, and the projection on a fiber tract (internal capsule) - red corresponds to possible activation and blue to inhibition - and the UI, the DBS lead, and a selection of brain structures. Figure from **Vorwerk** et al. (2020).

algorithms into an application for mobile operating systems is complex. Furthermore, this approach would complicate adjustments to the underlying algorithms as they are frequently necessary especially at the early development stage most of these algorithms are in. To circumvent these limitations, **Vorwerk** et al. (2020) proposed a platform to perform the computations on a server or desktop computer in near real-time and instantaneously visualize them on a tablet computer that is connected to the server via a local network. The tablet computer also provides a user interface that conveniently allows adjustments to the stimulation parameters.

For the visualization, **Vorwerk** et al. (2020) implemented an iOS application allowing the use on iPhones and iPads. The server application is available for Windows, macOS, and Linux operating systems. Whereas the server application is written in C++, it also allows the execution of Python scripts to obtain the simulation results. This approach offers high flexibility and enables rapid prototyping. **Vorwerk** et al. (2020) demonstrated the feasibility of this pipeline in two case studies.

For pre- and intraoperative planning, the implementation allows full flexibility with regard to electrode placement and DBS parameters. To enable the flexible electrode placement, a finite element mesh is generated within a few seconds based on predefined components. Following, a FEM simulation of the DBS is performed and a visualization is generated. A full execution of the pipeline including the mesh generation required about 10 s of

computation time. For a change of the DBS parameters without a change of the electrode positions, the execution required about 4 s.
For post-operative planning, i.e., an application during the initial programming session, the electrode position and accordingly also the finite element mesh were predefined based on the postoperative imaging. Thus, only the DBS parameters were flexible, and the simulation of DBS effects for a new set of parameters required about 4 s. Fig. 6.2 shows a visualization of the iPad app for post-operative planning.

7 Discussion

Accurate simulations of (bio-)electromagnetic fields in the human brain are important in several areas of neuroscience. Over the last decades, significant progress regarding the accuracy of these simulations has been made driven by an increase in available computational power and the development of novel computational methods. However, to reliably make use of such simulations, detailed knowledge about residual uncertainties inherent to the simulation results originating, e.g., from the sensitivity of the simulation results to model simplifications and parameter uncertainties, is important. In this thesis, novel computational methods to further reduce these uncertainties and studies to better understand the effects of the residual uncertainties - primarily for EEG/MEG source analysis - were presented. Furthermore, examples for applications of bioelectromagnetic field simulations using highly-realistic head volume conductor models in EEG/MEG source analysis and brain stimulation were introduced.

7.1 EEG/MEG Forward Problem

The St. Venant approach to solve the EEG/MEG forward problem as introduced by Buchner et al. (1997) was considered the best compromise between high numerical accuracy and computational effort for a long time. In Sec. 3.1, the multipole and the H(div) approach were introduced and shown to have a higher accuracy than the St. Venant approach while maintaining a comparable robustness and computational efficiency in solving the EEG/MEG forward problem. The H(div) approach performs especially well when the orientations of the dipole source are aligned with the mesh structure, whereas the accuracy of the multipole approach was shown to be independent of the local mesh structure.

The accuracy of the H(div) approach was further improved for highest eccentricities by Miinalainen et al. (2019). This was achieved by only considering basis functions that were supported on the gray matter compartment, while those that reached into other compartments (mainly CSF) were excluded. A similar approach was also implemented for the St. Venant and multipole approaches in Miinalainen et al. (2019) and **Vorwerk**

et al. (2019c) and led to a clear improvement of the accuracy at highest eccentricities compared to previous studies. No direct comparisons between the improved H(div) approach and multipole approach have been performed to date. However, the results of Miinalainen et al. (2019) and **Vorwerk** et al. (2019c) suggest that both approaches are robust, computationally efficient, and lead to very good accuracies even at the highest eccentricities. Thus, they can equally well be recommended for practical applications.
Neither the multipole nor H(div) approach have been evaluated for solving the MEG forward problem to date. However, based on prior studies, it can be assumed that the accuracy achieved in solving the EEG forward problem translates to the MEG forward problem. Therefore, they should currently also be considered as the best FEM approaches for solving the MEG forward problem.
Recently, Höltershinken et al. (2023) proposed a localized subtraction approach. This approach preserves the advantages of the subtraction approach, i.e., the analytical treatment of the dipole source, while severely reducing the computational effort by only performing the subtraction locally and thereby leading to a sparse right-hand side. This approach was shown to achieve a good numerical accuracy especially also for meshes with poorly shaped tetrahedrons, for which the accuracy of the multipole approach was to a certain degree reduced. The localized subtraction approach might therefore in the future become the recommended approach for FEM-based EEG/MEG forward simulations.
Mixed- and DG-FEM were shown to be more robust than CG-FEM towards skull meshing defects occurring particularly in hexahedral volume conductor models with a mesh resolution of 2 mm and coarser (Sec. 3.2). This was achieved by ensuring a current-preserving simulation of the electromagnetic fields. However, nowadays a mesh resolution of 1 mm is common for hexahedral meshes so that the risk of such defects is clearly decreased. Furthermore, pipelines that allow for a simple generation of accurate high-resolution tetrahedral volume meshes have been presented (Huang et al., 2019; Nielsen et al., 2018; Puonti et al., 2020). For tetrahedral meshes, Yavich et al. (2021) evaluated a mixed-hybrid FEM based on a subtraction approach for EEG and MEG forward solutions. Whereas no improvement over CG-FEM was found for fine grid resolutions, the mixed-hybrid FEM led to better accuracies in coarse meshes. Therefore, the use of Mixed- or DG-FEM approaches does currently not seem to provide significant advantages in the computation of EEG forward solutions as long as sufficiently finely resolved hexahedral or tetrahedral meshes are used.
As Mixed- and DG-FEM approaches allow for more realistic modeling of the volume currents evoked by neural activity inside the brain which contribute to the MEG signal, it was assumed that such approaches might also contribute to more accurate MEG forward solutions. Piastra et al. (2018) evaluated the subtraction DG-FEM and Yavich et al. (2021) evaluated a mixed-hybrid FEM subtraction approach for MEG forward solutions. Both studies found no significant differences in accuracy compared to CG-FEM for high mesh

resolutions, as they are nowadays commonly used. In conclusion, also for MEG forward solutions the CG-FEM currently seems to provide the best combination of numerical accuracy and computational effort.
Looking beyond FEM methods, Makarov et al. (2020) recently presented a boundary element fast multipole method (BEM-FMM) which joins concepts from BEM and the fast multipole method. The BEM-FMM avoids the complicated treatment of the dipole source as it is necessary for FEM approaches, and can handle a large number of unknowns, which is often a limiting factor for BEMs. Thereby, it is possible to calculate EEG/MEG forward solutions using detailed five-layer head volume conductor models. In a first comparison study, BEM-FMM achieved higher numerical accuracies than CG-FEM with regard to the RDM, however, this came at the cost of a significantly higher computation time (Lunkenheimer, 2021). Unbiased comparison studies where the mesh resolutions of BEM-FMM and CG-FEM are matched to obtain comparable computation times have not been performed to date to the best of our knowledge.
Exploiting novel technological developments in GPU-computing, Stenroos and Koponen (2019) implemented a BEM solver that allows for a fast computation of bioelectromagnetic field simulations for a five-layer realistic head volume conductor model. Whereas Stenroos and Koponen (2019) demonstrated the use for TMS, applying such an approach for EEG/MEG forward simulations might enable the use of realistic head volume conductor models with five or six conductive compartments with BEM, which is currently not possible due to the resulting computational effort.
Instead of explicitly describing the head geometry through a tetra- or hexahedral mesh, unfitted FEMs are based on a structured mesh that does not represent the geometry. The geometry is considered implicitly based on a description through level sets, which can be obtained from segmented volumetric images, usually MRIs. Such approaches have been presented for the EEG/MEG forward problem and were shown to achieve high accuracies (Erdbrügger et al., 2023; Nüßing et al., 2016). The use of these approaches might be especially interesting in scenarios where pipelines for automated mesh generation fail, e.g., when deviations of the head anatomy due to surgery or diseases exist, and manual corrections of the segmentation are necessary.
Several of the discussed FEM approaches have been implemented in the open-source toolbox DUNEuro (Schrader et al., 2021). Furthermore, integrated pipelines such as FieldTrip-SimBio (**Vorwerk** et al., 2018) and Brainstorm-DUNEuro (Medani et al., 2023) have been implemented, which allow to directly compute FEM forward simulations within a complete EEG/MEG processing pipeline. The H(div) approaches are furthermore implemented in the Zeffiro toolbox (He et al., 2020), which additionally provides several modern EEG/MEG source analysis methods. These efforts make it possible for many researchers to profit from the benefits of highly accurate EEG/MEG forward solutions in their research.

7.2 Head Volume Conductor Modeling

As demonstrated in **Vorwerk** et al. (2012), in most scenarios the effect of model simplifications on the EEG forward solution is much larger than that of numerical inaccuracies (Sec. 3.1.3). For EEG/MEG forward modeling, **Vorwerk** et al. (2014) have shown that especially the distinction of the different tissues enclosed by the skull, i.e., white matter, gray matter, and CSF in a six-compartment head volume conductor model, is important for accurate EEG/MEG forward solutions (Sec. 4.1.1). Subsequent studies demonstrated that the results of this forward modeling study for example translate to inaccuracies in beamformer source and connectivity analysis (Sec. 4.1.1; Cho, **Vorwerk**, et al. 2015; Neugebauer et al. 2017). Furthermore, Azizollahi et al. (2020) have shown that these effects are not only found for adults but similarly exist for head volume conductor models of neonates. Piastra et al. (2021) demonstrated that such model simplifications also skewed the expected SNR values for cortical and subcortical surfaces, again, potentially leading to errors in the interpretation of EEG/MEG source analysis results. The visualizations of the changes of the current flow within the head volume conductor in Wagner et al. (2013) and Wagner, **Vorwerk**, et al. (2012) allow to easily grasp the effects of head volume conductor simplifications on bioelectric field simulations.
Also further refinements of six-layer head volume conductors, e.g., distinguishing blood vessels (Sec. 4.1.2; Fiederer, **Vorwerk**, et al. 2016) or skull sutures (Lew et al., 2013; McCann and Beltrachini, 2022), were shown to have noticeable effects on EEG forward and inverse solutions. However, these effects were often only found locally around the simplifications. As these structures can currently not be automatically included in head volume conductor models, it is not feasible to distinguish them outside of modeling studies, but the possible errors should be considered in the evaluation of source analysis results.
The accurate (geometric) modeling of the skull was only a minor aspect in most of the previously discussed studies. As many of them only investigated the effect of distinguishing skull compacta and spongiosa instead of an homogenized skull with an optimized conductivity (Dannhauer et al., 2011), only small effects on EEG/MEG forward and inverse solutions were found, usually in temporal regions. Nevertheless, accurate modeling of the skull is one of the most important (and due to its bad MRI contrast also one of the most challenging) aspects of head volume conductor generation (Nielsen et al., 2018).
As a side effect, the results in Engwer*, **Vorwerk***, et al. (2017) and **Vorwerk** et al. (2016, 2018) already demonstrated that modeling the skin too thin or too thick severely affects the accuracy of EEG forward solutions (Sec. 3.2, 5.2). The severe influence of skull modeling defects on EEG source analysis was in detail shown by Lanfer et al. (2012) and Montes-Restrepo et al. (2014), whereas only a minor influence on MEG source analysis is assumed (Broek et al., 1998). However, Nielsen et al. (2018) demonstrated that modern segmentation algorithms - especially when combined with optimized MRI sequences -

obtain highly accurate representations of the skull, so that an inaccurate representation of the skull can be avoided.

Several studies have furthermore shown that besides an accurate geometric representation, the choice of skull conductivity has a strong influence on EEG source analysis (Sec. 4.2; Akalin Acar and Makeig 2013; Aydin, **Vorwerk**, et al. 2014; Chen et al. 2010; Gençer and Acar 2004; Vallaghé and Clerc 2008; Vanrumste et al. 2000). These studies showed that variations of the skull conductivity have the strongest influence on EEG forward solutions, especially regarding signal topography. Furthermore, a significant influence was also found for variations of the skin conductivity and of simultaneous variations of skull and skin conductivity. For quasi-tangential sources on sulcal walls, which represent a large portion of cortical sources, these variations mainly result in changes in the depth of the source localization up to a few centimeters. Furthermore, it was found that the correlation of skin and skull conductivity variations with the reconstructed source depth have opposite signs. Therefore, the effects might partially cancel out or even amplify depending on the specific variations. For sources on top of gyri and at the bottom of sulci, only a smaller change of source localization was observed.

Only few similarly detailed sensitivity studies have been performed for MEG source analysis. Gençer and Acar (2004) found that MEG forward simulations are mostly sensitive towards conductivity variations in the vicinity of the source, whereas changes in skin and skull conductivity did not have a major influence. These results help to understand the only small effects of skull modeling defects on the MEG forward solution found by Piastra et al. (2018). However, additional studies investigating the sensitivity of MEG source analysis to tissue conductivity uncertainties are desirable, especially also taking into account the characteristics of different existing (magnetometer, radial and tangential gradiometers) and newly developed (optically pumped magnetometers) sensor types.

The results of these sensitivity studies motivate the use of combined EEG/MEG source analysis as demonstrated in Aydin, **Vorwerk**, et al. (2015, 2014). Whereas MEG source analysis is assumed to be only slightly affected by conductivity uncertainties but cannot reliably reconstruct quasi-radial sources due to their weak MEG signal, the EEG source analysis only showed small deviations in source localization for those source positions that usually lead to quasi-radial sources.

However, to reliably perform combined EEG/MEG source analysis as a joint analysis, it is advisable to in advance perform a (skull) conductivity calibration. This can for example be performed based on a combined EEG/MEG measurement of SEPs or electrical impedance tomography (EIT) (Sec. 5.1.1; Aydin, **Vorwerk**, et al. 2014; Fernández-Corazza et al. 2017; Wolters et al. 2010). The performed sensitivity studies help to understand the potential and limits of EEG/MEG-based conductivity calibration. The strong influence of skull conductivity on the EEG signal topography found in these studies confirms the choice of this parameter as the primary target for conductivity calibration. Whereas skin

conductivity was also found to have a strong influence, it has to be assumed that the effects of skin and skull conductivity variations cannot be easily separated. In turn, it could be assumed that the effect of skin conductivity variations can already be compensated when fitting only the skull conductivity so that it might be unnecessary to add the skin conductivity as a second parameter to be fitted. The same might be true for the usually omitted modeling of the dura mater, which has also been shown to potentially have a non-negligible influence on EEG/MEG source analysis (Sec. 4.1.2; Fiederer, **Vorwerk**, et al. 2016). The influence of gray and white matter conductivity variations on the EEG signal topography is probably too small for reliable conductivity estimation. However, the influence of the gray matter conductivity on the magnitude and orientation of the reconstructed source for the EEG might offer a possibility for conductivity estimation. As Gençer and Acar (2004) found that also the MEG forward solution is sensitive to gray matter conductivity variations, it is not clear yet if such an approach could actually work in practice though. Therefore, the potential for improvements in EEG/MEG-based conductivity fitting should be investigated in future studies.

7.3 Applications

At the time of publication of the respective studies, the detailed six-layer head volume conductor model used in Cho, **Vorwerk**, et al. (2015) and **Vorwerk** et al. (2014) could only be created involving time-consuming manual corrections. Thus, these studies demonstrated the benefit/necessity of accurate head volume conductor modeling, but only few researchers had the resources to include such detailed head volume conductor models in their studies. Furthermore, while freely accessible under an open-source license, the FEM tools available at that time were not user-friendly and required advanced knowledge. Nevertheless, these studies allowed researchers to estimate the errors introduced by simplifications of the head volume conductor model in detail so that these could be considered in their analysis.
Aydin, **Vorwerk**, et al. (2015, 2014) demonstrated the possibility and benefits of performing combined EEG/MEG source analysis based on individually generated highly-detailed six-compartment head volume conductor models in PED. However, also the modeling pipeline derived for these studies still consisted of a variety of tools and scripts that needed to be combined manually.
Fortunately, since then huge improvements have been made regarding the user-friendly creation of highly accurate head volume conductor models and computation of FEM-based EEG/MEG forward solutions. Whereas the FieldTrip-SimBio pipeline (Sec. 5.2; **Vorwerk** et al. 2018) improved over the at that time state-of-the-art, but relied on rather basic head volume conductor models, nowadays open-source solutions that automatically generate highly-realistic head volume conductor models area available (Huang et al., 2019; Nielsen et al., 2018; Puonti et al., 2020) and modern FEM approaches are directly integrated

into several open-source toolboxes for EEG/MEG analysis (Medani et al., 2023; **Vorwerk** et al., 2018). Furthermore, also commercial toolboxes such as BESA (https://www.besa.de) and CURRY (https://compumedicsneuroscan.com/products/curry/) now implemented FEM-computed forward solutions.
Further improvements in automated head volume conductor model generation can be expected both through technical and methodological advancements, such as the growing availability of 7T MRI scanners and novel approaches for MRI segmentation, e.g., based on neural networks. Therefore, the consideration of further structures in head volume conductor models such as blood vessels, dura mater, or skull sutures, which for now could only be performed in single-subject studies (Sec. 4.1.2; Fiederer, **Vorwerk**, et al. 2016; Lew et al. 2013; McCann and Beltrachini 2022), could become more widespread in the future.
Despite the proven benefit of combined EEG/MEG source analysis, an increased application is currently not only limited by the additional measurement effort but also by the lack of access to MEG measurements in many research institutions. This is largely due to the currently high costs of maintaining an MEG system, which are often not considered to be justified by the expected benefits. Currently, MEG devices are mainly available at university hospitals or research centers, and only about 200 MEGs exist worldwide. However, MEG is becoming available at rapidly decreasing costs with new generations of optically pumped magnetometers (Labyt et al., 2018). New MEG systems based on OPMs might reduce hardware costs to about 400k €, which will enable MEG measurements also in smaller hospitals and research centers, where currently only EEG is available. In consequence, the use of combined EEG/MEG will potentially become much more accessible in the near future. Therefore, further research investigating the different sensitivity of EEG and MEG and how to optimally combine EEG and MEG in source analysis should be performed to advance applications such as PED.

7.4 Brain Stimulation

Due to the similarity of the underlying mathematical equations, the simulation and optimization of electric and magnetic brain stimulation can profit from insights and methods obtained in the research of EEG/MEG source analysis and vice versa. Therefore, brain stimulation was also treated as a side aspect within this thesis. For example, the core of the FEM implementation in the popular LeadDBS toolbox (Horn et al., 2019) is taken from the FieldTrip-SimBio pipeline (Sec. 5.2) and the pipeline for head volume conductor generation presented in Puonti et al. (2020), which is highly useful for EEG/MEG source analysis, was initiated in a research group focusing on brain stimulation research.
An accurate and detailed simulation of the electric currents within the brain might be even more important to understand and optimize both invasive and non-invasive brain

stimulation than in EEG/MEG source analysis. Especially for DBS, highly accurate simulations are assumed to be important, since huge gradients of the electric field occur around the stimulating electrodes, which is also the region of interest for estimating stimulation effects. More accurate simulations might help to improve the estimates of brain activation, which are derived based on simulations of the electric fields within the brain (Duffley et al., 2019). These estimates are fundamental, e.g., in the optimization of brain stimulation (Sec. 6.1.1; Anderson et al. 2018; **Vorwerk** et al. 2019b), explorative simulation studies (Anderson et al., 2019), or connectomic DBS (Horn, 2021; Horn et al., 2017). Therefore, possible benefits of an application of the current-preserving FEM approaches presented in Sec. 3.2 in the simulation of brain stimulation should be evaluated and first steps in this direction were recently taken (Schwendinger, 2024).

Besides the transfer of novel methodologies, coherent findings in sensitivity studies can also increase confidence in these results. For example, the effects of head volume conductor model detail described for tDCS simulations in Wagner et al. (2013) help to better understand the results of **Vorwerk** et al. (2014). Similarly, the effects of tissue conductivity uncertainties described for EEG source analysis (**Vorwerk** et al., 2019a, 2024) and tDCS (Saturnino et al., 2019; Schmidt et al., 2015) complement each other.

Looking forward, EEG/MEG and brain stimulation might not only complement each other in method development and sensitivity studies but also in practical applications. Already nowadays, EEG/MEG is used to retrospectively better understand the effects of brain stimulation (Litvak et al., 2021; Oswal et al., 2016), and the other way around EEG/MEG might also help to prospectively improve brain stimulation results by providing accurate, individual stimulation targets or individually adjusted head tissue conductivities for subsequent optimizations of stimulation patterns (Antonakakis et al., 2024; Khan et al., 2023).

8 Conclusion

The studies presented in this thesis considered different aspects influencing the accuracy of bioelectromagnetic field simulations in the human head with a focus on the accuracy of EEG/MEG source analysis. It was demonstrated that state-of-the-art FEM approaches reliably achieve high numerical accuracies. These approaches should optimally be used in combination with five- or six-compartment or even more detailed realistic head volume conductor models, which can nowadays easily be generated with automated pipelines. With technological and methodological improvements, it might be possible in the future to automatically generate even more accurate head volume conductor models.

Inter-individual variations of head tissue conductivities, particularly of the skull conductivity, remain a major source of uncertainty in EEG source analysis. Therefore, combined EEG/MEG source analysis and the use of head tissue conductivity calibration are recommendable whenever possible. Furthermore, approaches to determine and visualize the uncertainty in EEG/MEG source analysis resulting from tissue conductivity variations have been presented and could help to better consider these uncertainties in the evaluation of EEG/MEG source analysis results in the future.

The practicability and benefit of highly-detailed head volume conductor models, combined EEG/MEG source analysis, and skull conductivity calibration were demonstrated for an example from PED. Furthermore, an open-source toolbox to easily generate detailed head volume conductor models and FEM-calculated EEG forward solutions was presented, and progress in this area of research was discussed. Besides, applications based on bioelectromagnetic field simulations in the related field of brain stimulation were presented and the translatability of results between EEG/MEG source analysis and brain stimulation was discussed.

Future research should, amongst others, include in-depth research on the sensitivity of MEG source analysis to conductivity uncertainties, which could guide the further development of EEG/MEG-based conductivity calibration. Making the estimation and visualization of uncertainties accessible in (clinical) practice would result in better interpretability of EEG/MEG source analysis results. Several of the results and methods obtained for EEG/MEG source analysis could also be beneficial for other applications such as brain stimulation. For example, the use of current-preserving FEM approaches might help to

improve the accuracy of the simulation and optimization of brain stimulation. Such efforts could help to further increase the reliability of bioelectromagnetic field simulations in practice and advance neuroscience through, e.g., further improved EEG/MEG source analysis and accurately targeted brain stimulation.

Acknowledgments

I would like to thank all the wonderful people - be it scientists, family, or friends - without whom I would not be where I am today. My special thanks go to

- Carsten Wolters, Chris Butson, and Daniel Baumgarten for giving me the opportunity to be part of their research groups, their mentorship, and encouragement. Without them I would not have been able to pursue this scientific career.
- All the cooperation partners and collaborators with whom I have worked together, as co-authors on joint papers or in other research projects. Without them this habilitation would not have been possible.
- All the colleagues that made working at the IBB, SCI Institute, UMIT TIROL, and University of Innsbruck so fruitful and enjoyable.
- My parents and siblings for their support at all times.
- Victoria for everything, but especially your support, love and positive energy.

Furthermore, I am grateful to the German Research Foundation (DFG), mainly projects WO1425/2-1 and WO1425/5-1, US IGNITE, project 10037840, and the Austrian Science Fund (FWF), projects I 3790-B27 and especially P35949, for providing funding during my career and allowing me to focus on this research.

Bibliography

Akalin Acar, Z. and S. Makeig (2013). "Effects of forward model errors on EEG source localization". In: *Brain Topography* 26, pp. 378–396.

Akhtari, M., H. Bryant, A. Mamelak, E. Flynn, L. Heller, J. Shih, M. Mandelkem, A. Matlachov, D. Ranken, E. Best, M. DiMauro, R. Lee, and W. Sutherling (2002). "Conductivities of three-layer live human skull". In: *Brain Topography* 14, pp. 151–167.

Anderson, D. N., G. Duffley, **J. Vorwerk**, A. D. Dorval, and C. R. Butson (2019). "Anodic stimulation misunderstood: preferential activation of fiber orientations with anodic waveforms in deep brain stimulation". In: *Journal of Neural Engineering* 16.1, p. 016026.

Anderson, D. N., B. Osting, **J. Vorwerk**, A. D. Dorval, and C. R. Butson (2018). "Optimized programming algorithm for cylindrical and directional deep brain stimulation electrodes". In: *Journal of Neural Engineering* 15.2, p. 026005.

Antonakakis, M., F. Kaiser, S. Rampp, S. Kovac, H. Wiendl, W. Stummer, J. Gross, C. Kellinghaus, M. Khaleghi-Ghadiri, G. Möddel, and C. H. Wolters (2024). "Targeted and optimized multi-channel transcranial direct current stimulation for focal epilepsy: An N-of-1 trial". In: *Brain Stimulation: Basic, Translational, and Clinical Research in Neuromodulation*.

Antonakakis, M., S. Schrader, Ü. Aydin, A. Khan, J. Gross, M. Zervakis, S. Rampp, and C. H. Wolters (2020). "Inter-Subject Variability of Skull Conductivity and Thickness in Calibrated Realistic Head Models". In: *NeuroImage* 223, p. 117353.

Aydin, Ü., **J. Vorwerk**, M. Dümpelmann, P. Küpper, H. Kugel, M. Heers, J. Wellmer, C. Kellinghaus, J. Haueisen, S. Rampp, H. Stefan, and C. H. Wolters (2015). "Combined EEG/MEG can outperform single modality EEG or MEG source reconstruction in presurgical epilepsy diagnosis". In: *PloS one* 10.3, e0118753.

Aydin, Ü., **J. Vorwerk**, P. Küpper, M. Heers, H. Kugel, A. Galka, L. Hamid, J. Wellmer, C. Kellinghaus, S. Rampp, H. Stefan, and C. H. Wolters (2014). "Combining EEG and MEG for the reconstruction of epileptic activity using a calibrated realistic volume conductor model". In: *PloS one* 9.3, e93154.

Azizollahi, H., A. Aarabi, and F. Wallois (2020). "Effect of structural complexities in head modeling on the accuracy of EEG source localization in neonates". In: *Journal of Neural Engineering* 17.5, p. 056004.

Baccala, L. A., K. Sameshima, and D. Y. Takahashi (2007). "Generalized partial directed coherence". In: *2007 15th International conference on digital signal processing*. IEEE, pp. 163–166.

Baillet, S., L. Garnero, G. Marin, and J.-P. Hugonin (1999). "Combined MEG and EEG source imaging by minimization of mutual information". In: *IEEE Transactions on Biomedical Engineering* 46.5, pp. 522–534.

Barkley, G. L. and C. Baumgartner (2003). "MEG and EEG in epilepsy". In: *Journal of Clinical Neurophysiology* 20.3, pp. 163–178.

Bauer, M., S. Pursiainen, **J. Vorwerk**, H. Köstler, and C. H. Wolters (2015). "Comparison study for Whitney (Raviart–Thomas)-type source models in finite-element-method-based EEG forward modeling". In: *IEEE Transactions on Biomedical Engineering* 62.11, pp. 2648–2656.

Baumann, S. B., D. R. Wozny, S. K. Kelly, and F. M. Meno (1997). "The electrical conductivity of human cerebrospinal fluid at body temperature". In: *IEEE Transactions on Biomedical Engineering* 44.3, pp. 220–223.

Beltrachini, L. (2019). "The analytical subtraction approach for solving the forward problem in EEG". In: *Journal of Neural Engineering* 16.5, p. 056029.

Berger, H. (1929). "Über das Elektroenkephalogramm des Menschen". In: *Archiv für Psychiatrie und Nervenkrankheiten* 87.1, pp. 527–570.

Braess, D. (2007). *Finite elements: Theory, fast solvers, and applications in solid mechanics*. Cambridge University Press.

Broek, S. P. van den, F. Reinders, M. Donderwinkel, and M. Peters (1998). "Volume conduction effects in EEG and MEG". In: *Electroencephalography and Clinical Neurophysiology* 106.6, pp. 522–534.

Buchner, H., G. Knoll, M. Fuchs, A. Rienäcker, R. Beckmann, M. Wagner, J. Silny, and J. Pesch (1997). "Inverse localization of electric dipole current sources in finite element models of the human head". In: *Electroencephalography and clinical Neurophysiology* 102.4, pp. 267–278.

Buchner, H., T. D. Waberski, M. Fuchs, H. .-A. Wischmann, M. Wagner, and R. Drenckhahn (1995). "Comparison of realistically shaped boundary-element and spherical head models in source localization of early somatosensory evoked potentials". In: *Brain Topography* 8, pp. 137–143.

Butson, C. R., G. Tamm, S. Jain, T. Fogal, and J. Krüger (2012). "Evaluation of interactive visualization on mobile computing platforms for selection of deep brain stimulation parameters". In: *IEEE Transactions on Visualization and Computer Graphics* 19.1, pp. 108–117.

Calvetti, D., H. Hakula, S. Pursiainen, and E. Somersalo (2009). "Conditionally Gaussian hypermodels for cerebral source localization". In: *SIAM Journal on Imaging Sciences* 2.3, pp. 879–909.

Chen, F., H. Hallez, and S. Staelens (2010). "Influence of skull conductivity perturbations on EEG dipole source analysis". In: *Medical Physics* 37.8, pp. 4475–4484.

Cho, J.-H., **J. Vorwerk**, C. H. Wolters, and T. R. Knösche (2015). "Influence of the head model on EEG and MEG source connectivity analyses". In: *NeuroImage* 110, pp. 60–77.

Cohen, D. and B. Cuffin (1987). "A method for combining MEG and EEG to determine the sources". In: *Physics in Medicine & Biology* 32.1, p. 85.

Cohen, D. (1968). "Magnetoencephalography: evidence of magnetic fields produced by alpha-rhythm currents". In: *Science* 161.3843, pp. 784–786.

Cohen, D. (1972). "Magnetoencephalography: detection of the brain's electrical activity with a superconducting magnetometer". In: *Science* 175.4022, pp. 664–666.

Costa, F., H. Batatia, T. Oberlin, C. d'Giano, and J.-Y. Tourneret (2017). "Bayesian EEG source localization using a structured sparsity prior". In: *NeuroImage* 144, pp. 142–152.

Dannhauer, M., B. Lanfer, C. H. Wolters, and T. R. Knösche (2011). "Modeling of the human skull in EEG source analysis". In: *Human Brain Mapping* 32.9, pp. 1383–1399.

Dassios, G., A. S. Fokas, and D. Hadjiloizi (2007). "On the complementarity of electroencephalography and magnetoencephalography". In: *Inverse Problems* 23.6, p. 2541.

De Munck, J. C., B. W. Van Dijk, and H. Spekreijse (1988). "Mathematical dipoles are adequate to describe realistic generators of human brain activity". In: *IEEE Transactions on Biomedical Engineering* 35.11, pp. 960–966.

Delorme, A. and S. Makeig (2004). "EEGLAB: an open source toolbox for analysis of single-trial EEG dynamics including independent component analysis". In: *Journal of Neuroscience Methods* 134.1, pp. 9–21.

Deuschl, G., C. Schade-Brittinger, P. Krack, J. Volkmann, H. Schäfer, K. Bötzel, C. Daniels, A. Deutschländer, U. Dillmann, W. Eisner, et al. (2006). "A randomized trial of deep-brain stimulation for Parkinson's disease". In: *New England Journal of Medicine* 355.9, pp. 896–908.

Dimakopoulos, V. S., M. Antonakakis, G. Moeddel, J. Wellmer, S. Rampp, M. Zervakis, and C. H. Wolters (2019). "Combined EEG/MEG Source Reconstruction of Epileptic Activity using a Two-Phase Spike Clustering Approach". In: *2019 IEEE 19th International Conference on Bioinformatics and Bioengineering (BIBE)*. IEEE, pp. 877–881.

Drechsler, F., C. H. Wolters, T. Dierkes, H. Si, and L. Grasedyck (2009). "A full subtraction approach for finite element method based source analysis using constrained Delaunay tetrahedralisation". In: *NeuroImage* 46.4, pp. 1055–1065.

Duffley, G., D. N. Anderson, **J. Vorwerk**, A. D. Dorval, and C. R. Butson (2019). "Evaluation of methodologies for computing the deep brain stimulation volume of tissue activated". In: *Journal of Neural Engineering* 16.6, p. 066024.

Engwer*, C., **J. Vorwerk***, J. Ludewig, and C. H. Wolters (2017). "A discontinuous Galerkin method to solve the EEG forward problem using the subtraction approach". In: *SIAM Journal on Scientific Computing* 39.1, B138–B164. **The first two authors contributed equally to this work.*

Erdbrügger, T., A. Westhoff, M. Höltershinken, J.-O. Radecke, Y. Buschermöhle, A. Buyx, F. Wallois, S. Pursiainen, J. Gross, R. Lencer, C. Engwer, and C. H. Wolters (2023). "CutFEM forward modeling for EEG source analysis". In: *Frontiers in Human Neuroscience* 17.

Esch, L., C. Dinh, E. Larson, D. Engemann, M. Jas, S. Khan, A. Gramfort, and M. S. Hämäläinen (2019). "MNE: software for acquiring, processing, and visualizing MEG/EEG data". In: *Magnetoencephalography: From Signals to Dynamic Cortical Networks*, pp. 355–371.

Fernández-Corazza, M., S. Turovets, P. Luu, N. Price, C. H. Muravchik, and D. Tucker (2017). "Skull modeling effects in conductivity estimates using parametric electrical impedance tomography". In: *IEEE Transactions on Biomedical Engineering* 65.8, pp. 1785–1797.

Fiederer, L. D. J., **J. Vorwerk**, F. Lucka, M. Dannhauer, S. Yang, M. Dümpelmann, A. Schulze-Bonhage, A. Aertsen, O. Speck, C. H. Wolters, and T. Ball (2016). "The role of blood vessels in high-resolution volume conductor head modeling of EEG". In: *NeuroImage* 128, pp. 193–208.

Fischer, M. J., G. Scheler, and H. Stefan (2005). "Utilization of magnetoencephalography results to obtain favourable outcomes in epilepsy surgery". In: *Brain* 128.1, pp. 153–157.

Fuchs, M., J. Kastner, R. Tech, M. Wagner, and F. Gasca (2017). "MEG and EEG dipole clusters from extended cortical sources". In: *Biomedical Engineering Letters* 7.3, pp. 185–191.

Fuchs, M., M. Wagner, and J. Kastner (2001). "Boundary element method volume conductor models for EEG source reconstruction". In: *Clinical Neurophysiology* 112.8, pp. 1400–1407.

Fuchs, M., M. Wagner, and J. Kastner (2004). "Confidence limits of dipole source reconstruction results". In: *Clinical Neurophysiology* 115.6, pp. 1442–1451.

Fuchs, M., M. Wagner, H.-A. Wischmann, T. Köhler, A. Theißen, R. Drenckhahn, and H. Buchner (1998). "Improving source reconstructions by combining bioelectric and biomagnetic data". In: *Electroencephalography and Clinical Neurophysiology* 107.2, pp. 93–111.

Gao, C., S. Conte, J. E. Richards, W. Xie, and T. Hanayik (2019). "The neural sources of N170: Understanding timing of activation in face-selective areas". In: *Psychophysiology* 56.6, e13336.

Gençer, N. G. and C. E. Acar (2004). "Sensitivity of EEG and MEG measurements to tissue conductivity". In: *Physics in Medicine & Biology* 49.5, p. 701.

Geselowitz, D. B. (1967). "On bioelectric potentials in an inhomogeneous volume conductor". In: *Biophysical Journal* 7.1, pp. 1–11.

Gramfort, A., M. Luessi, E. Larson, D. A. Engemann, D. Strohmeier, C. Brodbeck, R. Goj, M. Jas, T. Brooks, L. Parkkonen, and M. Hämäläinen (2013). "MEG and EEG data analysis with MNE-Python". In: *Frontiers in Neuroscience*, p. 267.

Grosse-Wentrup, M., C. Liefhold, K. Gramann, and M. Buss (2009). "Beamforming in noninvasive brain–computer interfaces". In: *IEEE Transactions on Biomedical Engineering* 56.4, pp. 1209–1219.

Güllmar, D., J. Haueisen, and J. R. Reichenbach (2010). "Influence of anisotropic electrical conductivity in white matter tissue on the EEG/MEG forward and inverse solution. A high-resolution whole head simulation study". In: *NeuroImage* 51.1, pp. 145–163.

Hamalainen, M. S. and J. Sarvas (1989). "Realistic conductivity geometry model of the human head for interpretation of neuromagnetic data". In: *IEEE Transactions on Biomedical Engineering* 36.2, pp. 165–171.

Hämäläinen, M. S., R. Hari, R. J. Ilmoniemi, J. Knuutila, and O. V. Lounasmaa (1993). "Magnetoencephalography — theory, instrumentation, and applications to noninvasive studies of the working human brain". In: *Reviews of modern Physics* 65.2, p. 413.

Hämäläinen, M. S. and R. J. Ilmoniemi (1994). "Interpreting magnetic fields of the brain: minimum norm estimates". In: *Medical & Biological Engineering & Computing* 32.1, pp. 35–42.

Haueisen, J., C. Ramon, M. Eiselt, H. Brauer, and H. Nowak (1997). "Influence of tissue resistivities on neuromagnetic fields and electric potentials studied with a finite element model of the head". In: *IEEE Transactions on Biomedical Engineering* 44.8, pp. 727–735.

He, Q., A. Rezaei, and S. Pursiainen (2020). "Zeffiro user interface for electromagnetic brain imaging: a GPU accelerated FEM tool for forward and inverse computations in Matlab". In: *Neuroinformatics* 18, pp. 237–250.

Hoekema, R., G. Wieneke, F. Leijten, C. Van Veelen, P. Van Rijen, G. Huiskamp, J. Ansems, and A. Van Huffelen (2003). "Measurement of the conductivity of skull, temporarily removed during epilepsy surgery". In: *Brain Topography* 16.1, pp. 29–38.

Höltershinken, M., P. Lange, T. Erdbrügger, Y. Buschermöhle, F. Wallois, A. Buyx, S. Pursiainen, **J. Vorwerk**, C. Engwer, and C. H. Wolters (2023). "The localized subtraction approach for EEG and MEG forward modeling". In: *arXiv preprint arXiv:2302.12785*.

Horn, A. (2021). *Connectomic deep brain stimulation*. Academic Press.

Horn, A., N. Li, T. A. Dembek, A. Kappel, C. Boulay, S. Ewert, A. Tietze, A. Husch, T. Perera, W.-J. Neumann, M. Reisert, H. Si, R. Oostenveld, C. Rorden, F.-C. Yeh, Q. Fang, T. M. Herrington, J. Vorwerk, and A. A. Kühn (2019). "Lead-DBS v2: Towards a comprehensive pipeline for deep brain stimulation imaging". In: *NeuroImage* 184, pp. 293–316.

Horn, A., M. Reich, **J. Vorwerk**, N. Li, G. Wenzel, Q. Fang, T. Schmitz-Hübsch, R. Nickl, A. Kupsch, J. Volkmann, A. A. Kühn, and M. D. Fox (2017). "Connectivity predicts

deep brain stimulation outcome in P arkinson disease". In: *Annals of Neurology* 82.1, pp. 67–78.

Huang, M.-X., T. Song, D. J. Hagler Jr, I. Podgorny, V. Jousmaki, L. Cui, K. Gaa, D. L. Harrington, A. M. Dale, R. R. Lee, J. Elman, and E. Halgren (2007). "A novel integrated MEG and EEG analysis method for dipolar sources". In: *NeuroImage* 37.3, pp. 731–748.

Huang, Y., A. Datta, M. Bikson, and L. C. Parra (2019). "Realistic volumetric-approach to simulate transcranial electric stimulation—ROAST—a fully automated open-source pipeline". In: *Journal of Neural Engineering* 16.5, p. 056006.

Huang, Y., L. C. Parra, and S. Haufe (2016). "The New York Head—A precise standardized volume conductor model for EEG source localization and tES targeting". In: *NeuroImage* 140, pp. 150–162.

Iwasaki, M., E. Pestana, R. C. Burgess, H. O. Lüders, H. Shamoto, and N. Nakasato (2005). "Detection of epileptiform activity by human interpreters: blinded comparison between electroencephalography and magnetoencephalography". In: *Epilepsia* 46.1, pp. 59–68.

Jackson, J. D. (2021). *Classical electrodynamics*. John Wiley & Sons.

Jerbi, K., S. Baillet, J. C. Mosher, G. Nolte, L. Garnero, and R. M. Leahy (2004). "Localization of realistic cortical activity in MEG using current multipoles". In: *NeuroImage* 22.2, pp. 779–793.

Khan, A., M. Antonakakis, S. Suntrup-Krueger, R. Lencer, M. A. Nitsche, W. Paulus, J. Groß, and C. H. Wolters (2023). "Can individually targeted and optimized multi-channel tDCS outperform standard bipolar tDCS in stimulating the primary somatosensory cortex?" In: *Brain Stimulation* 16.1, pp. 1–16.

Knösche, T. R. and J. Haueisen (2022). *EEG/MEG Source Reconstruction: Textbook for Electro-and Magnetoencephalography*. Springer.

Köstler, H., C. Möller, J. Härdtlein, and A. Anwander (2007). "Numerical approaches for dipole modeling in finite element method based source analysis". In: *International Congress Series*. Vol. 1300. Elsevier, pp. 189–192.

Krauss, J. K., N. Lipsman, T. Aziz, A. Boutet, P. Brown, J. W. Chang, B. Davidson, W. M. Grill, M. I. Hariz, A. Horn, et al. (2021). "Technology of deep brain stimulation: current status and future directions". In: *Nature Reviews Neurology* 17.2, pp. 75–87.

Kreidenhuber, R., X. De Tiège, and S. Rampp (2019). "Presurgical functional cortical mapping using electromagnetic source imaging". In: *Frontiers in Neurology* 10, p. 628.

Kybic, J., M. Clerc, T. Abboud, O. Faugeras, R. Keriven, and T. Papadopoulo (2005). "A common formalism for the integral formulations of the forward EEG problem". In: *IEEE Transactions on Medical Imaging* 24.1, pp. 12–28.

Labyt, E., M.-C. Corsi, W. Fourcault, A. P. Laloy, F. Bertrand, F. Lenouvel, G. Cauffet, M. Le Prado, F. Berger, and S. Morales (2018). "Magnetoencephalography with optically

pumped 4 He magnetometers at ambient temperature". In: *IEEE Transactions on Medical Imaging* 38.1, pp. 90–98.

Lanfer, B., M. Scherg, M. Dannhauer, T. R. Knösche, M. Burger, and C. H. Wolters (2012). "Influences of skull segmentation inaccuracies on EEG source analysis". In: *NeuroImage* 62.1, pp. 418–431.

Lee, D. J., C. S. Lozano, R. F. Dallapiazza, and A. M. Lozano (2019). "Current and future directions of deep brain stimulation for neurological and psychiatric disorders: JNSPG 75th Anniversary Invited Review Article". In: *Journal of Neurosurgery* 131.2, pp. 333–342.

Lew, S., D. D. Sliva, M.-s. Choe, P. E. Grant, Y. Okada, C. H. Wolters, and M. S. Hämäläinen (2013). "Effects of sutures and fontanels on MEG and EEG source analysis in a realistic infant head model". In: *NeuroImage* 76, pp. 282–293.

Lew, S., C. Wolters, T. Dierkes, C. Röer, and R. MacLeod (2009). "Accuracy and run-time comparison for different potential approaches and iterative solvers in finite element method based EEG source analysis". In: *Applied Numerical Mathematics* 59.8, pp. 1970–1988.

Litvak, V., E. Florin, G. Tamás, S. Groppa, and M. Muthuraman (2021). "EEG and MEG primers for tracking DBS network effects". In: *NeuroImage* 224, p. 117447.

Lucka, F., S. Pursiainen, M. Burger, and C. H. Wolters (2012). "Hierarchical Bayesian inference for the EEG inverse problem using realistic FE head models: depth localization and source separation for focal primary currents". In: *NeuroImage* 61.4, pp. 1364–1382.

Lunkenheimer, P. (2021). "Comparison of Boundary Element Fast Multipole and Finite Element Methods for the solution of the EEG forward problem". Master's thesis in Mathematics. University of Münster. URL: http://www.sci.utah.edu/~wolters/PaperWolters/2021/MasterLunkenheimer.pdf.

Makarov, S. N., M. Hämäläinen, Y. Okada, G. M. Noetscher, J. Ahveninen, and A. Nummenmaa (2020). "Boundary element fast multipole method for enhanced modeling of neurophysiological recordings". In: *IEEE Transactions on Biomedical Engineering* 68.1, pp. 308–318.

Makeig, S., M. Westerfield, T.-P. Jung, S. Enghoff, J. Townsend, E. Courchesne, and T. J. Sejnowski (2002). "Dynamic brain sources of visual evoked responses". In: *Science* 295.5555, pp. 690–694.

McCann, H. and L. Beltrachini (2022). "Impact of skull sutures, spongiform bone distribution, and aging skull conductivities on the EEG forward and inverse problems". In: *Journal of Neural Engineering* 19.1, p. 016014.

McCann, H., G. Pisano, and L. Beltrachini (2019). "Variation in reported human head tissue electrical conductivity values". In: *Brain Topography* 32.5, pp. 825–858.

Medani, T., J. Garcia-Prieto, F. Tadel, M. Antonakakis, T. Erdbrügger, M. Höltershinken, W. Mead, S. Schrader, A. Joshi, C. Engwer, C. H. Wolters, J. C. Mosher, and R. M.

Leahy (2023). “Brainstorm-DUNEuro: An integrated and user-friendly Finite Element Method for modeling electromagnetic brain activity”. In: *NeuroImage* 267, p. 119851.

Meijs, J. W., O. W. Weier, M. J. Peters, and A. Van Oosterom (1989). “On the numerical accuracy of the boundary element method (EEG application)”. In: *IEEE Transactions on Biomedical Engineering* 36.10, pp. 1038–1049.

Miinalainen, T., A. Rezaei, D. Us, A. Nüßing, C. Engwer, C. H. Wolters, and S. Pursiainen (2019). “A realistic, accurate and fast source modeling approach for the EEG forward problem”. In: *NeuroImage* 184, pp. 56–67.

Montes-Restrepo, V., P. van Mierlo, G. Strobbe, S. Staelens, S. Vandenberghe, and H. Hallez (2014). “Influence of skull modeling approaches on EEG source localization”. In: *Brain Topography* 27, pp. 95–111.

Mosher, J. C., P. S. Lewis, and R. M. Leahy (1992). “Multiple dipole modeling and localization from spatio-temporal MEG data”. In: *IEEE Transactions on Biomedical Engineering* 39.6, pp. 541–557.

Murakami, S. and Y. Okada (2006). “Contributions of principal neocortical neurons to magnetoencephalography and electroencephalography signals”. In: *The Journal of Physiology* 575.3, pp. 925–936.

Neugebauer, F., G. Möddel, S. Rampp, and C. H. Wolters (2017). “The effect of head model simplification on beamformer source localization”. In: *Frontiers in Neuroscience* 11, p. 299489.

Neymotin, S. A., D. S. Daniels, B. Caldwell, R. A. McDougal, N. T. Carnevale, M. Jas, C. I. Moore, M. L. Hines, M. Hämäläinen, and S. R. Jones (2020). “Human Neocortical Neurosolver (HNN), a new software tool for interpreting the cellular and network origin of human MEG/EEG data”. In: *Elife* 9, e51214.

Nielsen, J. D., K. H. Madsen, O. Puonti, H. R. Siebner, C. Bauer, C. G. Madsen, G. B. Saturnino, and A. Thielscher (2018). “Automatic skull segmentation from MR images for realistic volume conductor models of the head: Assessment of the state-of-the-art”. In: *NeuroImage* 174, pp. 587–598.

Nolte, G., O. Bai, L. Wheaton, Z. Mari, S. Vorbach, and M. Hallett (2004). “Identifying true brain interaction from EEG data using the imaginary part of coherency”. In: *Clinical Neurophysiology* 115.10, pp. 2292–2307.

Nolte, G. and G. Curio (1997). “On the calculation of magnetic fields based on multipole modeling of focal biological current sources”. In: *Biophysical Journal* 73.3, pp. 1253–1262.

Nüßing, A. (2018). “Fitted and Unitted Finite Element Methods for Solving the EEG Forward Problem”. PhD thesis. University of Münster. URL: http://www.sci.utah.edu/~wolters/PaperWolters/2018/Dissertation_AndreasNuessing.pdf.

Nüßing, A., C. H. Wolters, H. Brinck, and C. Engwer (2016). "The unfitted discontinuous Galerkin method for solving the EEG forward problem". In: *IEEE Transactions on Biomedical Engineering* 63.12, pp. 2564–2575.

Okada, Y. (1993). "Empirical bases for constraints in current-imaging algorithms". In: *Brain Topography* 5.4, pp. 373–377.

Olivares, E. I., J. Iglesias, C. Saavedra, N. J. Trujillo-Barreto, and M. Valdés-Sosa (2015). "Brain signals of face processing as revealed by event-related potentials". In: *Behavioural Neurology* 2015.

Ollikainen, J. O., M. Vauhkonen, P. A. Karjalainen, and J. P. Kaipio (1999). "Effects of local skull inhomogeneities on EEG source estimation". In: *Medical Engineering & Physics* 21.3, pp. 143–154.

Oostenveld, R., P. Fries, E. Maris, and J.-M. Schoffelen (2011). "FieldTrip: open source software for advanced analysis of MEG, EEG, and invasive electrophysiological data". In: *Computational Intelligence and Neuroscience* 2011, pp. 1–9.

Oswal, A., M. Beudel, L. Zrinzo, P. Limousin, M. Hariz, T. Foltynie, V. Litvak, and P. Brown (2016). "Deep brain stimulation modulates synchrony within spatially and spectrally distinct resting state networks in Parkinson's disease". In: *Brain* 139.5, pp. 1482–1496.

Pantev, C., M. Hoke, B. Lütkenhöner, and K. Lehnertz (1989). "Tonotopic organization of the auditory cortex: pitch versus frequency representation". In: *Science* 246.4929, pp. 486–488.

Pascual-Marqui, R. D. (1999). "Review of methods for solving the EEG inverse problem". In: *International Journal of Bioelectromagnetism* 1.1, pp. 75–86.

Peña, E., S. Zhang, S. Deyo, Y. Xiao, and M. D. Johnson (2017). "Particle swarm optimization for programming deep brain stimulation arrays". In: *Journal of Neural Engineering* 14.1, p. 016014.

Piastra, M. C., A. Nüßing, **J. Vorwerk**, H. Bornfleth, R. Oostenveld, C. Engwer, and C. H. Wolters (2018). "The discontinuous Galerkin finite element method for solving the MEG and the combined MEG/EEG forward problem". In: *Frontiers in Neuroscience* 12, p. 30.

Piastra, M. C., A. Nüßing, **J. Vorwerk**, M. Clerc, C. Engwer, and C. H. Wolters (2021). "A comprehensive study on electroencephalography and magnetoencephalography sensitivity to cortical and subcortical sources". In: *Human Brain Mapping* 42.4, pp. 978–992.

Plonsey, R. (1977). "Action potential sources and their volume conductor fields". In: *Proceedings of the IEEE* 65.5, pp. 601–611.

Pohlmeier, R., H. Buchner, G. Knoll, A. RienÄcker, R. Beckmann, and J. Pesch (1997). "The influence of skull-conductivity misspecification on inverse source localization in realistically shaped finite element head models". In: *Brain Topography* 9, pp. 157–162.

Puonti, O., K. Van Leemput, G. B. Saturnino, H. R. Siebner, K. H. Madsen, and A. Thielscher (2020). "Accurate and robust whole-head segmentation from magnetic resonance images for individualized head modeling". In: *NeuroImage* 219, p. 117044.

Pursiainen, S. (2012). "Raviart–Thomas-type sources adapted to applied EEG and MEG: implementation and results". In: *Inverse Problems* 28.6, p. 065013.

Pursiainen, S., A. Sorrentino, C. Campi, and M. Piana (2011). "Forward simulation and inverse dipole localization with the lowest order Raviart—Thomas elements for electroencephalography". In: *Inverse Problems* 27.4, p. 045003.

Pursiainen, S., **J. Vorwerk**, and C. H. Wolters (2016). "Electroencephalography (EEG) forward modeling via H (div) finite element sources with focal interpolation". In: *Physics in Medicine & Biology* 61.24, p. 8502.

Ramon, C., P. Schimpf, J. Haueisen, M. Holmes, and A. Ishimaru (2004). "Role of soft bone, CSF and gray matter in EEG simulations". In: *Brain Topography* 16, pp. 245–248.

Rezaei, A., M. Antonakakis, M. C. Piastra, C. H. Wolters, and S. Pursiainen (2020). "Parametrizing the Conditionally Gaussian Prior Model for Source Localization with Reference to the P20/N20 Component of Median Nerve SEP/SEF". In: *Brain Sciences* 10.12, p. 934.

Riera, J. J., T. Ogawa, T. Goto, A. Sumiyoshi, H. Nonaka, A. Evans, H. Miyakawa, and R. Kawashima (2012). "Pitfalls in the dipolar model for the neocortical EEG sources". In: *Journal of Neurophysiology* 108.4, pp. 956–975.

Rosenow, F. and H. Lüders (2001). "Presurgical evaluation of epilepsy". In: *Brain* 124.9, pp. 1683–1700.

Rullmann, M., A. Anwander, M. Dannhauer, S. K. Warfield, F. H. Duffy, and C. H. Wolters (2009). "EEG source analysis of epileptiform activity using a 1 mm anisotropic hexahedra finite element head model". In: *NeuroImage* 44.2, pp. 399–410.

Ryvlin, P., J. H. Cross, and S. Rheims (2014). "Epilepsy surgery in children and adults". In: *The Lancet Neurology* 13.11, pp. 1114–1126.

Salanova, V., T. Witt, R. Worth, T. R. Henry, R. E. Gross, J. M. Nazzaro, D. Labar, M. R. Sperling, A. Sharan, E. Sandok, et al. (2015). "Long-term efficacy and safety of thalamic stimulation for drug-resistant partial epilepsy". In: *Neurology* 84.10, pp. 1017–1025.

Sarvas, J. (1987). "Basic mathematical and electromagnetic concepts of the biomagnetic inverse problem". In: *Physics in Medicine & Biology* 32.1, p. 11.

Saturnino, G. B., A. Thielscher, K. H. Madsen, T. R. Knösche, and K. Weise (2019). "A principled approach to conductivity uncertainty analysis in electric field calculations". In: *NeuroImage* 188, pp. 821–834.

Scherg, M. and D. Von Cramon (1985). "A new interpretation of the generators of BAEP waves I–V: results of a spatio-temporal dipole model". In: *Electroencephalography and Clinical Neurophysiology/Evoked Potentials Section* 62.4, pp. 290–299.

Schmidt, C., P. Grant, M. Lowery, and U. van Rienen (2012). "Influence of uncertainties in the material properties of brain tissue on the probabilistic volume of tissue activated". In: *IEEE Transactions on Biomedical Engineering* 60.5, pp. 1378–1387.

Schmidt, C., S. Wagner, M. Burger, U. van Rienen, and C. H. Wolters (2015). "Impact of uncertain head tissue conductivity in the optimization of transcranial direct current stimulation for an auditory target". In: *Journal of Neural Engineering* 12.4, p. 046028.

Schoffelen, J.-M. and J. Gross (2009). "Source connectivity analysis with MEG and EEG". In: *Human Brain Mapping* 30.6, pp. 1857–1865.

Schrader, S., A. Westhoff, M. C. Piastra, T. Miinalainen, S. Pursiainen, **J. Vorwerk**, H. Brinck, C. H. Wolters, and C. Engwer (2021). "DUNEuro—A software toolbox for forward modeling in bioelectromagnetism". In: *PloS one* 16.6, e0252431.

Schupp, H. T., T. Flaisch, J. Stockburger, and M. Junghöfer (2006). "Emotion and attention: event-related brain potential studies". In: *Progress in Brain Research* 156, pp. 31–51.

Schwendinger, T. (2024). "Simulation von Tiefer Hirnstimulation mit einem Mixed-FEM-Ansatz". Master's thesis in Mechatronics. UMIT TIROL.

Sekihara, K. and S. S. Nagarajan (2008). *Adaptive spatial filters for electromagnetic brain imaging*. ISBN: 978-3642098277. Springer Science & Business Media.

Sonntag, H., **J. Vorwerk**, C. H. Wolters, L. Grasedyck, J. Haueisen, and B. Maeß (2013). "Leakage effect in hexagonal FEM meshes of the EEG forward problem". In: *International Conference on Basic and Clinical Multimodal Imaging (BaCI)*. Vol. 102.

Stenroos, M. and L. M. Koponen (2019). "Real-time computation of the TMS-induced electric field in a realistic head model". In: *NeuroImage* 203, p. 116159.

Stubbemann, R. (2021). "Application of the Mixed-FEM approach for the MEG-Problem". Master's thesis in Mathematics. University of Münster. URL: http://www.sci.utah.edu/~wolters/PaperWolters/2021/MasterStubbemann.pdf.

Tadel, F., S. Baillet, J. C. Mosher, D. Pantazis, and R. M. Leahy (2011). "Brainstorm: a user-friendly application for MEG/EEG analysis". In: *Computational Intelligence and Neuroscience* 2011, pp. 1–13.

Tanaka, N. and S. M. Stufflebeam (2014). "Clinical application of spatiotemporal distributed source analysis in presurgical evaluation of epilepsy". In: *Frontiers in Human Neuroscience* 8, p. 62.

Vallaghé, S. and M. Clerc (2008). "A global sensitivity analysis of three-and four-layer EEG conductivity models". In: *IEEE Transactions on Biomedical Engineering* 56.4, pp. 988–995.

Van Veen, B. D., W. Van Drongelen, M. Yuchtman, and A. Suzuki (1997). "Localization of brain electrical activity via linearly constrained minimum variance spatial filtering". In: *IEEE Transactions on Biomedical Engineering* 44.9, pp. 867–880.

Vanrumste, B., G. Van Hoey, R. Van de Walle, M. D'havé, I. Lemahieu, and P. Boon (2000). "Dipole location errors in electroencephalogram source analysis due to volume

conductor model errors". In: *Medical and Biological Engineering and Computing* 38, pp. 528–534.

Vorwerk, **J.** (2011). "Comparison of Numerical Approaches to the EEG Forward Problem". Diploma thesis in Mathematics. University of Münster. URL: http://www.sci.utah.edu/~wolters/PaperWolters/VorwerkDiplom.pdf.

Vorwerk, **J.** (2016). "New finite element methods to solve the EEG/MEG forward problem". PhD thesis. University of Münster. URL: https://www.sci.utah.edu/~wolters/PaperWolters/2016/Vorwerk_Dissertation_2016.pdf.

Vorwerk, **J.**, Ü. Aydin, C. H. Wolters, and C. R. Butson (2019a). "Influence of head tissue conductivity uncertainties on EEG dipole reconstruction". In: *Frontiers in Neuroscience* 13, p. 531.

Vorwerk, **J.**, A. A. Brock, D. N. Anderson, J. D. Rolston, and C. R. Butson (2019b). "A retrospective evaluation of automated optimization of deep brain stimulation parameters". In: *Journal of Neural Engineering* 16.6, p. 064002.

Vorwerk, **J.**, J.-H. Cho, S. Rampp, H. Hamer, T. R. Knösche, and C. H. Wolters (2014). "A guideline for head volume conductor modeling in EEG and MEG". In: *NeuroImage* 100, pp. 590–607.

Vorwerk, **J.**, M. Clerc, M. Burger, and C. Wolters (2012). "Comparison of boundary element and finite element approaches to the EEG forward problem". In: *Biomedical Engineering/Biomedizinische Technik* 57.SI-1-Track-O, pp. 795–798.

Vorwerk, **J.**, C. Engwer, S. Pursiainen, and C. H. Wolters (2016). "A mixed finite element method to solve the EEG forward problem". In: *IEEE Transactions on Medical Imaging* 36.4, pp. 930–941.

Vorwerk, **J.**, A. Hanrath, C. H. Wolters, and L. Grasedyck (2019c). "The multipole approach for EEG forward modeling using the finite element method". In: *NeuroImage* 201, p. 116039.

Vorwerk, **J.**, D. McCann, J. Krüger, and C. R. Butson (2020). "Interactive computation and visualization of deep brain stimulation effects using Duality". In: *Computer Methods in Biomechanics and Biomedical Engineering: Imaging & Visualization* 8.1, pp. 3–14.

Vorwerk, **J.**, R. Oostenveld, M. C. Piastra, L. Magyari, and C. H. Wolters (2018). "The FieldTrip-SimBio pipeline for EEG forward solutions". In: *Biomedical Engineering Online* 17, pp. 1–17.

Vorwerk, **J.**, C. H. Wolters, and D. Baumgarten (2024). "Global Sensitivity of EEG Source Analysis to Tissue Conductivity Uncertainties". In: *Frontiers in Human Neuroscience* 18, p. 1335212.

Wagner, S., S. Rampersad, Ü. Aydin, **J. Vorwerk**, T. Oostendorp, T. Neuling, C. Herrmann, D. Stegeman, and C. Wolters (2013). "Investigation of tDCS volume conduction effects in a highly realistic head model". In: *Journal of Neural Engineering* 11.1, p. 016002.

Wagner, S., **J. Vorwerk**, L. Ruthotto, H. Kugel, M. Burger, T. Knösche, B. Maess, and C. Wolters (2012). "Sensitivity of EEG leads to volume conductor properties". In: *Biomedical Engineering/Biomedizinische Technik* 57.SI-1-Track-O, pp. 793–793.

Walsh, P., N. Kane, and S. Butler (2005). "The clinical role of evoked potentials". In: *Journal of Neurology, Neurosurgery & Psychiatry* 76.suppl 2, pp. ii16–ii22.

Weaver, F. M., K. Follett, M. Stern, K. Hur, C. Harris, W. J. Marks, J. Rothlind, O. Sagher, D. Reda, C. S. Moy, et al. (2009). "Bilateral deep brain stimulation vs best medical therapy for patients with advanced Parkinson disease: a randomized controlled trial". In: *Jama* 301.1, pp. 63–73.

Weinstein, D., L. Zhukov, and C. Johnson (2000). "Lead-field bases for electroencephalography source imaging". In: *Annals of Biomedical Engineering* 28, pp. 1059–1065.

Weise, K., L. Di Rienzo, H. Brauer, J. Haueisen, and H. Toepfer (2015). "Uncertainty analysis in transcranial magnetic stimulation using nonintrusive polynomial chaos expansion". In: *IEEE Transactions on Magnetics* 51.7, pp. 1–8.

Wendel, K., N. G. Narra, M. Hannula, P. Kauppinen, and J. Malmivuo (2008). "The influence of CSF on EEG sensitivity distributions of multilayered head models". In: *IEEE Transactions on Biomedical Engineering* 55.4, pp. 1454–1456.

Wolters, C. H., M. Antonakakis, A. Khan, M. C. Piastra, and **J. Vorwerk** (2021). "Characterization of the Somatosensory System". In: *Translational Methods for Multiple Sclerosis Research*, pp. 153–169.

Wolters, C. H., A. Anwander, X. Tricoche, D. Weinstein, M. A. Koch, and R. S. Macleod (2006). "Influence of tissue conductivity anisotropy on EEG/MEG field and return current computation in a realistic head model: a simulation and visualization study using high-resolution finite element modeling". In: *NeuroImage* 30.3, pp. 813–826.

Wolters, C. H., L. Grasedyck, and W. Hackbusch (2004). "Efficient computation of lead field bases and influence matrix for the FEM-based EEG and MEG inverse problem". In: *Inverse Problems* 20.4, p. 1099.

Wolters, C. H., H. Köstler, C. Möller, J. Härdtlein, L. Grasedyck, and W. Hackbusch (2008). "Numerical mathematics of the subtraction method for the modeling of a current dipole in EEG source reconstruction using finite element head models". In: *SIAM Journal on Scientific Computing* 30.1, pp. 24–45.

Wolters, C. H., S. Lew, R. S. MacLeod, and M. Hämäläinen (2010). "Combined EEG/MEG source analysis using calibrated finite element head models". In: *Biomedizinische Technik/Biomedical Engineering. Rostock, Germany: Walter de Gruyter* 55.Suppl 1, pp. 64–68.

Wolters, C. H., M. Kuhn, A. Anwander, and S. Reitzinger (2002). "A parallel algebraic multigrid solver for finite element method based source localization in the human brain". In: *Computing and Visualization in Science* 5, pp. 165–177.

Xiao, Y., E. Pena, and M. D. Johnson (2015). "Theoretical optimization of stimulation strategies for a directionally segmented deep brain stimulation electrode array". In: *IEEE Transactions on Biomedical Engineering* 63.2, pp. 359–371.

Yan, Y., P. Nunez, and R. Hart (1991). "Finite-element model of the human head: scalp potentials due to dipole sources". In: *Medical and Biological Engineering and Computing* 29.5, pp. 475–481.

Yavich, N., N. Koshev, M. Malovichko, and M. Fedorov (2021). "Conservative finite element modeling of EEG and MEG on unstructured grids". In: *IEEE Transactions on Medical Imaging* 41.3, pp. 647–656.

Original Publications

Biomed Tech 2012; 57 (Suppl. 1) © 2012 by Walter de Gruyter · Berlin · Boston. DOI 10.1515/bmt-2012-4152

Comparison of Boundary Element and Finite Element Approaches to the EEG Forward Problem

J. Vorwerk[1], M. Clerc[2], M. Burger[3], C.H. Wolters[1]
j.vorwerk@uni-muenster.de

[1] Institute for Biomagnetism and Biosignalanalysis, University of Münster, 48149, Münster, Germany
[2] Inria Sophia-Antipolis—Méditerranée, 06904, Sophia-Antipolis Cedex, France
[3] Institute for Computational and Applied Mathematics, University of Münster, 48149, Münster, Germany

Abstract

The accurate simulation of the electric fields evoked by neural activity is crucial for solving the inverse problem of EEG.
Nowadays, boundary element methods (BEM) are frequently applied to achieve this goal, usually relying on the simplification of approximating the human head by three nested compartments with isotropic conductivities (skin, skull, brain). Here, including the highly-conducting cerebrospinal fluid (CSF) is a difficult task due to the complex geometrical structure of the CSF, demanding a high number of additional nodes for an accurate modeling and thus a strongly increased computational effort. Though, CSF conductivity is well-known and nearly not varying inter-individually and its significant influence on EEG forward simulation has been shown.
The CSF can be included at negligible computational costs when applying finite element (FE) forward approaches.
In this study we compare the accuracy and performance of state-of-the-art BE and FE approaches in both artificial and realistic three layer head models, showing that all approaches lead to high numerical accuracies. Furthermore, we give an impression of the significant influence of modeling the CSF compartment as disregarding this compartment leads to model errors that lie clearly above the observed numerical errors.

1 Introduction

The goal of EEG source reconstruction is to determine the active brain areas from measured potentials at the head surface [1–3]. To solve this problem, the accurate simulation of the electric field evoked by dipole sources in the brain is crucial. Therefore, it is necessary to apply numerical methods that are able to take the realistic shape of the head into account as several studies have shown [1], [2], [4–8].
One approach to achieve this goal are boundary element methods (BEM) [1], [4], [9], [10]. Approximating the head by a volume conductor consisting of compartments with constant, isotropic conductivities, the forward problem can be transformed to a boundary integral equation, which can then be solved numerically. A double layer BE approach was developed by Geselowitz [1]. To improve numerical accuracy, the isolated skull approach (ISA) has been proposed [4]. In our study we make use of the SimBio-toolbox[1], which implements a *linear collocation ISA BE approach* [2].
The recently proposed *symmetric BE approach* is based on a reformulation of the boundary integral equation using Newtonian potentials [9], [10]. It is implemented in the open-source toolbox OpenMEEG[2]. It has been shown that the symmetric BEM outperforms the double-layer BEM in three layer sphere models. Using an adaptive integration scheme, the achieved accuracy can be further increased [9], [10].
These approaches have the advantage of a relatively standardized model generation (three nested and non-intersecting compartments) and a relatively low computational complexity.
As a drawback of BE methods must be seen that anisotropy, e.g., in the white or gray matter compartment, whose influence on source analysis has been shown [8], cannot be taken into account. Furthermore, the distinction of tissue structures like, e.g., skull compacta and spongiosa [6] or the brain surface, which is needed to take the current-channeling CSF compartment into account [7], [11], [12], leads to an increase in computational complexity and memory demand due to the high mesh resolution needed to resolve their shape correctly. Additionally, most current BEM implementations are restricted to nested shell topographies.
The finite element methods developed for source analysis do not suffer from these specific problems, being able to handle both anisotropy and complex geometries [3], [5–7], [13], [14]. The computational complexity can be reduced by the introduction of transfer matrix or reciprocity approaches and fast iterative solver methods, which lead to an overall linear dependence on the number of FE nodes, enabling the practical usage of FE methods [3], [13], [14]. Three different FE approaches are considered here, differing in the treatment of the singularity introduced through the source term. Two of them are direct approaches, i.e., the source is approximated locally by a distribution of electrical monopoles. This distribution can be computed by means of an application of the law of St.

[1] https://www.mrt.uni-jena.de/simbio/
[2] http://www-sop.inria.fr/athena/software/OpenMEEG/

NeuroImage 100 (2014) 590–607

Contents lists available at ScienceDirect

NeuroImage

journal homepage: www.elsevier.com/locate/ynimg

A guideline for head volume conductor modeling in EEG and MEG

Johannes Vorwerk [a,*], Jae-Hyun Cho [b], Stefan Rampp [c], Hajo Hamer [c], Thomas R. Knösche [b], Carsten H. Wolters [a]

[a] Institut für Biomagnetismus und Biosignalanalyse, Westfälische Wilhelms-Universität, Münster, Germany
[b] Max Planck Institute for Human Cognitive and Brain Sciences, Leipzig, Germany
[c] Epilepsiezentrum, Universitätsklinikum Erlangen, Erlangen, Germany

ARTICLE INFO

Article history:
Accepted 18 June 2014
Available online 25 June 2014

Keywords:
EEG
MEG
Volume conductor modeling
FEM
Forward problem
Tissue conductivity anisotropy

ABSTRACT

For accurate EEG/MEG source analysis it is necessary to model the head volume conductor as realistic as possible. This includes the distinction of the different conductive compartments in the human head. In this study, we investigated the influence of modeling/not modeling the conductive compartments skull spongiosa, skull compacta, cerebrospinal fluid (CSF), gray matter, and white matter and of the inclusion of white matter anisotropy on the EEG/MEG forward solution. Therefore, we created a highly realistic 6-compartment head model with white matter anisotropy and used a state-of-the-art finite element approach. Starting from a 3-compartment scenario (skin, skull, and brain), we subsequently refined our head model by distinguishing one further of the above-mentioned compartments. For each of the generated five head models, we measured the effect on the signal topography and signal magnitude both in relation to a highly resolved reference model and to the model generated in the previous refinement step. We evaluated the results of these simulations using a variety of visualization methods, allowing us to gain a general overview of effect strength, of the most important source parameters triggering these effects, and of the most affected brain regions. Thereby, starting from the 3-compartment approach, we identified the most important additional refinement steps in head volume conductor modeling. We were able to show that the inclusion of the highly conductive CSF compartment, whose conductivity value is well known, has the strongest influence on both signal topography and magnitude in both modalities. We found the effect of gray/white matter distinction to be nearly as big as that of the CSF inclusion, and for both of these steps we identified a clear pattern in the spatial distribution of effects. In comparison to these two steps, the introduction of white matter anisotropy led to a clearly weaker, but still strong, effect. Finally, the distinction between skull spongiosa and compacta caused the weakest effects in both modalities when using an optimized conductivity value for the homogenized compartment. We conclude that it is highly recommendable to include the CSF and distinguish between gray and white matter in head volume conductor modeling. Especially for the MEG, the modeling of skull spongiosa and compacta might be neglected due to the weak effects; the simplification of not modeling white matter anisotropy is admissible considering the complexity and current limitations of the underlying modeling approach.

Introduction

Electro- and magnetoencephalography (EEG and MEG) have become important tools in the analysis of brain activity in a variety of applications in both science and medicine, e.g., brain research or clinical analysis. In many of these applications, the aim is to reconstruct the sources inside the brain volume that underlie the measured signal. Therefore, it is necessary to solve an ill-posed inverse problem which requires the simulation of the electric/magnetic field caused by a point-like source inside the brain volume: the so-called forward problem of EEG/MEG (Brette and Destexhe, 2012). The achievable accuracy in the inverse problem strongly depends on an accurate forward solution. The influence of the head modeling accuracy on the forward solution—and also on the related inverse solution—has been subject to several studies.

Early EEG/MEG source analysis used (multi-layer) sphere models to approximate the human head (de Munck and Peters, 1993), which may have, of course, led to extreme inaccuracies in the forward simulation. As a first step towards more realistic head modeling, the impact of using realistically shaped 3-layer head models distinguishing the boundaries between skin, skull, and a homogenized brain compartment was demonstrated (Brette and Destexhe, 2012). However, such models are still based on a variety of simplifications. The introduction of a homogenized brain compartment inside the inner skull surface neglects the highly conductive cerebrospinal fluid (CSF) (Lanfer et al., 2012a; Ramon et al., 2004; Wendel et al., 2008), whose conductivity is well

* Corresponding author at: Institute for Biomagnetism and Biosignalanalysis, University of Münster, Malmedyweg 15, 48149 Münster, Germany. Fax: +49 251 83 56874.
E-mail address: j.vorwerk@uni-muenster.de (J. Vorwerk).

http://dx.doi.org/10.1016/j.neuroimage.2014.06.040
1053-8119/

OPEN ACCESS Freely available online

PLOS ONE

Combining EEG and MEG for the Reconstruction of Epileptic Activity Using a Calibrated Realistic Volume Conductor Model

Ümit Aydin[1]*, Johannes Vorwerk[1], Philipp Küpper[1,2], Marcel Heers[3], Harald Kugel[4], Andreas Galka[5], Laith Hamid[5], Jörg Wellmer[3], Christoph Kellinghaus[2], Stefan Rampp[6], Carsten Hermann Wolters[1]

1 Institute for Biomagnetism and Biosignalanalysis, Westfälische Wilhelms-Universität Münster, Münster, Germany, **2** Department of Neurology, Klinikum Osnabrück, Osnabrück, Germany, **3** Ruhr-Epileptology Department of Neurology, Universitätsklinikum Knappschaftskrankenhaus Bochum, Bochum, Germany, **4** Department of Clinical Radiology, Universitätsklinikum Münster, Münster, Germany, **5** Department of Neuropediatrics, Universitätsklinikum Schleswig-Holstein, Kiel, Germany, **6** Epilepsy Center, Department of Neurology, Universitätsklinikum Erlangen, Erlangen, Germany

Abstract

To increase the reliability for the non-invasive determination of the irritative zone in presurgical epilepsy diagnosis, we introduce here a new experimental and methodological source analysis pipeline that combines the complementary information in EEG and MEG, and apply it to data from a patient, suffering from refractory focal epilepsy. Skull conductivity parameters in a six compartment finite element head model with brain anisotropy, constructed from individual MRI data, are estimated in a calibration procedure using somatosensory evoked potential (SEP) and field (SEF) data. These data are measured in a single run before acquisition of further runs of spontaneous epileptic activity. Our results show that even for single interictal spikes, volume conduction effects dominate over noise and need to be taken into account for accurate source analysis. While cerebrospinal fluid and brain anisotropy influence both modalities, only EEG is sensitive to skull conductivity and conductivity calibration significantly reduces the difference in especially depth localization of both modalities, emphasizing its importance for combining EEG and MEG source analysis. On the other hand, localization differences which are due to the distinct sensitivity profiles of EEG and MEG persist. In case of a moderate error in skull conductivity, combined source analysis results can still profit from the different sensitivity profiles of EEG and MEG to accurately determine location, orientation and strength of the underlying sources. On the other side, significant errors in skull modeling are reflected in EEG reconstruction errors and could reduce the goodness of fit to combined datasets. For combined EEG and MEG source analysis, we therefore recommend calibrating skull conductivity using additionally acquired SEP/SEF data.

Citation: Aydin Ü, Vorwerk J, Küpper P, Heers M, Kugel H, et al. (2014) Combining EEG and MEG for the Reconstruction of Epileptic Activity Using a Calibrated Realistic Volume Conductor Model. PLoS ONE 9(3): e93154. doi:10.1371/journal.pone.0093154

Editor: Gareth Robert Barnes, University College of London - Institute of Neurology, United Kingdom

Received January 23, 2014; **Accepted** February 28, 2014; **Published** March 26, 2014

Funding: This research has been supported by the German Research Foundation (DFG) through projects WO1425/2-1, STE380/14-1 and SFB 855 (http://dfg.de), and by the Medical Faculty, Ruhr University Bochum, by a FoRUM research grant (K062-11). The funders had no role in study design, data collection and analysis, decision to publish, or preparation of the manuscript.

Competing Interests: The authors have declared that no competing interests exist.

* E-mail: umitaydin@ieee.org

Introduction

Epilepsy surgery is an important option to treat pharmaco-resistant focal epilepsy and its success depends heavily on the correct determination of the epileptogenic zone. The epileptogenic zone is defined as "the minimum amount of cortex that must be resected (inactivated or completely disconnected) to produce seizure freedom" [1]. It is estimated prior to surgery by considering information available from initial seizure semiology, lesions in magnetic resonance images (MRI), video and electro-encephalography (EEG) long-term monitoring, magnetoencepha-lography (MEG), single photon emission computed tomography (SPECT), positron emission tomography (PET), neuropsycholog-ical examination and others. The *irritative zone*, one of the important zones for locating the epileptogenic zone, is identified by EEG and/or MEG. The irritative zone is defined as the brain area producing synchronous discharges of nerve cell clusters between seizures (interictal). The identification of the irritative zone has not only localizatory, but also prognostic value [2–4]. Multifocal or contralateral epileptic discharges are correlated to a less favorable postoperative outcome regarding seizure freedom [3]. Although the irritative zone might not always be identical to the epileptogenic zone, as in some patients with bitemporal spikes that became seizure free after the resection of one temporal lobe [1], it holds important information regarding the location of the epileptogenic zone. An accurate identification of the irritative zone can therefore be of high importance. We propose here a new experimental and methodological source analysis pipeline for the non-invasive identification of this zone using combined or single modality EEG/MEG source analysis in a calibrated realistic head model. The methodology will be applied in a case study with a patient suffering from refractory focal epilepsy who showed a sufficient amount of interictal spikes for the purpose of this study. In this way, we will be able to show the advantages, but also the risks of combined EEG/MEG and single modality EEG or MEG

NeuroImage 110 (2015) 60–77

Contents lists available at ScienceDirect

NeuroImage

journal homepage: www.elsevier.com/locate/ynimg

Influence of the head model on EEG and MEG source connectivity analyses

Jae-Hyun Cho [a,*], Johannes Vorwerk [b], Carsten H. Wolters [b], Thomas R. Knösche [a]

[a] Max Planck Institute for Human Cognitive and Brain Sciences, Leipzig, Germany
[b] Institute for Biomagnetism and Biosignal Analysis, University of Münster, Münster, Germany

ARTICLE INFO

Article history:
Accepted 23 January 2015
Available online 29 January 2015

Keywords:
EEG
MEG
Head modeling
Forward problem
Finite element model
Source reconstruction
Beamforming
Connectivity
Imaginary coherence
Generalized partial directed coherence

ABSTRACT

The results of brain connectivity analysis using reconstructed source time courses derived from EEG and MEG data depend on a number of algorithmic choices. While previous studies have investigated the influence of the choice of source estimation method or connectivity measure, the effects of the head modeling errors or simplifications have not been studied sufficiently.

In the present simulation study, we investigated the influence of particular properties of the head model on the reconstructed source time courses as well as on source connectivity analysis in EEG and MEG. Therefore, we constructed a realistic head model and applied the finite element method to solve the EEG and MEG forward problems. We considered the distinction between white and gray matter, the distinction between compact and spongy bone, the inclusion of a cerebrospinal fluid (CSF) compartment, and the reduction to a simple 3-layer model comprising only the skin, skull, and brain. Source time courses were reconstructed using a beamforming approach and the source connectivity was estimated by the imaginary coherence (ICoh) and the generalized partial directed coherence (GPDC).

Our results show that in both EEG and MEG, neglecting the white and gray matter distinction or the CSF causes considerable errors in reconstructed source time courses and connectivity analysis, while the distinction between spongy and compact bone is just of minor relevance, provided that an adequate skull conductivity value is used. Large inverse and connectivity errors are found in the same regions that show large topography errors in the forward solution. Moreover, we demonstrate that the very conservative ICoh is relatively safe from the crosstalk effects caused by imperfect head models, as opposed to the GPDC.

Introduction

While in the past the localization of brain activity was the main focus of neuroimaging, connectivity analysis is nowadays considered crucial for understanding brain function in neuroscience as well as in clinical research (Bassett and Gazzaniga, 2011; Castellanos et al., 2011; He et al., 2011; Palva and Palva, 2012; Schnitzler and Gross, 2005; Schoffelen and Gross, 2009). The notion of brain connectivity encompasses at least three major concepts: effective, functional, and structural connectivity (Friston, 1994; Horwitz, 2003). Functional and effective connectivity patterns in the human brain have been estimated from functional magnetic resonance imaging (fMRI) or from electroencephalography (EEG) and magnetoencephalography (MEG). Although the spatial resolution of EEG and MEG is lower than that of fMRI, they have high temporal resolution in the millisecond range and directly reflect neuronal activity caused by synchronous changes of membrane potentials in large numbers of neurons. For these reasons, EEG and MEG have been widely used to detect networks of neuronal activities and to estimate causality within these networks (David et al., 2006; Kamiński and Blinowska, 1991; Kiebel et al., 2006; Kus et al., 2004; Lachaux et al., 1999; Nolte et al., 2004; Rappelsberger and Petsche, 1988; Varela et al., 2001).

Functional connectivity between time courses recorded at multiple EEG and MEG sensors has been estimated using various methods, for example linear correlation in time or frequency domain (Nolte et al., 2004; Rappelsberger and Petsche, 1988) or analysis of phase synchrony (Lachaux et al., 1999; Varela et al., 2001). Likewise, directional information flow (effective connectivity) between signals has also been estimated using various methods (Baccalá and Sameshima, 2001; David et al., 2006; Granger, 1969; Kamiński and Blinowska, 1991; Kiebel et al., 2006). However, the interpretation of connectivity in sensor space is difficult because of signal mixing caused by volume conduction. Moreover, it is difficult to associate an anatomical meaning with the connections, as the measured signals do not generally locate in direct spatial proximity to the underlying sources (Castellanos et al., 2011; Palva and Palva, 2012; Schoffelen and Gross, 2009).

* Corresponding author at: Max Planck Institute for Human Cognitive and Brain Sciences, Stephanstraße 1A, 04103 Leipzig, Germany. Fax: +49 341 9940 2204.
E-mail address: jhcho@cbs.mpg.de (J.-H. Cho).

http://dx.doi.org/10.1016/j.neuroimage.2015.01.043

PLOS ONE

RESEARCH ARTICLE

Combined EEG/MEG Can Outperform Single Modality EEG or MEG Source Reconstruction in Presurgical Epilepsy Diagnosis

Ümit Aydin[1,2]*, Johannes Vorwerk[1], Matthias Dümpelmann[3], Philipp Küpper[1,4], Harald Kugel[5], Marcel Heers[3,6], Jörg Wellmer[6], Christoph Kellinghaus[4], Jens Haueisen[2], Stefan Rampp[6,7], Hermann Stefan[7], Carsten H. Wolters[1]

1 Institute for Biomagnetism and Biosignalanalysis, Westfälische Wilhelms-Universität Münster, Münster, Germany, **2** Institute for Biomedical Engineering and Informatics, Technische Universität Ilmenau, Ilmenau, Germany, **3** Epilepsy Center, Universitätsklinikum Freiburg, Freiburg im Breisgau, Germany, **4** Department of Neurology, Klinikum Osnabrück, Osnabrück, Germany, **5** Department of Clinical Radiology, Universitätsklinikum Münster, Münster, Germany, **6** Ruhr-Epileptology Department of Neurology, Universitätsklinikum Knappschaftskrankenhaus Bochum, Bochum, Germany, **7** Epilepsy Center, Department of Neurology, Universitätsklinikum Erlangen, Erlangen, Germany

* umitaydin@ieee.org

Citation: Aydin Ü, Vorwerk J, Dümpelmann M, Küpper P, Kugel H, Heers M, et al. (2015) Combined EEG/MEG Can Outperform Single Modality EEG or MEG Source Reconstruction in Presurgical Epilepsy Diagnosis. PLoS ONE 10(3): e0118753. doi:10.1371/journal.pone.0118753

Academic Editor: Daniele Marinazzo, Universiteit Gent, BELGIUM

Received: September 12, 2014

Accepted: January 6, 2015

Published: March 11, 2015

Data Availability Statement: All relevant data are within the paper and its supporting information files.

Funding: This work was supported by DFG (Deutsche Forschungsgemeinschaft) project WO1425/2-1 and the Priority Program 1665 of the DFG (WO1425/5-1) for ÜA, JV and CHW; DFG project STE380/14-1 for SR and HS; and by the Medical Faculty of Ruhr University Bochum, by a FoRUM research grant (K062-11) for MH and JW. The funders had no role in study design, data collection and analysis, decision to publish, or preparation of the manuscript.

Abstract

We investigated two important means for improving source reconstruction in presurgical epilepsy diagnosis. The first investigation is about the optimal choice of the number of epileptic spikes in averaging to (1) sufficiently reduce the noise bias for an accurate determination of the center of gravity of the epileptic activity and (2) still get an estimation of the extent of the irritative zone. The second study focuses on the differences in single modality EEG (80-electrodes) or MEG (275-gradiometers) and especially on the benefits of combined EEG/MEG (EMEG) source analysis. Both investigations were validated with simultaneous stereo-EEG (sEEG) (167-contacts) and low-density EEG (ldEEG) (21-electrodes). To account for the different sensitivity profiles of EEG and MEG, we constructed a six-compartment finite element head model with anisotropic white matter conductivity, and calibrated the skull conductivity via somatosensory evoked responses. Our results show that, unlike single modality EEG or MEG, combined EMEG uses the complementary information of both modalities and thereby allows accurate source reconstructions also at early instants in time (epileptic spike onset), i.e., time points with low SNR, which are not yet subject to propagation and thus supposed to be closer to the origin of the epileptic activity. EMEG is furthermore able to reveal the propagation pathway at later time points in agreement with sEEG, while EEG or MEG alone reconstructed only parts of it. Subaveraging provides important and accurate information about both the center of gravity and the extent of the epileptogenic tissue that neither single nor grand-averaged spike localizations can supply.

A Mixed Finite Element Method to Solve the EEG Forward Problem

J. Vorwerk,* C. Engwer, S. Pursiainen, and C. H. Wolters

***Abstract*— Finite element methods have been shown to achieve high accuracies in numerically solving the EEG forward problem and they enable the realistic modeling of complex geometries and important conductive features such as anisotropic conductivities. To date, most of the presented approaches rely on the same underlying formulation, the continuous Galerkin (CG)-FEM. In this article, a novel approach to solve the EEG forward problem based on a mixed finite element method (Mixed-FEM) is introduced. To obtain the Mixed-FEM formulation, the electric current is introduced as an additional unknown besides the electric potential. As a consequence of this derivation, the Mixed-FEM is, by construction, current preserving, in contrast to the CG-FEM. Consequently, a higher simulation accuracy can be achieved in certain scenarios, e.g., when the diameter of thin insulating structures, such as the skull, is in the range of the mesh resolution. A theoretical derivation of the Mixed-FEM approach for EEG forward simulations is presented, and the algorithms implemented for solving the resulting equation systems are described. Subsequently, first evaluations in both sphere and realistic head models are presented, and the results are compared to previously introduced CG-FEM approaches. Additional visualizations are shown to illustrate the current preserving property of the Mixed-FEM. Based on these results, it is concluded that the newly presented Mixed-FEM can at least complement and in some scenarios even outperform the established CG-FEM approaches, which motivates a further evaluation of the Mixed-FEM for applications in bioelectromagnetism.**

***Index Terms*— EEG, forward problem, source analysis, mixed finite element method, realistic head modeling.**

I. Introduction

THE EEG forward problem is to simulate the electric potential on the head surface that is generated by a minimal patch of active brain tissue. Its accurate solution is fundamental for precise EEG source analysis. An accurate solution can be achieved via numerical methods that allow to take the realistic head geometry into account. In this context, finite element methods (FEM) achieve high numerical accuracies and enable to realistically model tissue boundaries with complicated shapes, such as the gray matter/CSF interface, and to incorporate tissue conductivity anisotropy. The importance of incorporating these model features for the computation of accurate forward solutions and, in consequence, also for precise source analysis has been shown in multiple studies [1]–[3].

Different FEM approaches to solve the EEG forward problem have been proposed, e.g., St. Venant, partial integration, Whitney, or subtraction approaches [4]–[9]. These approaches differ in the way the dipole source is modeled, but the underlying discretization of the continuous partial differential equation (PDE) is the same: a conforming Galerkin-FEM (CG-FEM) with most often linear Ansatz-functions. The necessary discretization of the head volume can be achieved using either tetrahedral or hexahedral head models. Hexahedral models have the advantage that they can be directly generated from voxel-based magnetic resonance images (MRI), whereas the generation of surface-based tetrahedral meshes can be complicated. Therefore, hexahedral meshes are more and more frequently used in praxis [10], [11] and have, furthermore, recently been positively validated in an animal study [12].

In this article, a mixed finite element method (Mixed-FEM) to solve the EEG forward problem is introduced. Compared to the CG-FEM, it has the advantage that the current source can be represented in a direct way, whereas either an approximation using electrical monopoles has to be derived or the subtraction approach has to be applied when using the CG-FEM. Furthermore, the Mixed-FEM is current preserving and thereby prevents the effects of the (local) current leakages through the skull that might occur for the CG-FEM [13], [14]. Mixed- and CG-FEM are compared in such a leakage scenario in Section IV-C. An accurate simulation of the currents penetrating the skull is important, as the influence of an accurate representation of the skull for accurate forward simulations has been shown [15]–[17]. The accuracy of the Mixed-FEM in comparison to CG-FEM approaches and a recently presented approach based on a discontinuous Galerkin (DG) FEM formulation [14] is evaluated in sphere and realistic head models. It is shown that the Mixed-FEM achieves higher accuracies in solving the EEG forward problem than the CG-FEM for highly eccentric sources in sphere models and than both CG- and DG-FEM in realistic head models.

Manuscript received October 9, 2016; accepted October 26, 2016. Date of publication November 2, 2016; date of current version April 1, 2017. This work was supported by the Priority Program 1665 of the Deutsche Forschungsgemeinschaft (DFG) (WO1425/5-2, WO1425/7-1) and the EU project ChildBrain (Marie Curie Innovative Training Networks, grant agreement no. 641652). C.E. was supported by the Cluster of Excellence 1003 of the Deutsche Forschungsgemeinschaft (DFG EXC 1003 Cells in Motion). S. P. was supported by the Academy of Finland (Centre of Excellence in Inverse Problems Research and Key Project number 305055). *Asterisk indicates corresponding author.*

*J. Vorwerk is with the Institute for Biomagnetism and Biosignalanalysis, University of Münster, 48149 Münster, Germany and also with the Scientific Computing and Imaging (SCI) Institute, University of Utah, Salt Lake City, UT 84112, USA (e-mail: jvorwerk@sci.utah.edu).

C. Engwer is with the Institute for Applied Mathematics, University of Münster, 48149 Münster, Germany and also with the Cluster of Excellence EXC 1003, Cells in Motion, CiM, 48149 Münster, Germany.

S. Pursiainen is with the Department of Mathematics, Tampere University of Technology, 33101 Tampere, Finland.

C. H. Wolters is with the Institute for Biomagnetism and Biosignalanalysis, University of Münster, 48149 Münster, Germany.

Digital Object Identifier 10.1109/TMI.2016.2624634

IOP Publishing | Institute of Physics and Engineering in Medicine Physics in Medicine & Biology

Phys. Med. Biol. **61** (2016) 8502–8520 doi:10.1088/0031-9155/61/24/8502

Electroencephalography (EEG) forward modeling via *H*(div) finite element sources with focal interpolation

S Pursiainen[1,4], J Vorwerk[2,3] and C H Wolters[2]

[1] Department of Mathematics, Tampere University of Technology, PO Box 553, FI-33101 Tampere, Finland
[2] Institute for Biomagnetism and Biosignalanalysis, University of Münster, Malmedyweg 15, 84149 Münster, Germany
[3] Scientific Computing and Imaging (SCI) Institute, University of Utah, 72 S Central Campus Drive, Salt Lake City, UT 84112, USA

E-mail: sampsa.pursiainen@tut.fi

Received 16 August 2015, revised 21 September 2016
Accepted for publication 18 October 2016
Published 15 November 2016

Abstract

The goal of this study is to develop focal, accurate and robust finite element method (FEM) based approaches which can predict the electric potential on the surface of the computational domain given its structure and internal primary source current distribution. While conducting an EEG evaluation, the placement of source currents to the geometrically complex grey matter compartment is a challenging but necessary task to avoid forward errors attributable to tissue conductivity jumps. Here, this task is approached via a mathematically rigorous formulation, in which the current field is modeled via divergence conforming *H*(div) basis functions. Both linear and quadratic functions are used while the potential field is discretized via the standard linear Lagrangian (nodal) basis. The resulting model includes dipolar sources which are interpolated into a random set of positions and orientations utilizing two alternative approaches: the position based optimization (PBO) and the mean position/orientation (MPO) method. These results demonstrate that the present dipolar approach can reach or even surpass, at least in some respects, the accuracy of two classical reference methods, the partial integration (PI) and St. Venant (SV) approach which utilize monopolar loads instead of dipolar currents.

Keywords: biomedical engineering, electroencephalography, source modeling, finite element method, divergence conforming elements, neuroscience, EEG

(Some figures may appear in colour only in the online journal)

[4] Author to whom any correspondence should be addressed.

NeuroImage 128 (2016) 193–208

Contents lists available at ScienceDirect

NeuroImage

journal homepage: www.elsevier.com/locate/ynimg

The role of blood vessels in high-resolution volume conductor head modeling of EEG

L.D.J. Fiederer [a,b,c,d,*], J. Vorwerk [e], F. Lucka [e,f,l], M. Dannhauer [g,m], S. Yang [h], M. Dümpelmann [a,c], A. Schulze-Bonhage [c,d], A. Aertsen [b,d], O. Speck [h,i,j,k], C.H. Wolters [e], T. Ball [a,c,d]

[a] Intracranial EEG and Brain Imaging Lab, Epilepsy Center, University Hospital Freiburg, Germany
[b] Neurobiology and Biophysics, Faculty of Biology, University of Freiburg, Germany
[c] BrainLinks-BrainTools Cluster of Excellence, University of Freiburg, Germany
[d] Bernstein Center Freiburg, University of Freiburg, Germany
[e] Institute for Biomagnetism and Biosignalanalysis, University of Münster, Germany
[f] Institute for Computational and Applied Mathematics, University of Münster, Germany
[g] Scientific Computing and Imaging Institute, 72 So. Central Campus Drive, Salt Lake City, Utah 84112, USA
[h] Dept. of Biomedical Magnetic Resonance, Otto-von-Guericke University Magdeburg, Germany
[i] Leibniz Institute for Neurobiology, Magdeburg, Germany
[j] German Center for Neurodegenerative Diseases (DZNE), Site Magdeburg, Germany
[k] Center for Behavioral Brain Sciences, Magdeburg, Germany
[l] Department of Computer Science, University College London, WC1E 6BT London, UK
[m] Center for Integrative Biomedical Computing, University of Utah, 72 S. Central Campus Drive, 84112, Salt Lake City, UT, USA

ARTICLE INFO

Article history:
Received 2 October 2015
Accepted 22 December 2015
Available online 31 December 2015

Keywords:
FEM
7 T MRI
Blood vessel modeling
Submillimeter volume conductor head model
Forward problem
Inverse problem
EEG source localization
Extended source model

ABSTRACT

Reconstruction of the electrical sources of human EEG activity at high spatio-temporal accuracy is an important aim in neuroscience and neurological diagnostics. Over the last decades, numerous studies have demonstrated that realistic modeling of head anatomy improves the accuracy of source reconstruction of EEG signals. For example, including a cerebro-spinal fluid compartment and the anisotropy of white matter electrical conductivity were both shown to significantly reduce modeling errors. Here, we for the first time quantify the role of detailed reconstructions of the cerebral blood vessels in volume conductor head modeling for EEG. To study the role of the highly arborized cerebral blood vessels, we created a submillimeter head model based on ultra-high-field-strength (7 T) structural MRI datasets. Blood vessels (arteries and emissary/intraosseous veins) were segmented using Frangi multi-scale vesselness filtering. The final head model consisted of a geometry-adapted cubic mesh with over 17×10^6 nodes. We solved the forward model using a finite-element-method (FEM) transfer matrix approach, which allowed reducing computation times substantially and quantified the importance of the blood vessel compartment by computing forward and inverse errors resulting from ignoring the blood vessels. Our results show that ignoring emissary veins piercing the skull leads to focal localization errors of approx. 5 to 15 mm. Large errors (>2 cm) were observed due to the carotid arteries and the dense arterial vasculature in areas such as in the insula or in the medial temporal lobe. Thus, in such predisposed areas, errors caused by neglecting blood vessels can reach similar magnitudes as those previously reported for neglecting white matter anisotropy, the CSF or the dura — structures which are generally considered important components of realistic EEG head models. Our findings thus imply that including a realistic blood vessel compartment in EEG head models will be helpful to improve the accuracy of EEG source analyses particularly when high accuracies in brain areas with dense vasculature are required.

Introduction

Realistic head models are important tools in neuroscience (Pascual-Marqui, 1999; Michel et al., 2004; Grech et al., 2008; Michel and Murray, 2012; Schneider, 1972; Opitz et al., 2011; Datta et al., 2013; Sadleir et al., 2010; Fernández-Corazza et al., 2013; Bayford and Tizzard, 2012; Vonach et al., 2012; Carter et al., 2005; Miller et al., 2010; Voo et al., 1996; Yang et al., 2009; Panzer et al., 2012; Wendel et al., 2009; Lau et al., 2014; Heers et al., 2012; Rampp and Stefan, 2007). The present paper focuses on realistic head models for EEG research that are used as volume conductor head models (VCHMs) for computing the electric fields created by electrical sources in the brain.

* Corresponding author at: Engesserstr. 4, 5th floor, EEG Lab AG Ball, 79108 Freiburg, Germany.
E-mail address: lukas.fiederer@uniklinik-freiburg.de (L.D.J. Fiederer).

http://dx.doi.org/10.1016/j.neuroimage.2015.12.041

SIAM J. SCI. COMPUT.
Vol. 39, No. 1, pp. B138–B164

A DISCONTINUOUS GALERKIN METHOD TO SOLVE THE EEG FORWARD PROBLEM USING THE SUBTRACTION APPROACH*

CHRISTIAN ENGWER†, JOHANNES VORWERK‡, JAKOB LUDEWIG§, AND CARSTEN H. WOLTERS¶

Abstract. In order to perform electroencephalography (EEG) source reconstruction, i.e., to localize the sources underlying a measured EEG, the electric potential distribution at the electrodes generated by a dipolar current source in the brain has to be simulated, which is the so-called EEG forward problem. To solve it accurately, it is necessary to apply numerical methods that are able to take the individual geometry and conductivity distribution of the subject's head into account. In this context, the finite element (FE) method (FEM) has shown high numerical accuracy with the possibility to model complex geometries and conductive features, e.g., white matter conductivity anisotropy. In this article, we introduce and analyze the application of a discontinuous Galerkin (DG) method, an FEM that includes features of the finite volume framework, to the EEG forward problem. The DG-FEM approach fulfills the conservation property of electric charge also in the discrete case, making it attractive for a variety of applications. Furthermore, as we show, this approach can alleviate modeling inaccuracies that might occur in head geometries when using classical FE methods, e.g., so-called "skull leakage effects," which may occur in areas where the thickness of the skull is in the range of the mesh resolution. Therefore, we derive a DG formulation of the FEM subtraction approach for the EEG forward problem and present numerical results that highlight the advantageous features and the potential benefits of the proposed approach.

Key words. discontinuous Galerkin, finite element method, conservation properties, EEG, dipole, subtraction method, realistic head modeling

AMS subject classifications. 35J25, 35J75, 35Q90, 65N12, 65N30, 68U20, 92C50

DOI. 10.1137/15M1048392

1. Introduction.

Electroencephalography (EEG) source reconstruction is nowadays widely used in both research and clinical routine to investigate the activity of the human brain, as it is a noninvasive, easy to perform, and relatively cheap technique [29, 17]. To reconstruct the active brain areas from the electric potentials measured at the head surface, it is necessary to simulate the electric potential generated by a dipolar current source in the gray matter compartment of the brain, the so-called EEG forward problem. The achievable accuracy in solving the forward problem strongly depends on a realistic modeling of shape and conductive features of the volume conductor, i.e., the human head. Therefore, it is necessary to apply numerical methods

*Submitted to the journal's Computational Methods in Science and Engineering section November 16, 2015; accepted for publication (in revised form) November 9, 2016; published electronically February 23, 2017.

http://www.siam.org/journals/sisc/39-1/M104839.html

Funding: This work was partially supported by the Deutsche Forschungsgemeinschaft (DFG), project WO1425/7-1, the Priority Program 1665 of the Deutsche Forschungsgemeinschaft (DFG) (WO1425/5-1, 5-2), the Cluster of Excellence 1003 of the Deutsche Forschungsgemeinschaft (DFG EXC 1003 Cells in Motion), and by EU project ChildBrain (Marie Curie Innovative Training Networks, grant agreement 641652).

†Institute for Computational and Applied Mathematics, University of Münster, Einsteinstraße 62, 48149 Münster, Germany (christian.engwer@uni-muenster.de).

‡Institute for Biomagnetism and Biosignalanalysis, University of Münster, Malmedyweg 15, 48149 Münster, Germany (j.vorwerk@uni-muenster.de).

§Cluster of Excellence EXC 1003, Cells in Motion CiM Münster, Germany (jakobludewig@gmx.net).

¶Scientific Computing and Imaging (SCI) Institute, University of Utah, 72 S Central Campus Drive, Salt Lake City, UT 84112 (carsten.wolters@uni-muenster.de).

Vorwerk *et al. BioMed Eng OnLine (2018) 17:37*
https://doi.org/10.1186/s12938-018-0463-y

BioMedical Engineering OnLine

SOFTWARE Open Access

The FieldTrip-SimBio pipeline for EEG forward solutions

Johannes Vorwerk[1,2*†], Robert Oostenveld[3,4†], Maria Carla Piastra[1], Lilla Magyari[3,5] and Carsten H. Wolters[1]

*Correspondence:
j.vorwerk@uni-muenster.de
†Johannes Vorwerk
and Robert Oostenveld
contributed equally to this
work
[1] Institute for Biomagnetism
and Biosignalanalysis,
University of Münster,
Malmedyweg 15,
48149 Münster, Germany
Full list of author information
is available at the end of the
article

Abstract

Background: Accurately solving the electroencephalography (EEG) forward problem is crucial for precise EEG source analysis. Previous studies have shown that the use of multicompartment head models in combination with the finite element method (FEM) can yield high accuracies both numerically and with regard to the geometrical approximation of the human head. However, the workload for the generation of multicompartment head models has often been too high and the use of publicly available FEM implementations too complicated for a wider application of FEM in research studies. In this paper, we present a MATLAB-based pipeline that aims to resolve this lack of easy-to-use integrated software solutions. The presented pipeline allows for the easy application of five-compartment head models with the FEM within the FieldTrip toolbox for EEG source analysis.

Methods: The FEM from the SimBio toolbox, more specifically the St. Venant approach, was integrated into the FieldTrip toolbox. We give a short sketch of the implementation and its application, and we perform a source localization of somatosensory evoked potentials (SEPs) using this pipeline. We then evaluate the accuracy that can be achieved using the automatically generated five-compartment hexahedral head model [skin, skull, cerebrospinal fluid (CSF), gray matter, white matter] in comparison to a highly accurate tetrahedral head model that was generated on the basis of a semiautomatic segmentation with very careful and time-consuming manual corrections.

Results: The source analysis of the SEP data correctly localizes the P20 component and achieves a high goodness of fit. The subsequent comparison to the highly detailed tetrahedral head model shows that the automatically generated five-compartment head model performs about as well as a highly detailed four-compartment head model (skin, skull, CSF, brain). This is a significant improvement in comparison to a three-compartment head model, which is frequently used in praxis, since the importance of modeling the CSF compartment has been shown in a variety of studies.

Conclusion: The presented pipeline facilitates the use of five-compartment head models with the FEM for EEG source analysis. The accuracy with which the EEG forward problem can thereby be solved is increased compared to the commonly used three-compartment head models, and more reliable EEG source reconstruction results can be obtained.

Keywords: Source analysis, Forward modeling, Finite element method, Volume conductor modeling

NeuroImage 201 (2019) 116039

Contents lists available at ScienceDirect

NeuroImage

journal homepage: www.elsevier.com/locate/neuroimage

The multipole approach for EEG forward modeling using the finite element method

Johannes Vorwerk [a,b,*,1], Anne Hanrath [d,1], Carsten H. Wolters [b,c], Lars Grasedyck [d]

[a] Institute of Electrical and Biomedical Engineering, UMIT - Private University for Health Sciences, Medical Informatics and Technology, Hall in Tirol, Austria
[b] Institute for Biomagnetism and Biosignalanalysis, University of Münster, Münster, Germany
[c] Otto Creutzfeldt Center for Cognitive and Behavioral Neuroscience, University of Münster, Münster, Germany
[d] Institut für Geometrie und Praktische Mathematik, RWTH Aachen, Aachen, Germany

ARTICLE INFO

Keywords:
EEG
Source analysis
Finite element method
Source modeling
Quadrupole
Multipole

ABSTRACT

For accurate EEG forward solutions, it is necessary to apply numerical methods that allow to take into account the realistic geometry of the subject's head. A commonly used method to solve this task is the finite element method (FEM). Different approaches have been developed to obtain EEG forward solutions for dipolar sources with the FEM. The St. Venant approach is frequently applied, since its high numerical accuracy and stability as well as its computational efficiency was demonstrated in multiple comparison studies. In this manuscript, we propose a variation of the St. Venant approach, the multipole approach, to improve the numerical accuracy of the St. Venant approach even further and to allow for the simulation of additional source scenarios, such as quadrupolar sources. Exploiting the multipole expansion of electric fields, we demonstrate that the newly proposed multipole approach achieves even higher numerical accuracies than the St. Venant approach in both multi-layer sphere and realistic head models. Additionally, we exemplarily show that the multipole approach allows to not only simulate dipolar but also quadrupolar sources.

1. Introduction

Electroencephalography (EEG) is a frequently used tool to observe brain activity in both neuroscience and clinical applications, since it provides a unique time resolution in the millisecond range. In many of these applications, it is desirable to perform EEG source analysis, i.e., to reconstruct the active brain areas evoking a measured signal. To achieve this reconstruction it is necessary to simulate the EEG signal that is generated by activity in a certain region of the brain. This task is called the EEG forward problem (Brette and Destexhe, 2012).

The EEG forward problem can only be solved analytically in simple geometries, such as multi-layer sphere models (de Munck et al., 1988; de Munck and Peters, 1993). To realistically model the subject's head, the use of numerical techniques such as boundary element methods (BEM, Gramfort et al., 2010), finite volume methods (FVM, Cook and Koles, 2006), finite difference methods (FDM, Vatta et al., 2009; Montes-Restrepo et al., 2014), or finite element methods (FEM, Wolters et al., 2007a) is necessary. For all these techniques, the major challenge is to deal with the strong singularity caused by the assumption of a dipolar source to represent brain activity, as it is common in EEG source analysis (de Munck et al., 1988; Hämäläinen et al., 1993; Sarvas, 1987).

Two classes of approaches to solve this problem when applying FEM exist: In the subtraction approach (Wolters et al., 2007b; Engwer et al., 2017), the dipolar source is subtracted from the original equation by using the analytical solution for an infinite, homogeneous volume conductor. Subsequently, a correction potential that accounts for the inhomogeneous conductivity distribution within the head is computed, and the EEG forward solution is obtained by summing up analytical solution and correction potential. In the direct approaches, such as St. Venant (Buchner et al., 1997), partial integration (Yan et al., 1991), and Whitney approach (Tanzer et al., 2005; Pursiainen et al., 2011), the dipole source is approximated by a discrete distribution of current sinks and sources placed on the vertices of the finite element mesh. Each of the approaches follows a different assumption to select these vertices and to determine the strength of the sinks and sources.

Whereas all of these approaches lead to accurate EEG forward

* Corresponding author. Institute of Electrical and Biomedical Engineering, UMIT - Private University for Health Sciences, Medical Informatics and Technology, Hall in Tirol, Austria.
E-mail address: johannes.vorwerk@umit.at (J. Vorwerk).
[1] The first two authors contributed equally to this work.

https://doi.org/10.1016/j.neuroimage.2019.116039
Received 21 February 2019; Received in revised form 14 June 2019; Accepted 19 July 2019
Available online 29 July 2019

frontiers in Neuroscience

ORIGINAL RESEARCH
published: 04 June 2019
doi: 10.3389/fnins.2019.00531

Influence of Head Tissue Conductivity Uncertainties on EEG Dipole Reconstruction

Johannes Vorwerk[1,2,3], *Ümit Aydin*[2,4], *Carsten H. Wolters*[2,5] *and Christopher R. Butson*[1,6,7]*

[1] *Scientific Computing & Imaging (SCI) Institute, University of Utah, Salt Lake City, UT, United States,* [2] *Institute for Biomagnetism and Biosignalanalysis, University of Münster, Münster, Germany,* [3] *Institute of Electrical and Biomedical Engineering, UMIT - University for Health Sciences, Medical Informatics and Technology, Hall in Tirol, Austria,* [4] *Multimodal Functional Imaging Lab, Department of Physics and PERFORM Centre, Concordia University, Montreal, QC, Canada,* [5] *Otto Creutzfeldt Center for Cognitive and Behavioral Neuroscience, University of Münster, Münster, Germany,* [6] *Departments of Biomedical Engineering, Neurology, and Psychiatry, University of Utah, Salt Lake City, UT, United States,* [7] *Department of Neurosurgery, Clinical Neurosciences Center, University of Utah, Salt Lake City, UT, United States*

Reliable EEG source analysis depends on sufficiently detailed and accurate head models. In this study, we investigate how uncertainties inherent to the experimentally determined conductivity values of the different conductive compartments influence the results of EEG source analysis. In a single source scenario, the superficial and focal somatosensory P20/N20 component, we analyze the influence of varying conductivities on dipole reconstructions using a generalized polynomial chaos (gPC) approach. We find that in particular the conductivity uncertainties for skin and skull have a significant influence on the EEG inverse solution, leading to variations in source localization by several centimeters. The conductivity uncertainties for gray and white matter were found to have little influence on the source localization, but a strong influence on the strength and orientation of the reconstructed source, respectively. As the CSF conductivity is most accurately determined of all conductivities in a realistic head model, CSF conductivity uncertainties had a negligible influence on the source reconstruction. This small uncertainty is a further benefit of distinguishing the CSF in realistic volume conductor models.

Keywords: EEG source analysis, EEG dipole reconstruction, head modeling, sensitivity analysis, conductivity uncertainty, conductivity estimation, finite element method, generalized polynomial chaos

OPEN ACCESS

Edited by:
Takashi Hanakawa, National Center of Neurology and Psychiatry, Japan

Reviewed by:
Okito Yamashita, Advanced Telecommunications Research Institute International (ATR), Japan
Victoria Eugenia Montes Restrepo, VU University Medical Center, Netherlands

***Correspondence:**
Christopher R. Butson
butson@sci.utah.edu

Specialty section:
This article was submitted to Neural Technology, a section of the journal Frontiers in Neuroscience

Received: *16 January 2019*
Accepted: *08 May 2019*
Published: *04 June 2019*

Citation:
Vorwerk J, Aydin Ü, Wolters CH and Butson CR (2019) Influence of Head Tissue Conductivity Uncertainties on EEG Dipole Reconstruction. Front. Neurosci. 13:531. doi: 10.3389/fnins.2019.00531

1. INTRODUCTION

Electroencephalography (EEG) source analysis is an important tool in a variety of both clinical and scientific applications to identify the active brain areas that evoke a measured signal (Brette and Destexhe, 2012). In practice, EEG source analysis consists of two problems: simulating the EEG signal evoked by activity in a certain brain region (EEG forward problem) and, based on these simulations, reconstructing the active brain areas underlying a measured EEG signal (EEG inverse problem). The accuracy of the EEG inverse solution depends on various factors, for example the signal-to-noise ratio (SNR) of the measurement (Arridge et al., 2006; Bast et al., 2006), the number of EEG sensors (Lantz et al., 2003; Grieve et al., 2004), the applied inverse method (Pascual-Marqui, 2002; Lucka et al., 2012), or the accuracy of the EEG forward solution (Acar and Makeig, 2013; Cho et al., 2015). Of course, the amount of influence of each of these factors on the source analysis

OPEN ACCESS
IOP Publishing
Journal of Neural Engineering
J. Neural Eng. **16** (2019) 064002 (14pp)
https://doi.org/10.1088/1741-2552/ab35b1

Note

A retrospective evaluation of automated optimization of deep brain stimulation parameters

Johannes Vorwerk[1,2], Andrea A Brock[1,3], Daria N Anderson[1,3,4], John D Rolston[1,3,4] and Christopher R Butson[1,3,4,5,6]

[1] Scientific Computing & Imaging (SCI) Institute, University of Utah, Salt Lake City, UT, United States of America
[2] Institute of Electrical and Biomedical Engineering, UMIT—Private University for Health Sciences, Medical Informatics and Technology, Hall in Tirol, Austria
[3] Department of Neurosurgery, University of Utah, Salt Lake City, UT, United States of America
[4] Department of Biomedical Engineering, University of Utah, Salt Lake City, UT, United States of America
[5] Departments of Psychiatry and Neurology, University of Utah, Salt Lake City, UT, United States of America

E-mail: johannes.vorwerk@umit.at and butson@sci.utah.edu

Received 23 October 2018, revised 17 July 2019
Accepted for publication 25 July 2019
Published 6 November 2019

Abstract

Objective. We performed a retrospective analysis of an optimization algorithm for the computation of patient-specific multipolar stimulation configurations employing multiple independent current/voltage sources. We evaluated whether the obtained stimulation configurations align with clinical data and whether the optimized stimulation configurations have the potential to lead to an equal or better stimulation of the target region as manual programming, while reducing the time required for programming sessions. *Approach.* For three patients (five electrodes) diagnosed with essential tremor, we derived optimized multipolar stimulation configurations using an approach that is suitable for the application in clinical practice. To evaluate the automatically derived stimulation settings, we compared them to the results of the monopolar review. *Main results.* We observe a good agreement between the findings of the monopolar review and the optimized stimulation configurations, with the algorithm assigning the maximal voltage in the optimized multipolar pattern to the contact that was found to lead to the best therapeutic effect in the clinical monopolar review in all cases. Additionally, our simulation results predict that the optimized stimulation settings lead to the activation of an equal or larger volume fraction of the target compared to the manually determined settings in all cases. *Significance.* Our results demonstrate the feasibility of an automatic determination of optimal DBS configurations and motivate a further evaluation of the applied optimization algorithm.

[6] Author to whom any correspondence should be addressed.

COMPUTER METHODS IN BIOMECHANICS AND BIOMEDICAL ENGINEERING: IMAGING & VISUALIZATION
2020, VOL. 8, NO. 1, 3–14
https://doi.org/10.1080/21681163.2018.1484817

Taylor & Francis
Taylor & Francis Group

RESEARCH PAPER

Interactive computation and visualization of deep brain stimulation effects using Duality

J. Vorwerk[a], D. McCann[a], J. Krüger[a,b] and C. R. Butson[a]

[a]Scientific Computing & Imaging (SCI) Institute, Department of Bioengineering, University of Utah, Salt Lake City, UT, USA; [b]Center of Visual Data Analysis and Computer Graphics (COVIDAG) & HPC Group, University of Duisburg-Essen, Duisburg, Germany

ABSTRACT

Deep brain stimulation (DBS) is an established treatment for movement disorders such as Parkinson's disease or essential tremor. Currently, the selection of optimal stimulation settings is performed by iteratively adjusting the stimulation parameters and is a time consuming procedure that requires multiple clinic visits of several hours. Recently, computational models to predict and visualize the effect of DBS have been developed with the goal to simplify and accelerate this procedure by providing visual guidance and such models have been made available also on mobile devices. However, currently available visualization software still either lacks mobility, i.e. it is running on desktop computers and no easily available in clinical praxis, or flexibility, as the simulations that are visualized on mobile devices have to be precomputed. The goal of the pipeline presented in this paper is to close this gap: Using Duality, a newly developed software for the interactive visualization of simulation results, we implemented a pipeline that allows to compute DBS simulations in near-real time and instantaneously visualize the result on a tablet computer. We carry out a performance analysis and present the results of a case study in which the pipeline was applied.

ARTICLE HISTORY
Received 15 January 2018
Accepted 1 June 2018

KEYWORDS
DBS; neuromodulation; computational steering; finite element method; telemedicine

1. Introduction

The goal of neuromodulation is to achieve therapeutic effects by stimulating specific target regions in the human brain using electric or magnetic fields. Both non-invasive and invasive procedures to reach this goal exist. As an invasive procedure, deep brain stimulation (DBS) has become an established treatment for movement disorders, such as Parkinson's disease or essential tremor, where Level 1 evidence for the efficacy of DBS exists (Deuschl et al. 2006; Weaver et al. 2009). DBS is furthermore under current investigation as a treatment for a variety of other disorders, such as depression, obsessive-compulsive disorder, Alzheimer's disease, or traumatic brain injury. Depending on the disease to be treated, a target region in the brain, commonly a subcortical brain structure, such as subthalamic nucleus (STN) or globus pallidus interna (GPi) for Parkinson's disease (Deuschl et al. 2006; Weaver et al. 2009), is determined and the DBS lead is introduced into this structure in a surgical procedure.

A DBS lead commonly has at least four contacts; each contact can be either circular in shape or, for newer DBS leads, also segmented contacts exist, which allow for a better targeted stimulation. The DBS lead is connected to an implanted pulse generator (IPG) that is subcutaneously placed in the patient's chest. The IPG generates electric potentials with a specific waveform and frequency, which are then applied to the electrode contacts.

The major task to achieve a successful DBS treatment, is the determination of an optimal stimulation pattern, i.e. the selection of the active electrode contacts as well as stimulation waveform and pattern. In most cases, either one contact is chosen to be active with the stimulator case as reference (unipolar stimulation) or two contacts are active with one as anode and one as cathode (bipolar stimulation). Stimulation voltages are in the range of a few volts, pulse widths between 60 and 210 μs, and frequencies around 130 Hz (Volkmann et al. 2002; Butson and McIntyre 2006). Classically, the optimal stimulation pattern has to be found in a trial-and-error approach, i.e. based on the personal experience of the treating physician, the parameter space is sampled and the chosen settings are adjusted based on the observation of the patient. This usually requires multiple outpatient visits for programming sessions and each of them may last multiple hours (Hunka et al. 2005; Ondo and Bronte-Stewart 2005).

Recently, a variety of studies has been published that aims at simplifying the process of finding optimal stimulation settings. Decision-support applications have been developed that allow the visualization of the stimulated brain area together with segmentations of the target structures within the brain (Butson et al. 2007a, 2013; Horn and Kühn 2015). The goal of these applications is to simplify the manual optimization of the patient programming through the visualization of predicted stimulation effects. A common concept in this context is the volume of tissue activated

CONTACT C. R. Butson butson@sci.utah.edu

frontiers | Frontiers in Human Neuroscience

TYPE Original Research
PUBLISHED 12 March 2024
DOI 10.3389/fnhum.2024.1335212

OPEN ACCESS

EDITED BY
George Alexandrakis,
University of Texas at Arlington, United States

REVIEWED BY
Joonas Iivanainen,
Aalto University, Finland
Seppo P. Ahlfors,
Massachusetts General Hospital and Harvard Medical School, United States

*CORRESPONDENCE
Johannes Vorwerk
✉ johannes.vorwerk@umit-tirol.at

RECEIVED 08 November 2023
ACCEPTED 22 January 2024
PUBLISHED 12 March 2024

CITATION
Vorwerk J, Wolters CH and Baumgarten D (2024) Global sensitivity of EEG source analysis to tissue conductivity uncertainties. *Front. Hum. Neurosci.* 18:1335212. doi: 10.3389/fnhum.2024.1335212

Global sensitivity of EEG source analysis to tissue conductivity uncertainties

Johannes Vorwerk[1]*, Carsten H. Wolters[2,3] and Daniel Baumgarten[1]

[1]Institute of Electrical and Biomedical Engineering, UMIT TIROL—Private University for Health Sciences and Health Technology, Hall in Tirol, Austria, [2]Institute for Biomagnetism and Biosignalanalysis, University of Münster, Münster, Germany, [3]Otto Creutzfeldt Center for Cognitive and Behavioral Neuroscience, University of Münster, Münster, Germany

Introduction: To reliably solve the EEG inverse problem, accurate EEG forward solutions based on a detailed, individual volume conductor model of the head are essential. A crucial—but often neglected—aspect in generating a volume conductor model is the choice of the tissue conductivities, as these may vary from subject to subject. In this study, we investigate the sensitivity of EEG forward and inverse solutions to tissue conductivity uncertainties for sources distributed over the whole cortex surface.

Methods: We employ a detailed five-compartment head model distinguishing skin, skull, cerebrospinal fluid, gray matter, and white matter, where we consider uncertainties of skin, skull, gray matter, and white matter conductivities. We use the finite element method (FEM) to calculate EEG forward solutions and goal function scans (GFS) as inverse approach. To be able to generate the large number of EEG forward solutions, we employ generalized polynomial chaos (gPC) expansions.

Results: For sources up to a depth of 4 cm, we find the strongest influence on the signal topography of EEG forward solutions for the skull conductivity and a notable effect for the skin conductivity. For even deeper sources, e.g., located deep in the longitudinal fissure, we find an increasing influence of the white matter conductivity. The conductivity variations translate to varying source localizations particularly for quasi-tangential sources on sulcal walls, whereas source localizations of quasi-radial sources on the top of gyri are less affected. We find a strong correlation between skull conductivity and the variation of source localizations and especially the depth of the reconstructed source for quasi-tangential sources. We furthermore find a clear but weaker correlation between depth of the reconstructed source and the skin conductivity.

Discussion: Our results clearly show the influence of tissue conductivity uncertainties on EEG source analysis. We find a particularly strong influence of skull and skin conductivity uncertainties.

KEYWORDS

EEG, forward modeling, finite element method, source analysis, sensitivity analysis, uncertainty quantification

1 Introduction

Electroencephalography (EEG) is a frequently used tool for functional brain imaging in both research and clinical care (Brette and Destexhe, 2012). A huge advantage of EEG over, e.g., functional magnetic resonance imaging (fMRI), is its time resolution in the millisecond range. To localize the brain activity underlying a measured signal it is necessary to solve the EEG inverse problem (Knösche and Haueisen, 2022). As a prerequisite for solving the EEG inverse problem, it is necessary to model the propagation of the electric fields evoked by brain activity through the head tissues,